Pseudotyped lentiviral systems for studying viral entry proteins from emerging viruses with pandemic potential

Katharine H. D. Crawford

A dissertation
submitted in partial fulfillment of the
requirements for the degree of

Doctor of Philosophy

University of Washington

2021

Reading Committee:

Jesse D. Bloom, Chair

Neil P. King

Helen Y. Chu

Program Authorized to Offer Degree:
Genome Sciences

University of Washington

Abstract

Pseudotyped lentiviral systems for studying viral entry proteins from emerging viruses with pandemic potential

Katharine H. D. Crawford

Chair of the Supervisory Committee:
Associate Member Jesse D. Bloom
Fred Hutchinson Cancer Research Center

Viral entry proteins facilitate viral entry into host cells through receptor binding and membrane fusion. They play a critical role in the viral life cycle and, as prominent surface proteins, are common targets of the host immune response. Mutations in viral entry proteins can allow viruses to infect new hosts (including humans), better spread between hosts, or evade immune responses and some therapeutics. A better understanding of how viral entry proteins interact with host proteins, elicit host antibody responses, or are affected by mutations is important for being tackling current and emerging viral threats.

However, viral entry proteins are also heavily glycosylated, multimeric, metastable proteins that are challenging to work with. Furthermore, studying viral entry proteins in their native viral context is challenging due to inefficient reverse genetics systems or the need to work under high biosafety level containment. As such, many viral entry proteins—especially those from emerging viruses—cannot be studied with many high-throughput experimental techniques, such as mutational scanning experiments.

Pseudotyping viral entry proteins on easier- and safer-to-work-with viral particles is one way to facilitate research of viral entry proteins from emerging viruses. When SARS-CoV-2 was first identified in late 2019, there was an urgent need to develop tools to safely

and easily study the virus. Working with SARS-CoV-2 itself requires a biosafety level 3 facility, but pseudotyping its entry protein, spike, onto lentiviral particles allows SARS-CoV-2 spike to be studied under commonly available biosafety level 2 conditions.

In the following chapters, I describe a protocol for pseudotyping lentiviral particles with SARS-CoV-2 spike to facilitate research into this emerging virus. I also describe the use of spike-pseudotyped lentiviral particles to investigate the neutralizing antibody response to SARS-CoV-2 and the effects of mutations to spike on its function as a viral entry protein. Spike-pseudotyped lentiviral particles are especially useful for measuring SARS-CoV-2-neutralizing antibodies and I provide a detailed protocol for a SARS-CoV-2 neutralization assay using spike-pseudotyped lentiviral particles I then use this assay to investigate the dynamics of the neutralizing antibody response to SARS-CoV-2 in the first several months following infection. Titers of SARS-CoV-2 neutralizing antibodies decline modestly from $\approx$1 to $\approx$3 months post symptom onset, which is typical of the neutralizing antibody response to other acute respiratory viruses.

The SARS-CoV-2 pandemic has also provided an example of the importance of prospectively characterizing the effects of mutations to viral entry proteins. Pseudotyped lentiviral particles provide a genetically tractable system for assessing the effects of mutations to viral entry proteins from emerging viruses at high-throughput. As such, I have worked to develop a pseudotyped lentivirus-based system for screening the functional and antigenic effects of mutations to viral entry proteins from emerging viruses in high-throughput. This system is still being developed, but I briefly discuss current progress and describe a Python package I helped write to facilitate the analysis of such deep mutational scanning experiments.

In summary, the following chapters describe the use of pseudotyped lentiviral particles as a a flexible, rapidly deployable tool for studying viral entry proteins from emerging

viruses, such as SARS-CoV-2. Using spike-pseudotyped lentiviral particles, I contributed to some of our earliest understanding of the dynamics of the neutralizing antibody response to SARS-CoV-2 in the first several months following infection. Nonetheless, I think the full potential of using pseudotyped lentiviral particles to study viral entry proteins from emerging viruses has yet to be realized. As such, I also discuss current progress (including computational tools) and future work towards using pseudotyped lentiviral particles to measure the functional and antigenic effects of mutations to viral entry proteins from emerging viruses at high-throughput.

TABLE OF CONTENTS

LIST OF FIGURES

LIST OF TABLES

ACKNOWLEDGMENTS

I am very grateful to have had the opportunity to be mentored by Jesse Bloom and complete my thesis research in his lab. Jesse's scientific guidance helped the projects described in this thesis come to fruition, but, more importantly, his mentorship helped me become a capable and confident scientist. Jesse managed to find the right balance between letting me try things on my own and giving me enough direction to be successful. I am also grateful for his kindness and the support he provided during the challenges of this past year. I think one of my grant reviewers put it best when they said that Jesse and I "really do seem to make a good team."

I would also like to thank my thesis committee—Neil King, Julie Overbaugh, Helen Chu, and Stan Fields. I have truly enjoyed getting to discuss my work with them and their guidance and insight proved invaluable numerous times. I have also been lucky enough to get to collaborate with Neil, Julie, and Helen on several projects—including some discussed in this dissertation. I could not have asked for better collaborators during my graduate studies. A special thank you goes to the members of Helen, Julie, and Neil's labs with whom I worked directly: Caitlin Wolf, Naomi Wilcox, Ted Gobillot, Meghan Garrett, Caitlin Stoddard, and Dan Ellis.

I am also grateful for the scientific community at the Fred Hutch and in the UW Genome Sciences department. Specifically, thank you to the Thursday morning virology group for excellent advice, astute questions, a sense of community, and (pre-2020) bagels.

My previous mentors also deserve a big thank you for helping me get to where I am. Thank you to the Saccomanno Research Institute in Grand Junction, Colorado for wel-

coming me as an eager high school student and teaching me the basics of molecular biology. At Williams College, I was fortunate to work with Professors Lois Banta and Claire Ting, both extremely supportive mentors who helped me develop my confidence as a young scientist. Thank you to the summer undergraduate research program at Cold Spring Harbor Laboratory and specifically Drs. Darryl Pappin, Jon Ipsaro, and John Wilson for taking me under their wing, introducing me to the word of high-throughput assay development, and trusting me with the mass-spectrometers. Finally, thank you to Dr. Jennifer Whangbo who was my mentor in the Ritz lab at Dana Farber Cancer Research Center between undergraduate and graduate school. Jennifer is not only an excellent scientific mentor, but was very supportive in helping me figure out my next steps.

I would also like to thank Julie Tall and the ARCS program for funding support during the initial years of my PhD.

Due to the nature of my MD/PhD training, I have been affiliated with the Bloom lab for the past 6 years and in many ways I feel like I've been able to "grow up" with the lab. From chats with Mike Doud and Orr Ashenberg during my first rotation in the summer of 2015 to now brainstorming with Andrea Loes about how to make sure the lab continues to be a supportive and fun place to do science, I cannot think of a better place to have completed my PhD. I am grateful to all members of the Bloom lab past and present for having made the lab not only an excellent place to do science, but also a place I wanted to be filled with people I wanted to spend time with—I can honestly say I will miss the lab.

I feel lucky that in the course of my PhD I have worked closely with almost everyone in the lab (perhaps this is because I have sat at the most desks of anyone in lab—new students take note). I cannot possibly do justice here to how much I have valued each of those collaborations and conversations, but I am leaving the Bloom lab a better scientist thanks to the collective contributions of all its members and for that I am grateful.

Although its members have changed over the years, I would especially like to thank the ”HIV corner” for camaraderie and fruitful discussions during my PhD. Coffee walks with Sarah Hilton got me through some particularly challenging parts of graduate school. Adam Dingens's willingness to let me bounce ideas off of him ad nauseum facilitated my progression throughout my PhD and helped mold my scientific thinking for the better. David Bacsik has been an excellent cohort-mate, house-mate, lab-mate, etc.—I couldn't ask for a better friend throughout this journey.

Thank you also to Rachel Eguia who helped me with much of the work described in the following chapters—she is an excellent scientist and somehow managed to make setting up dozens of neutralization assays almost fun. Keara Malone and Andrea also made the work described herein possible and helped keep me sane. Thank you also to Tyler Starr for schooling me at ping pong and providing much needed mentorship when I needed an opinion other than Jesse's. Thank you to Allie Greaney for always believing I could accomplish my goals and reminding me of that when I needed it. And thank you to Lauren Gentles for a steady relentlessness in the projects we worked on together—including Girls Who Code!

Finally, I worked closely with Caelan Radford on the majority of my PhD research, most of which unfortunately did not make it into this written dissertation. Caelan and I proved to be good foils for each other during graduate school. He always seemed to be optimistic about our platform development when I was not and vice versa. It was a pleasure working with him and I'm excited to see where he takes this work in the coming years.

Outside of lab, I spent a majority of my time playing ultimate frisbee. Thank you to Tom for making me promise I'd try the sport when I came to graduate school. If 2020 taught me anything it is that without ultimate frisbee and my teammates (on Element, Freeze, Underground, and Birdfruit), I'm not sure how I would have gotten through graduate school.

The competitive outlet, the friendship, and the opportunity to throw myself (quite literally) at something with such abandon have been invaluable.

A huge thank you also goes to my family, especially my parents Dodie and Henry Dusenbury who attended several of my talks during my PhD. They were a great grounding presence and being able to make them proud has been the most gratifying part of my graduate studies. Thank you also to my big brother John Dusenbury for believing in his little sister, but also asking tough questions and not letting me get too much of a big head.

The biggest thanks goes to Tom, without whom I would be lost. I hope he enjoyed being +1 doctorate on me for a couple of years.

Chapter 1

INTRODUCTION

In this introduction, I will provide background on viral entry proteins and pseudotyped lentiviral particles, as well as common assays using such particles. I will also introduce SARS-CoV-2 and its entry protein, spike, which is the focus of Chapters 2 and 3.

Finally, I will briefly introduce viral entry protein deep mutational scanning and highlight the computational need that my work in Chapter 4 addresses.

1.1 Introduction to viral entry proteins

Viral entry proteins are the proteins on the surface of a virus involved in receptor binding and/or membrane fusion [164]. Since viruses rely on cellular machinery to replicate and reproduce, entry into a host cell is a critical first step in the viral life cycle and, thus, viral pathogenesis. For enveloped viruses, including the common human pathogens influenza, HIV, and severe acute respiratory syndrome coronavirus 2 (SARS-CoV-2), this process is particularly complex as the viral envelope must fuse with a host membrane to allow viral components to enter the cell. Therefore, viral entry proteins from enveloped viruses must mediate both receptor binding and membrane fusion [63].

Many enveloped viruses encode a single glycoprotein that mediates both receptor binding and membrane fusion. This includes influenza hemagglutinin (HA), HIV envelope (Env), SARS-CoV-2 spike, Ebola virus glycoprotein (EBOV GP), and Lassa virus glycoprotein (LASV GP) [165, 45, 14, 164, 64]. These ”dual-function” viral entry proteins are

the focus of this dissertation.

Other viruses, including herpesviruses and paramyxoviruses, such as measles virus or Nipah virus, encode separate glycoproteins for receptor binding and membrane fusion [164]. Many of the concepts and approaches described in this dissertation could be extended with some experimental modifications to apply to viral entry proteins that mediate only binding *or* fusion. However, the work described herein focuses on developing and applying tools to facilitate research of viral entry proteins that mediate both receptor binding *and* membrane fusion, with a particular focus on SARS-CoV-2 spike.

1.1.1 Three classes of viral fusion proteins

Despite the large diversity of enveloped viruses, most viral fusion proteins employ a common mechanism for mediating membrane fusion [124]. The first step in virus-mediated membrane fusion is typically priming of the viral fusion protein through proteolytic cleavage of the fusion protein itself or an associated chaperon protein. This cleavage involves minimal structural rearrangements, but is typically required for a viral fusion proteins to be fusogenic [63]. Next, a triggering event, such as receptor binding or exposure to low pH, initiates substantial structural rearrangements that lead to the insertion of the hydrophobic ”fusion peptide” or ”fusion loop” into the host membrane and trimerization of the fusion protein (if it is not already a trimer) [63]. In this extended ”prehairpin” intermediate form, the fusion protein is anchored to the virus by its transmembrane domain and the cellular membrane by its fusion peptide. The fusion protein then begins to fold in on itself, transitioning into a low-energy postfusion form described as a ”trimer-of-hairpins.” This structural transition brings the two membranes together. As the membranes juxtapose, they first go through a hemifusion intermediate, where the outermost membrane leaflets from each membrane fuse, and then fuse completely, forming a fusion pore through which viral components can enter the cell [124].

Along with sharing a common fusion mechanism, most viral fusion proteins share structural characteristics and can be classified into one of three classes based on their typical 3-dimensional structures [164, 124, 63]. Below I highlight the steps of viral fusion that distinguish each fusion protein class.

Class I

Class I viral fusion proteins include some of the most well-studied viral fusion proteins including influenza HA, HIV Env, and SARS-CoV-2 spike—the focus of this dissertation. These viral fusion proteins are homotrimers that protrude perpendicularly from the viral surface. The structure of class I fusion proteins is dominated by α-helices and, in their postfusion form, they collapse into a six-helix-bundle structure [164]. To become fusion competent, class I fusion proteins must be proteolytically cleaved, often by host proteases [164]. This cleavage separates the fusion protein into multiple subunits and primes the fusion peptide so that it can insert into the host membrane once triggered. Class I fusion proteins can be triggered by a variety of conditions including receptor binding, low pH, a combination of the two, or other unknown triggers [164].

Class II

The prototypical class II viral fusion protein is the flavivirus envelope protein, such as Dengue virus E [124, 164]. Unlike class I fusion proteins, class II fusion proteins are arranged parallel to the surface of the virus and are largely comprised of β-sheet secondary structure [164]. These fusion proteins form anti-parallel homodimers that pack into an icosahedrally symmetric array encasing the viral membrane [124, 63]. Class II fusion proteins associate with a separate viral ”chaperon” protein that protects the fusion peptide during viral maturation and must be cleaved for the fusion protein to become fusogenic. All known class II fusion proteins are then triggered by exposure to low pH, such as in a

target cell's acidified endosome [164].

Class III

Class III viral fusion proteins are a relatively small class of fusion proteins. The prototypical class III viral fusion protein is vesicular stomatitis virus glycoprotein (VSV G), but other rhabdoviruses, herpesviruses, baculoviruses, and some thogotoviruses also have class III viral fusion proteins [124]. Class III viral fusion proteins have characteristics similar to both class I and class II fusion proteins. Like class I fusion proteins, they exist as trimers in both their pre and postfusion conformations, but their fusion domain is comprised largely of β-sheet secondary structure and more closely resembles that of class II fusion proteins [124]. Most notably, class III viral fusion proteins do not undergo a proteolytic cleavage priming step, meaning that, at least for VSV G, the conformational changes they undergo prior to membrane fusion are reversible [164]. Unlike class I and class II viral fusion proteins, if VSV G is triggered prematurely by exposure to low pH, it will not irreversibly transition to their postfusion state. Rather, upon exposure to neutral pH, VSV G can reverse the low pH-induced conformational changes and return to a fusogenic prefusion state. It remains unknown if the trigger-induced structural rearrangements of other class III viral fusion proteins are also reversible [164].

Other viral fusion proteins

Although most viral fusion proteins fit into these three main classes, several viruses have fusion proteins with unique structures that defy this classification. Interestingly, several genera in the *Flaviviridae* family have fusion proteins that do not appear to fit the typical class II fusion protein structure. Additionally hepatitis B virus and poxviruses have unique viral fusion protein complexes that are distinct from all three classes [124]. As viral entry proteins from enveloped viruses, many of the pseudotyping techniques described in future

sections would potentially still be applicable to these other viral fusion proteins, but my initial work has focused on class I viral fusion proteins as those have the most previous research upon which I have been able to build.

1.1.2 Selective pressures on viral entry proteins

Viral entry proteins mediate cell entry through direct interaction with host receptors and, therefore, are important determinants of host tropism [106]. Mutations to viral entry proteins can allow viruses to infect new hosts, including humans [153, 100] or more efficiently infect an already susceptible host [81].

As prominent surface proteins, viral entry proteins are also often targeted by the host's neutralizing antibody response [13, 66, 127, 75, 120]. Thus, these proteins face selective pressure to evade the host immune response. Pressure from such antibodies often drives accumulation of mutations in these proteins. Indeed, possible signatures of antibody selection in LASV GP have been identified in naturally circulating strains in West Africa [5], and pressure from the host neutralizing antibody response also drives mutations to accumulate in HIV Env or influenza HA [66, 180]. Mutations that allow the virus to escape from antibody or serum neutralization have also been identified in SARS-CoV-2 spike [94, 55].

Tools to better understand how mutations to viral entry proteins from emerging viruses affect viral entry proteins' basic functions of receptor binding and/or membrane fusion are scientifically important for shedding light on these complex proteins. With the context that mutations to viral entry proteins can have important effects on host tropism and/or escape from the host immune response, understanding the effects of mutations to these proteins is especially important as it can directly inform our ability to effectively tackle emerging viral threats.

1.1.3 Challenges of studying viral entry proteins

Viral entry proteins are oligomeric, heavily glycosylated, and metastable proteins that are difficult to study even under ideal conditions [164, 124]. Some viral entry proteins such as influenza HA, HIV Env, and now SARS-CoV-2 spike have been highly studied, but others, including LASV GP or Ebola virus GP, have only just begun to be characterized in detail. Notably, prior to 2020, very little was known about coronavirus entry proteins and the first β-coronavirus spike structures—for the spikes from mouse hepatitis virus and the HKU1 human coronavirus—were solved only 5 years ago [158, 78]. Many emerging viruses have pandemic potential and, as we learned this past year, it is very difficult to predict what virus might cause the next pandemic [112]. Therefore, continued research of the viral entry proteins from emerging viruses is crucial.

Unfortunately, our ability to study viral entry proteins from many emerging viruses remains limited. Many emerging viruses must be studied under high biosafety conditions because they cause severe disease with high case fatality rates and limited treatment options [7]. This containment makes these viruses difficult to study. Thus, important questions about emerging viruses remain unanswered simply because many techniques, including many high-throughput assays, cannot be easily applied.

In the past year, the SARS-CoV-2 pandemic has challenged the scientific community to improve the speed and ease with which we study emerging viruses. The work described in Chapters 2 and 3 is one small part of the progress we have made to better understanding this emerging virus in a short time frame.

1.2 Introduction to pseudotyped lentiviral particles

One way to study viral entry proteins from viruses that are challenging to work with, either due to requiring high biosafety level containment or lacking an easily tractable reverse genetics system, is to ”pseudotype” them onto the surface of a non-replicative viral particle

[148, 173, 90, 34, 80]. The resulting viral particles rely on the heterologous, ”pseudotyped” viral entry protein for entry into host cells, thereby facilitating research into viral entry proteins from viruses that are difficult to work with in their native viral context. Importantly non-replicative viral particles can typically be studied under biosafety level 2 conditions that are commonly available in any laboratory with facilities for mammalian cell culture [2]. Therefore, a pseudotyped virus system greatly expands the scientific community's capacity to conduct experiments with viral entry proteins from most emerging viruses.

Lentiviral vectors derived from HIV-1 are commonly pseudotyped with viral entry proteins from other viruses [34, 80]. HIV was initially identified as a potential vector for heterologous pseudotyping following observations in the late 1980s that cells co-infected with HIV and another virus, such as VSV or herpes simplex virus, would produce progeny that packaged the HIV genetic material, but used the viral entry protein from the coinfecting virus to infect target cells [179]. Further studies determined that HIV-based viral particles could be produced that package the HIV genomic RNA with only a heterologous viral entry protein on their surface [114, 108]. Such lentiviral vectors were initially designed for their ability to transduce a wide variety of target cells, resulting in the stable expression of a gene of interest in infected cells [108]. For studies of viral entry, encoding a simple reporter gene expressing green fluorescent protein or luciferase on the lentiviral backbone provides an easy readout for identifying infected cells [34].

To make HIV-1-derived lentiviral vectors safe to use in biosafety level 2 facilities, they have been engineered to be non-replicative [108]. This has been accomplished by moving the genes required for lentiviral virion assembly onto separate plasmids and only encoding the sequences that are minimally necessary for RNA packaging on the lentiviral backbone plasmid [108, 44, 182, 181]. Co-transfecting 293T ”producer” cells with plasmids encoding Gag/Pol, Tat, or Rev, a lentiviral backbone plasmid expressing a reporter protein, and a plasmid encoding a heterologous viral entry protein, such as VSV G or SARS-CoV-2

spike, produces high titers non-replicative pseudotyped lentiviral particles that rely on the heterologous viral entry protein for entry [32]. These lentiviral particles can then be used for numerous downstream assays, typically at much higher throughput than would be possible if directly studying the virus from which the viral entry protein was derived.

1.2.1 Assays using pseudotyped lentiviral particles

Pseudotyped lentiviral particles were initially developed for use as gene therapy vectors since they transduce target cells resulting in stable expression of a gene-of-interest [34, 151]. Much of the research into pseudotyping lentiviral vectors with different viral entry proteins has therefore focused on trying to extend what cell types these vectors can transduce [34]. However, pseudotyped lentiviral particles are also very useful for studying the pseudotyping viral entry protein itself.

A pseudotyped lentiviral particle does not perfectly recapitulate all aspects of viral entry mediated by the pseudotyping viral entry protein. In particular, some cell types that the native virus can infect may not be infectable with a pseudotyped lentiviral particle due to restriction of the lentiviral processes required to express the reporter gene [114]. Nonetheless, pseudotyped lentiviral particles provide a tractable starting point for studying the cell tropism and function of the viral entry proteins from otherwise very challenging to study viruses [139]. Due to their ease of use and high titers, pseudotyped lentiviral vectors also provide a good starting point for high-throughput screens of the effects of mutations to viral entry proteins. Although the effects of mutations to viral entry proteins in a pseudotyped system may not perfectly recapitulate mutation effects in the native virus and vice versa, many mutations will likely have similar effects in both contexts. For instance, the D614G mutation to SARS-CoV-2 spike increases infectivity of both native SARS-CoV-2 and spike-pseudotyped lentiviral particles [81].

Since neutralizing antibodies typically target a virus's entry protein, pseudotyped lentivi-

ral particles have proven to be an easily accessible system for studying the neutralizing antibody response to viral entry proteins from emerging viruses [30, 110, 168, 79, 148, 151]. Such assays simply involve incubating pseudotyped lentiviral particles with antibodies or serum samples prior to infecting target cells and measuring how effectively such samples prevent infection of target cells (as measured by expression of the reporter gene) compared to ”no antibody/serum” control infections. Importantly, the measurement of neutralizing antibody titers using a pseudotyped lentiviral system has been shown to correlate well with neutralization of native virus for many viral entry proteins [167, 75]. One caveat in using pseudotyped lentiviral particles to measure serum neutralization is that individuals who are HIV+ may be taking anti-retroviral drugs that will inhibit viral entry independent of antibody activity targeting the viral entry protein. Nonetheless, pseudotyped lentivirus particles have proven very useful for developing easily accessible assays to measure the neutralizing antibody response to many emerging viruses [151].

1.3 SARS-CoV-2

SARS-CoV-2 was first identified in late 2019 [178, 177, 170] and has led to an ongoing global pandemic. Infection with SARS-CoV-2 causes COVID-19, which ranges in severity from an asymptomatic infection to a severe illness requiring hospitalization and potentially resulting in death [71]. COVID-19 has caused $>$3.3 million deaths since its identification less than 18 months ago [50]. Clearly, the human toll of this pandemic has been immense.

1.3.1 Brief introduction to SARS-CoV-2 biology

SARS-CoV-2 is a β-coronavirus of the *sarbecovirus* subgenus [154]. Coronaviruses are single-stranded positive-sense RNA viruses with the largest genomes of known RNA viruses [154]. The majority of the coronavirus genome is comprised of two open reading frames (ORFs) called ORF1a and ORF1b that produce the numerous non-structural

proteins that make up the viral replication and transcription complexes [154]. These open reading frames are translated immediately upon virus entry into a host cell and the resulting proteins then begin transcribing negative sense full-length and subgenomic RNAs. These negative sense RNAs then serve as templates for the generation of subgenomic mRNAs to produce the viral structural proteins (including spike) and new positive-sense genomic RNAs to package into progeny virions [154]. Progeny virions assemble in the host endoplasmic reticulum and bud into host secretory vesicles that are then released from host cells via exocytosis [154]. Several steps in the complex coronavirus lifecycle are currently being studied to improve our understanding of and treatment options for SARS-CoV-2, but my work has focused on SARS-CoV-2 entry mediated by the spike protein.

1.3.2 SARS-CoV-2 spike

SARS-CoV-2 spike is a class I fusion protein and it shares its main structural features with other coronavirus spikes [92]. Thanks in part to previous work that identified key mutations that could stabilize coronavirus spikes in their prefusion form [115], the SARS-CoV-2 prefusion spike structure was solved in February 2020, only about one month after the viral sequence was made publicly available [157, 166, 170].

Like other class I fusion proteins, spike is a homotrimeric glycoprotein that must be proteolytically cleaved to become fusogenic [92]. SARS-CoV-2 spike, and other closely related coronavirus spikes, must undergo two cleavage steps to fully prime for fusion [92]. One cleavage occurs at the S1/S2 boundary to separate spike into the S1 and S2 subunits and the other occurs at the S2' site in the S2 subunit to release the fusion peptide [154]. Unlike other *sarbecoviruses*, the cleavage site at the S1/S2 boundary in SARS-CoV-2 spike is a polybasic cleavage site that can be readily cleaved by furin proteases in the producing cell [154]. Following this cleavage the S1 and S2 subunits remain non-covalently linked until receptor binding triggers S1 shedding and subsequent

membrane fusion [154]. Notably, transmembrane serine protease 2 (TMPRSS2) has also been shown to be important for SARS-CoV-2 entry and plays an important role in the proteolytic processing of SARS-CoV-2 spike during natural infection [70].

The S1 subunit of SARS-CoV-2 spike contains the receptor binding domain (RBD) as well as an N-terminal domain (NTD), the function of which is currently uncertain. The RBD interacts directly with angiotensin converting enzyme 2 (ACE2), the receptor for SARS-CoV-2, to initiate the process of viral entry into host cells [70, 91].

The S2 domain contains the fusion peptide and fusion machinery [154, 92]. Following receptor binding and S1 shedding, the S2 domain undergoes several important structural rearrangements (briefly described in Section 1.1.1) to facilitate membrane fusion. The S2 domain is also more conserved between human coronaviruses than S1 and is a potential site of cross-reactive antibody binding [138].

In the past year, there has been intense scientific interest in SARS-CoV-2 spike. Research into the effects of mutations to SARS-CoV-2 spike has identified mutations that increase the infectivity or transmissibility of SARS-CoV-2 or allow spike to escape from infection- or vaccination-elicited antibodies [143, 81, 55, 56]. Additionally, research into the antibody response to spike has identified potential therapeutic antibodies, highlighted the main regions of spike important for antibody neutralization, and increased our understanding of the development of neutralizing antibodies following infection [1, 3, 155, 137, 9, 118]. An important component of much of this research has been the use of spike-pseudotyped viral particles.

Previous research on human coronaviruses had shown that pseudotyped lentiviral particles could be efficiently pseudotyped with coronavirus spike proteins [148, 58]. As such, following the publication of the SARS-CoV-2 genome sequence in early 2020, I began developing a pseudotyped lentiviral system to study SARS-CoV-2 spike. I initially applied this spike-pseudotyped lentiviral system to measuring neutralizing antibodies against SARS-

CoV-2 spike and this work is described in Chapters 2 and 3. Additionally, we shared the protocols and reagents for this assay widely, further facilitating research into SARS-CoV-2 spike.

1.4 Viral entry protein deep mutational scanning

One goal of developing a pseudotyped lentivirus system for SARS-CoV-2 spike was to develop a high-throughput, virus-based system for assessing the effects of mutations to spike. Since viruses, including SARS-CoV-2, evolve rapidly, prospectively characterizing the effects of mutations to viral entry proteins provides important and actionable insight into viral evolution and antibody escape. Deep mutational scanning allows for the high-throughput characterization of the effects of mutations to viral proteins. Briefly, deep mutational scanning of viral entry proteins uses high-throughput mutagenesis to create a mutant plasmid library containing all single amino-acid mutations to the viral entry protein of interest. Reverse genetics is then used to generate a mutant viral library from the plasmid library, where each virus expresses and encodes a single viral entry protein mutant. Growing these mutant viral libraries in cell culture selects for functional variants that can mediate infection [41, 61]. Infecting cells with these libraries in the presence of antibodies selects for those variants that can escape antibody neutralization. Deep sequencing the viruses that can infect cells under these conditions allows for the quantification of the functional and antigenic effects of mutations to a viral entry protein [42, 39].

The Bloom lab has pioneered the use of deep mutational scanning for studying viral evolution. The lab has used these methods to study influenza HA evolution and to characterize HIV Env antibody escape mutations [87, 37]. This past year, the lab developed a yeast-display system to use deep mutational scanning to study the SARS-CoV-2 RBD [143] However, current approaches are either completely removed from a viral system—as with SARS-CoV-2 RBD—or require that mutant viral entry protein libraries are

grown in the context of an otherwise wildtype virus—such as for influenza or HIV. Therefore, to measure the functional effects of mutations to a new viral entry protein a new reverse genetics and deep mutational scanning system would need to be set up. This is not only time-consuming, but infeasible for emerging viruses that lack efficient reverse genetics systems or must be studied under high containment.

Lentiviral particles can be pseudotyped with viral entry proteins from are a wide range of enveloped viruses, are genetically tractable, and can be grown to high titer in biosafety level 2 facilities [34]. Therefore, pseudotyped lentiviral particles provide a good starting point for building a general viral entry protein deep mutational scanning system that can be applied to SARS-CoV-2 spike, as well as the viral entry proteins from other emerging viruses, such as Lassa virus or Ebola virus. This system is still in development and current progress is discussed briefly in Chapter 5.

An additional benefit of the genetic tractability of a pseudotyped lentiviral system is the ability to link all mutations in a viral entry protein variant with a unique molecular barcode. Due to their compact genomes and commonly overlapping reading frames, it is often difficult to insert exogenous DNA sequences into a viral genome adjacent to the viral entry protein gene [47]. However, barcodes can easily be added following the viral entry protein variants in a lentiviral system. Long-read PacBio sequencing can then be used to link barcodes with all mutations in their associated variants and downstream selection experiments then only require short-read Illumina sequencing of the nucleotide barcodes to determine what variants are present [99].

Barcoding variants for viral entry protein deep mutational scanning is an important step forward in assessing the effects of multiple mutations on viral entry protein function and the role of epistasis in shaping viral entry protein evolution. However, parsing mutation and barcode information from long-read PacBio sequencing is non-trivial. The Python package described in Chapter 4 was written to facilitate this process of aligning long

sequencing reads to a known sequence and then extracting information about pre-defined features, such as a barcode or a viral entry protein gene. Although designed with the analysis of barcoded deep mutational scanning libraries in mind, this package is broadly applicable to any long-read sequencing data where the sequencing reads need to be aligned to a target sequence and features of interest parsed for additional analyses.

Although a generalizable viral entry protein deep mutational scanning system is not yet fully operational, the work discussed in the following chapters describes important progress towards that goal. My dissertation work has helped establish a pseudotyped lentivirus system in the Bloom lab, demonstrated such a system's utility for studying viral entry proteins from emerging viruses, and helped develop computational tools for long-read sequencing data. In sum, this work establishes important groundwork for using pseudotyped lentiviral particles to conduct deep mutational scanning of viral entry proteins from emerging viruses.

Chapter 2

PROTOCOL AND REAGENTS FOR PSEUDOTYPING LENTIVIRAL PARTICLES WITH SARS-COV-2 SPIKE PROTEIN AND THEIR USES

A version of this chapter has been previously published as:

Crawford KHD, Eguia R, Dingens AS, Loes AN, Malone KD, et al. Protocol and Reagents for Pseudotyping Lentiviral Particles with SARS-CoV-2 Spike Protein for Neutralization Assays. Viruses. 2020 May 6;12(5):513. doi: 10.3390/v12050513.

This chapter contains updates and improvements to the original protocol and system. These updates have also been included in a version of this protocol on protocols.io entitled "Pseudotyping lentiviral particles with SARS-CoV-2 Spike protein for neutralization assays V.2". This protocol is available at the doi: 10.17504/protocols.io.br44m8yw

The **Applications** section (Section 2.7) at the end of this chapter includes several vignettes where the assays introduced in this chapter were used for additional research into SARS-CoV-2 spike. These vignettes were originally published as parts of the following manuscripts:

Dingens AS, Crawford KHD, Adler A, Steele SL, Lacombe K, et al. Serological identification of SARS-CoV-2 infections among children visiting a hospital during the initial Seattle outbreak. Nat Commun. 2020 Sep 1;11(1):4378. doi: 10.1038/s41467-020-18178-1.

Addetia A, Crawford KHD, Dingens A, Zhu H, Roychoudhury P, Huang ML, Jerome

KR, Bloom JD, Greninger AL. Neutralizing antibodies correlate with protection from SARS-CoV-2 in humans during a fishery vessel outbreak with high attack rate. J Clin Microbiol. 2020 Aug 21:02107-20. doi:10.1128/JCM.02107-20.

Hodcroft EB, Zuber M, Nadeau S, Vaugh TG, Crawford KHD, et al. Spread of a SARS-CoV-2 variant through Europe in the summer of 2020. Nature. 2021. doi:10.1038/s41586-021-03677-y

Ellis D, Brunette N, Crawford KHD, Walls AC, Pham MN, et al. Stabilization of the SARS-CoV-2 S receptor binding domain by deep mutational scanning and structure-based design. bioRxiv. 2021. doi:10.1101/2021.05.15.444222

2.1 Abstract

SARS-CoV-2 enters cells using its spike protein, which is also the main target of neutralizing antibodies. Therefore, assays to measure how antibodies and sera affect spike-mediated viral infection are important for studying immunity. Because SARS-CoV-2 is a biosafety-level-3 virus, one way to simplify such assays is to pseudotype biosafety-level-2 viral particles with spike. Such pseudotyping has now been described for single-cycle lentiviral, retroviral, and vesicular stomatitis virus (VSV) particles, but the reagents and protocols were not widely available. Here, we detailed how to effectively pseudotype lentiviral particles with SARS-CoV-2 spike and infect 293T cells engineered to express the SARS-CoV-2 receptor, ACE2. We also made all the key experimental reagents available in the BEI Resources repository of ATCC and the NIH. Furthermore, we demonstrated how these pseudotyped lentiviral particles could be used to measure the neutralizing activity of human sera or plasma against SARS-CoV-2 in convenient luciferase-based assays, thereby providing a valuable complement to ELISA-based methods that measure antibody binding rather than neutralization.

2.2 Introduction

Infection with SARS-CoV-2 elicits antibodies that bind to the virus [75, 77, 176, 169, 95, 111]. However, as is the case for all viruses [13, 119, 66, 59], only some of these antibodies neutralize the virus's ability to enter cells [169, 95, 97, 120]. Whereas studies of immunity to SARS-CoV-2 are limited, for many other viruses, neutralizing antibodies are more strongly correlated with protection against reinfection or disease than antibodies that bind but do not neutralize [13, 119, 66, 59, 150, 28, 18]. Indeed, for other coronaviruses, neutralizing antibodies are protective in mouse models of infection [29, 102, 128, 145, 76] and associated with at least some reduced susceptibility to re-infection or disease in humans [18, 17, 123]. Furthermore, anecdotal reports have suggested that the passive transfer of neutralizing antibodies to sick patients may help alleviate disease from SARS-CoV-2 and its close relative, SARS-CoV [141, 23, 43].

However, while there are now well-characterized and high-throughput methods (such as ELISA assays) to measure total antibody binding to SARS-CoV-2 or some of its key constituent proteins [77, 111, 3], quantifying neutralizing antibody activity is more difficult. The most biologically relevant method is to directly measure how antibodies or sera inhibit infection of cells by replication-competent SARS-CoV-2. Such live-virus assays have now been performed to quantify neutralizing activity in the sera of infected patients or characterize the potency of individual antibodies [75, 111, 120, 22]. However, the throughput and accessibility of live-virus neutralization assays with SARS-CoV-2 is limited by the fact that the virus is a biosafety-level-3 agent that must be worked with in specialized facilities.

An alternative approach that alleviates these biosafety limitations leverages the fact that all known neutralizing antibodies to SARS-CoV-2 (and other coronaviruses that lack a hemagglutinin-esterase protein) target the virus's spike protein [75, 120, 22]. Spike protrudes prominently from the surface of SARS-CoV-2 virions, and is necessary and sufficient to enable the virus to bind and enter cells [157]. Spike from several coronaviruses

can be “pseudotyped” onto safer nonreplicative viral particles in place of their endogenous entry protein, thereby making entry of these particles into cells dependent on spike [91, 52, 148, 19, 173, 58, 90, 103]. For SARS-CoV-2, such pseudotyping has recently been reported using HIV-based lentiviral particles [169, 22, 113], MLV-based retroviral particles [120, 122], and VSV [91, 172, 109, 70]. In the data reported to date, results from such pseudovirus neutralization assays have correlated well with measurements made using live SARS-CoV-2 [75, 120, 22, 172]. However, the detailed protocols and reagents to perform such assays are not yet widely available to the scientific community.

Here, we filled this gap by providing a detailed description of how to pseudotype lentiviral particles with spike. We explained how these pseudotyped particles could be used to conveniently measure spike-mediated cell entry via fluorescent or luciferase reporters, and to quantify the neutralizing activity of human plasma. Finally, we described all the necessary experimental reagents and make them available in the BEI Resources reagent repository (`https://www.beiresources.org/`).

2.3 Results

2.3.1 General Approach for Pseudotyping Lentiviral Particles with SARS-CoV-2 Spike

The basic strategy for pseudotyping HIV-1-derived lentiviral particles is shown in Figure 2.1A. It involves transfecting 293T cells with a lentiviral backbone plasmid encoding a fluorescent or luminescent reporter protein, a plasmid expressing spike, and plasmids expressing the minimal set of lentiviral proteins necessary to assemble viral particles. The transfected cells then produce Spike-pseudotyped lentiviral particles that can be used to infect permissive cells that express the SARS-CoV-2 receptor protein, ACE2 [157, 91, 70, 166].

We used an HIV-based lentiviral system to produce viral particles pseudotyped with spike. As shown in Figure 2.1A, this system requires co-transfecting cells with a lentivi-

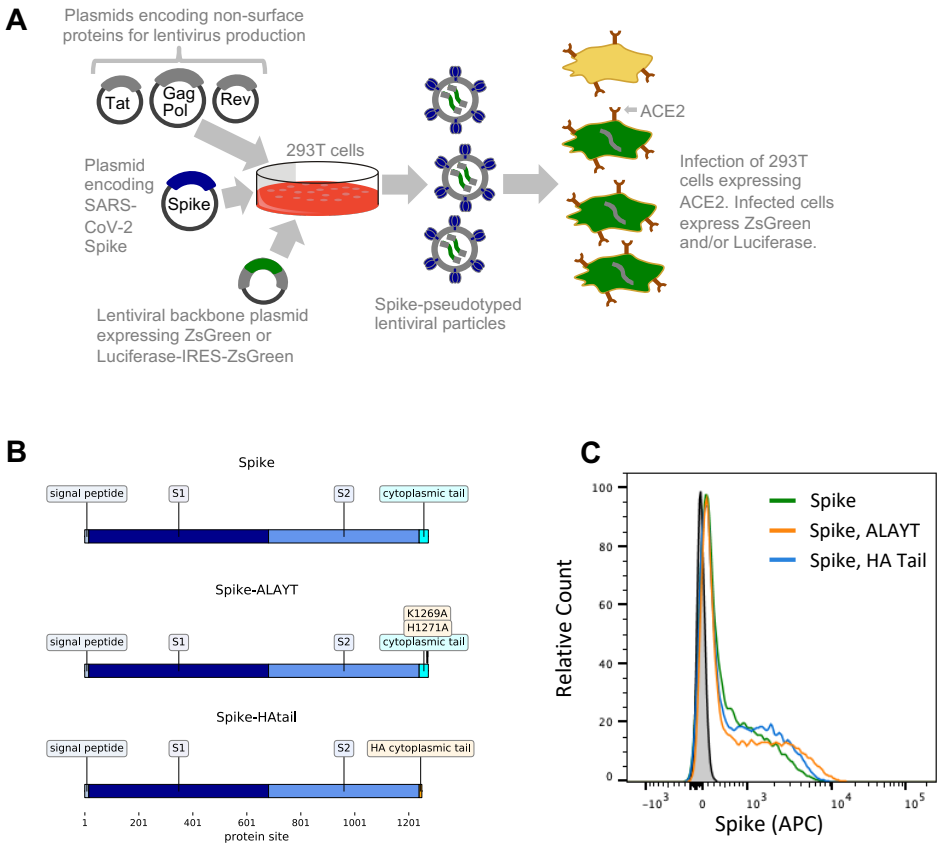

Figure 2.1: **General approach for lentiviral pseudotyping. (A)** 293T cells are transfected with a plasmid encoding a lentiviral backbone (genome) expressing a marker protein, a plasmid expressing spike, and plasmids expressing the other HIV proteins needed for virion formation (Tat, Gag-Pol, and Rev). The transfected cells produce lentiviral particles with spike on their surface. These viral particles can infect cells that express the ACE2 receptor. **(B)** We used three variants of spike: The codon-optimized spike from SARS-CoV-2 strain Wuhan-Hu-1, a variant containing mutations K1269A and H1271A in the cytoplasmic tail (such that the C-terminal five amino acids are ALAYT), and a variant in which the cytoplasmic tail of spike has been replaced with that from influenza hemagglutinin (HA). **(C)** Spike expression on the surface of 293T cells transfected with the plasmids expressing our three spike constructs was measured using flow cytometry 24 h post-transfection. Spike expression was measured by staining with in-house produced CR3022 antibody [149, 175, 74] at a concentration of 10 μg/mL followed by staining with an anti-human Fc antibody conjugated to APC (Jackson Labs, 109-135-098) at a 1:100 dilution.

ral backbone encoding the reporter protein(s), a plasmid expessing spike, and plasmids encoding the other HIV proteins necessary for virion formation (Tat, Gag-Pol, and Rev). We used two different lentiviral backbones: One that used a CMV promoter to drive expression of just ZsGreen, and another that used a CMV promoter to drive expression of luciferase followed by an internal ribosome entry site (IRES) and ZsGreen (hereafter referred to as the ZsGreen and Luciferase-IRES-ZsGreen backbones).

The spike protein was from SARS-CoV-2 strain Wuhan-Hu-1 using the NCBI-annotated start site [170], with the nucleotide sequence codon optimized for expression in human cells. We initially used three variants of spike (Figure 2.1B). The first variant was simply the codon-optimized spike. The second variant had two amino acid mutations to basic residues in spike's cytoplasmic tail (K1269A and H1271A) that changed the sequence of the five most C-terminal residues to ALAYT. This variant is hereafter referred to as spike-ALAYT. The rationale for spike-ALAYT was that for the original SARS-CoV, the two analagous mutations were shown to improve plasma membrane expression of Spike by eliminating an endoplasmic reticulum retention signal [101, 132]. The third variant had the cytoplasmic tail of spike replaced with that from influenza hemagglutinin (HA). This variant is hereafter referred to as spike-HAtail. The rationale for spike-HAtail was that for the original SARS-CoV, deleting spike's cytoplasmic tail or replacing it with that from other viruses was shown to improve pseudotyping efficiency [52, 54, 136, 105]. We validated that there was expression of spike on the surface of 293T cells transfected with plasmids expressing each of these three variants (Figure 2.1C).

Following initial studies with full-length spike, spike-ALAYT, and spike-HAtail, additional data accumulated that indicated simply deleting the spike cytoplasmic tail improves the titers of spike-pseudotyped viral particles [135, 36, 129]. Given these additional data, we decided to test the effects of deleting the cytomplasmic tail from spike in our pseudotyped lentivirus system. Other groups have tested deleting the last 18, 19, or 21 amino acids of

Spike in VSV-[36, 20, 159], MLV-[129], or HIV-based[113, 24] pseudotyped virus systems. We chose to test the 18 and 21 amino acid truncations, hereafter referred to as spike-$\triangle$18 and spike-$\triangle$21.

The sequences of all of the spike and lentiviral plasmids are available on GitHub at `https://github.com/jbloomlab/SARS-CoV-2_lentiviral_pseudotype/tree/master/plasmid_maps`, and the plasmids are available from BEI Resources (see Materials and Methods for BEI catalog numbers). Although not used in this study, the available plasmids also include a spike expression plasmid (BEI NR-53765) with the final 21 amino acids of spike deleted and the D614G mutation that is now the dominant sequence and has been shown to increase titers of spike-pseudotyped viruses [81].

2.3.2 Target 293T Cells Constitutively Expressing Spike's ACE2 Receptor

To create a target cell line that is efficiently infected by the SARS-CoV-2 spike-pseudotyped lentiviral particles, we transduced 293T cells with a lentiviral vector expressing human ACE2 under an EF1a promoter (lentiviral backbone plasmid is available from BEI Resources as item NR-52512). To create a clonal cell line from the bulk transduction, we sorted single transduced cells by flow cytometry and re-expanded into large populations (note that there was not a selectable marker in these cells). We identified an expanded clone that expressed high levels of ACE2 (Figure 2.2A). This ACE2 expression appears stable overtime and has not noticeably decreased through 12 passages at the time of writing. This clone is hereafter referred to as 293T-ACE2 and is available from BEI Resources as item NR-52511.

We validated that the 293T-ACE2 cells were susceptible to infection by SARS-CoV-2 spike-pseudotyped lentiviral particles by incubating 293T-ACE2 and parental 293T with equivalent amounts of viral particles carrying ZsGreen. As shown in Figure 2.2B, all Spike-pseudotyped viruses could infect the 293T-ACE2 but not the 293T cells. Virus

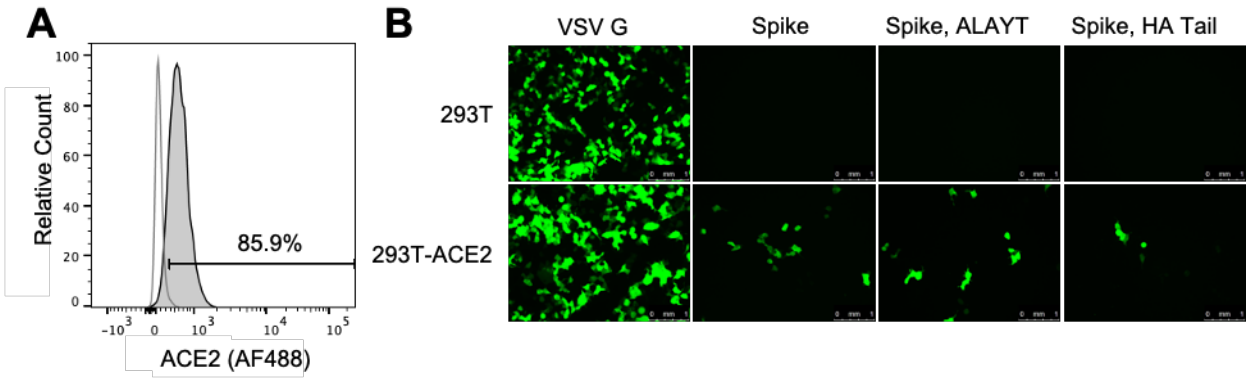

Figure 2.2: **293T-ACE2 cells are infectable with SARS-CoV-2 Spike-pseudotyped lentiviral particles**. **(A)** Flow cytometry plot showing expression of human ACE2 by the 293T-ACE2 cells (grey shaded) at passage 12 compared to parental 293T cells (white fill) as quantified by staining with an anti-ACE2 antibody (see Section 2.5.2) for detailed methods). The gate was set so the parental 293T cells were 2% positive. **(B)** Microscope images showing ZsGreen expression in 293T-ACE2 or 293T cells at 58 h after incubation with spike- or VSV G-pseudotyped lentiviral particles with the ZsGreen backbone. For each viral entry protein, 293T and 293T-ACE2 cells were incubated with equal volumes of virus. Cells were incubated with 1/20th the volume of VSV G-pseudotyped lentivirus compared to spike-pseudotyped lentivirus. The decrease in infected cells for the spike-HAtail virus compared to the other spike-pseudotyped lentiviruses is consistent with this virus having somewhat lower titers (see Figure 2.3A).

pseudotyped with VSV G, an amphotropic viral entry protein that is not dependent on ACE2, efficiently infected both cell lines (Figure 2.2B).

2.3.3 Titers of Pseudotyped Lentiviral Particles with Different Spike Cytoplasmic Tail Variants

To quantify the titers of lentiviral particles pseudotyped with each of the spike variants, we produced particles with each of these spikes, as well as a positive control using VSV G and a negative control without a viral entry protein. We first produced viral particles using the ZsGreen backbone, and titered by flow cytometry to determine the number of

transducing particles per ml. As shown in Figure 2.3A, the full-length, spike-ALAYT, and spike-HAtail spikes produced titers $\approx 10^4$ transduction units per mL. These titers were about two orders of magnitude lower than those achieved with VSV G, but we considered them to be encouragingly high given that lentiviral particles can be further concentrated by a variety of methods [73, 33]. Furthermore, we found that pseudotyped lentiviral particles pseudotyped with spike-$\Delta 18$ or spike-$\Delta 21$ yielded titers almost 10-fold higher than full-length spike, providing an even more promising construct for spike-pseudotyping (Figure 2.4A).

We then produced viral particles using the Luciferase-IRES-ZsGreen backbone and found that we could achieve titers of $>10^6$ relative luciferase units (RLUs) per mL in 96-well plate infections for the full-length, spike-ALAYT, and spike-HAtail spikes (Figure 2.3B). The truncated spikes produced lentiviral particles with $>$10-fold higher RLU-based titers (Figure 2.4B). Spike-pseudotyped lentiviral titers remained about one to two orders of magnitude lower than those achieved using VSV G. As expected, the magnitude of the fluorescent signal from ZsGreen was lower for the Luciferase-IRES-ZsGreen backbone than for the ZsGreen-only backbone (Figure 2.3C), since the ZsGreen in the former construct was driven by an IRES rather than the primary promoter.

2.3.4 Neutralization Assays with Spike-Pseudotyped Lentiviral Particles

We next used the Luciferase-IRES-ZsGreen viruses to perform neutralization assays in 96-well plates. Because $<10^5$ RLUs per well of a 96-well plate are necessary to achieve a signal $>$1000-fold above the background luciferase activity of virus-only controls, this assay required only a relatively modest volume of virus for a full 96-well plate neutralization assay.

We performed neutralization assays using plasma from a confirmed SARS-CoV-2-infected patient collected at 19 days post symptom onset, and with soluble ACE2 protein

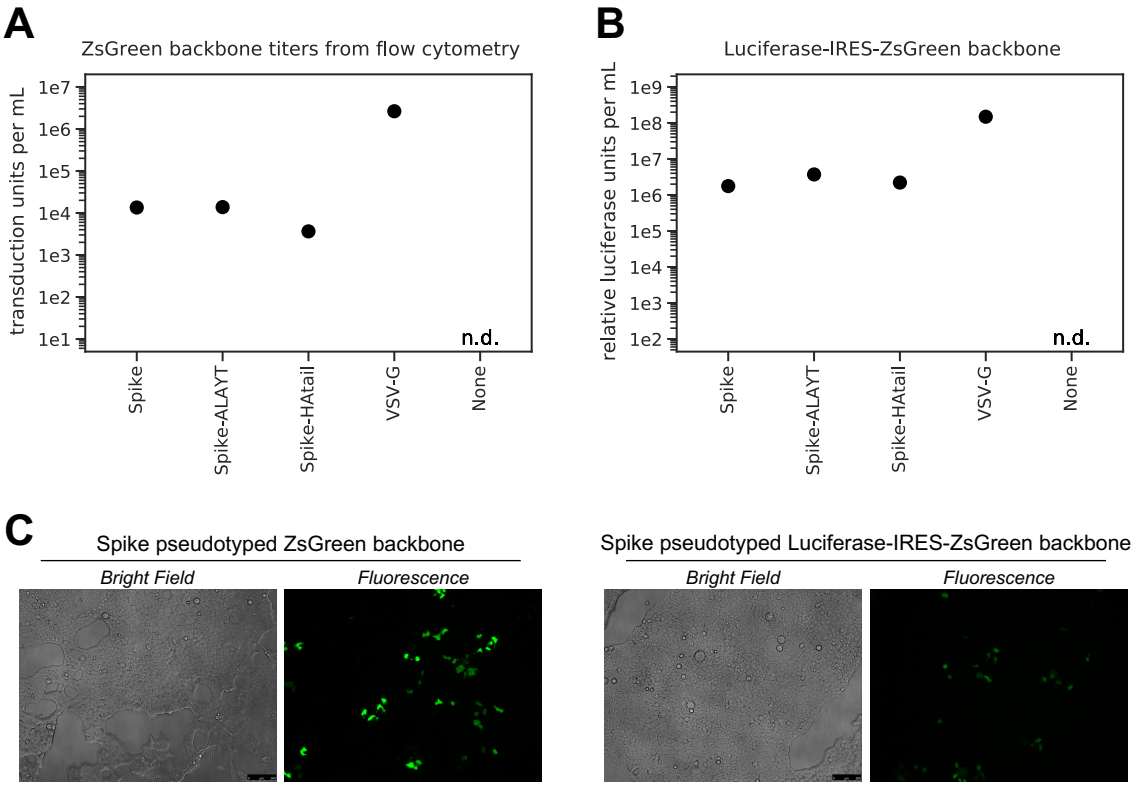

Figure 2.3: **Titers of spike-pseudotyped lentiviral particles in 293T-ACE2 cells. (A)** Titers of the ZsGreen backbone pseudotyped with the three Spike variants or VSV G, as determined by counting green cells via flow cytometry analysis at 48 h post-infection and then calculating transduction-competent viral particles per mL from the percentage of green cells. The "n.d." indicates that the titer was not detectable. Data shown are from a single representative example. **(B)** Titers of the Luciferase-IRES-ZsGreen backbone as determined by measuring relative luciferase units (RLUs). RLUs were determined at 48 h after infecting 2.3×10^4 293T-ACE2 cells per well in 96-well plates. The RLUs per mL for the Spike-pseudotyped viruses are the average of three three-fold serial dilutions of virus starting at 50 μL virus in a total volume of 150 μL. For the VSV G-pseudotyped virus, RLUs per mL were averaged from two three-fold dilutions starting at 3 μL virus in a total volume of 150 μL. **(C)** Microscope images showing 293T-ACE2 cells transduced with Spike pseudotyped virus with either the ZsGreen or Luciferase-IRES-ZsGreen backbone at 60 h post-infection. As can be seen from the images, the ZsGreen backbone gave a stronger fluorescent signal than the Luciferase-IRES-ZsGreen backbone, presumably because this protein was expressed more strongly as the sole CMV-promoter driven transcript than as the second transcript driven by an IRES.

Figure 2.4: **Titers of truncated spike-pseudotyped lentiviral particles in 293T-ACE2 cells (BEI Resources, NR-52511) (A, B) and neutralization of these viruses with serum from an individual previously infected with SARS-CoV-2 (C)**. **(A)** Titers of pseudotyped lentivirus with a ZsGreen backbone (BEI, NR-52520) pseudotyped with full-length spike (BEI, NR-52514), spike with either the last 18 ($\triangle$18) or 21 ($\triangle$21) amino acids truncated, VSV G, or no viral entry protein. Titers were determined as described in Section 2.5. Positive cells were counted via flow cytometry at 60 h post-infection. The "n.d." indicates that the titer was not detectable. Data shown are from a single representative example. **(B)** Titers of Luciferase-IRES-ZsGreen backbone virus pseudotyped with the specified viral entry proteins. Titers were determined by measuring relative luciferase units (RLUs) per mL and then normalizing to the titers of full-length spike pseudotyped lentivirus. RLUs were determined at 52 h post-infection. The RLUs per mL for the spike-pseudotyped viruses are the average of seven wells of a 1:3 dilution of virus in a total volume of 150 μL. For the VSV G-pseudotyped virus, RLUs per mL were averaged from six three-fold dilutions starting at a 1:48 dilution in a total volume of 150 μL. **(C)** Neutralization assay with serum collected from an individual previously infected with SARS-CoV-2, 43 days post symptom onset (p.s.o.). The full-length neutralization curve shows data averaged from duplicate measurements. The $\triangle$18 and $\triangle$21 neutralization curves display data from a single replicate. The IC50s for the full-length, $\triangle$18, and $\triangle$21 viruses are 1:345, 1:345, and 1:370, respectively. These values all fall within the range of IC50 values we have measured previously for this same serum sample with virus pseudotyped with full-length spike (1:320-1:375).

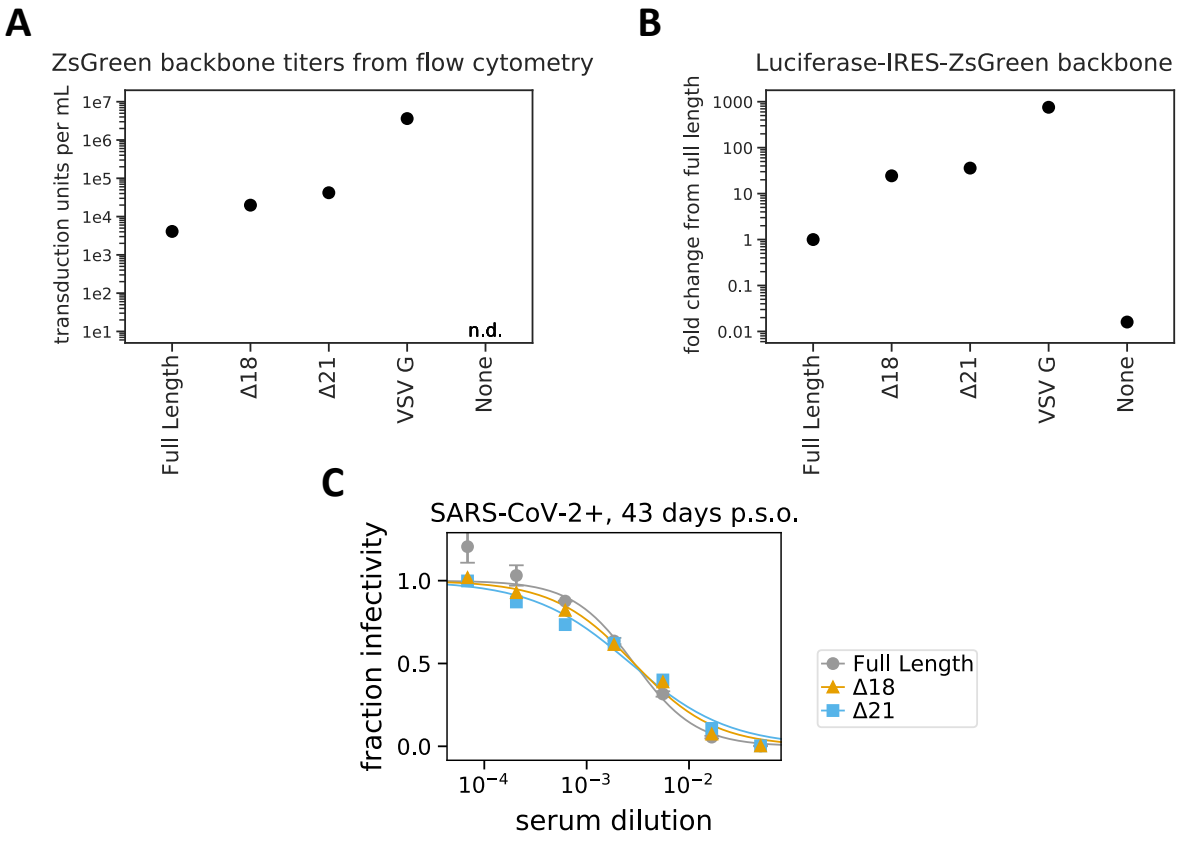
A
ZsGreen backbone titers from flow cytometry
transduction units per mL
1e7
1e6
1e5
1e4
1e3
1e2
1e1
n.d.
Full Length
Δ18
Δ21
VSV G
None
B
Luciferase-IRES-ZsGreen backbone
fold change from full length
1000
100
10
1
0.1
0.01
Full Length
Δ18
Δ21
VSV G
None
C
SARS-CoV-2+, 43 days p.s.o.
fraction infectivity
1.0
0.5
0.0
10−4
10−3
10−2
serum dilution
Full Length
Δ18
Δ21

fused to an IgG Fc domain (which neutralizes SARS-CoV-2 by acting as a decoy receptor [88]). As negative controls (not expected to neutralize), we used sera collected prior to the emergence of SARS-CoV-2 in late 2019. For these assays, we first made serial dilutions of the plasma, sera, or soluble ACE2-Fc in a 96-well plate. We then incubated these dilutions for 60 min with a volume of pseudotyped lentiviral particles sufficient to achieve 2×10^5 RLUs of luciferase signal per well. Finally, we added the mix to a pre-seeded plate of 293T-ACE2 cells. We measured the luciferase signal at 60 h post-infection (see Materials and Methods (Section 2.5) for a more detailed protocol).

Both the plasma from the confirmed SARS-CoV-2-infected patient and the soluble ACE2-Fc effectively neutralized the virus (Figure 2.5A,B). For the plasma, the inhibitory concentrations 50% (IC50s) were $\approx$1:1600 ($\pm$25%) for all three Spike variants, which is in the range of values that have been reported for sera and plasma from other SARS-CoV-2 patients at a similar time post-infection [169]. For soluble ACE2-Fc, the IC50 was $\approx$2 μg/mL with the spike and spike-ALAYT-pseudotyped lentiviral particles, but was notably lower for the spike-HAtail pseudotyped lentiviral particles (Figure 2.5B). Our measurement of $\approx$2 μg/mL for the unmodified Spike is higher than a previously reported IC50 of 0.1 μg/mL for soluble ACE2-IgG [88]. We suspect that the difference could be because our 293T-ACE2 target cells expressed high levels of ACE2, making them more resistant to neutralization by soluble ACE2. Additionally, following the initial publication of this protocol we became aware that the ACE2-Fc construct we were using was the macaque ACE2 sequence rather than the human ACE2 sequence due to a plasmid mixup. Since this ACE2 is clearly still neutralizing, this does not meaningfully change the interpretation of our results, but could potentially explain the difference in our calculated IC50 value compared to [88]. As expected, there was no neutralization of the pseudotyped virus by either pooled or individual human sera collected at dates prior to the emergence of SARS-CoV-2 (Figure 2.5C).

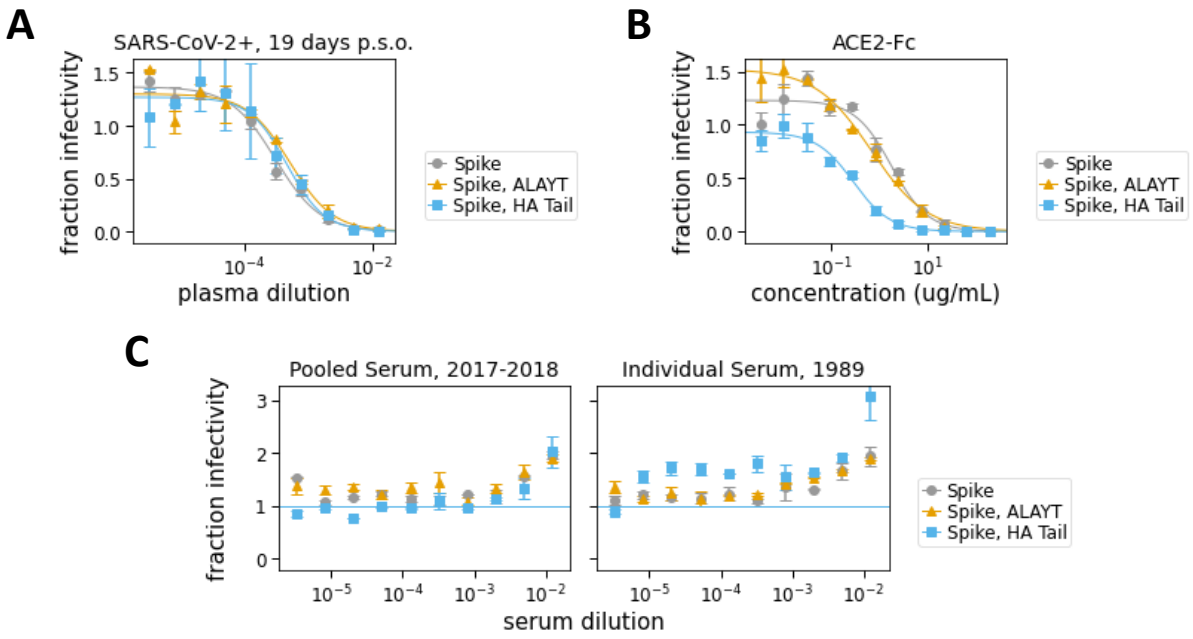

Figure 2.5: **Neutralization assays. (A)** Neutralization assay using plasma collected from a confirmed SARS-CoV-2-infected patient at 19 days post symptom onset ("p.s.o."). The IC50 for this plasma was 1:2076 for the spike-pseudotype, 1:1334 for the spike, ALAYT-pseudotype, and 1:1605 for the spike, HA tail-pseudotype. **(B)** Neutralization assay using soluble ACE2 protein fused to the Fc domain from IgG (ACE2-Fc). The IC50 for ACE2-Fc was 2.49 μg/mL for the spike-psdeudotype, 1.75 μg/mL for the spike, ALAYT-pseudotype, and 0.25 μg/mL for the spike, HA tail-pseudotype. **(C)** Negative control sera collected prior to the emergence of SARS-CoV-2 did not neutralize the spike-pseudotyped lentiviral particles. The serum from 1989 was from a person of a similar age at the time of serum collection as the confirmed SARS-CoV-2 infected patient whose plasma was tested in A. High concentrations of naïve serum seemed to enhance luciferase signal, perhaps because of components that improve cell-growth. Each point shows the average of duplicate values with error bars showing standard error.

Lentiviral particles pseudotyped with the truncated spikes (spike-$\triangle$18 and spike-$\triangle$21) were tested alongside full-length spike in a separate neutralization assay using a serum sample collected 43 days post symptom onset from another individual previously infected with SARS-CoV-2 (Figure 2.4C). The IC50s for full-length spike and the two truncated spikes were all $\approx$1:350, which are also within the range of IC50 values typical of individuals $\approx$1-month post symptom onset [31]. We did not test particles pseudotyped with the truncated spikes in neutralization assays using ACE2-Fc.

Our results indicate that some cytoplasmic tail modifications could potentially alter neutralization sensitivity. For the plasma/serum neutralization, all spike variants (spike, spike-ALAYT, spike-HAtail, spike-$\triangle$18, and spike-$\triangle$21) exhibited similar neutralization profiles (Figures 2.5A and 2.4C). However, for the soluble ACE2, the spike-HAtail virus was notably more neutralization sensitive than the other two spike variants tested (Figure 2.5B). Whereas the mechanism underlying the distinct neutralization sensitivity observed is unclear, it is possible that some modifications to the spike's cytoplasmic tail may alter opening of the receptor-binding domains [157]. Therefore, we recommend testing any potential spike modifications in neutralization assays prior to wide-spread use to ensure the modifications do not have unexpected antigenic effects. Nonetheless, due to the large increase in titer seen with the cytoplasmic tail deletions and the lack of any change in antigenicity in the serum neutralization assay, we recommend using the spike-$\triangle$21 construct in future studies.

2.4 Discussion

We described a detailed protocol for producing SARS-CoV-2 spike-pseudotyped lentiviral particles and performing neutralization assays. Although this basic pseudotyping approach has been described previously [169, 120, 22, 91, 113, 122, 172, 109, 70], we provided the first detailed protocol that made all reagents available in a public reposi-

tory (https://www.beiresources.org/). We hope this protocol and reagents will more easily enable others to assess the neutralizing activity of antibodies and sera reactive to SARS-CoV-2.

We also found that although our initial modifications to the cytoplasmic tail of SARS-CoV-2 spike (spike-ALAYT and spike-HAtail) did not greatly improve titers of spike-pseudotyped lentiviral particles, simply deleting the last 18 or 21 amino acids of spike increased titers $\approx$10-fold. Notably, one cytoplasmic tail modification we tested (spike-HAtail) potentially altered the neutralization sensitivity of the pseudotyped lentiviral particles, suggesting that it may be undesirable. Whereas we did not test the full suite of cytoplasmic tail modifications that have been used for pseudotyping with spike from the original SARS-CoV [52, 54, 136, 105], our results suggest that whiile many modifications to the cytoplasmic tail of the SARS-CoV-2 spike are compatible with pseudotyped lentivirus production, each modification should be tested for antigenic effects prior to routine use. Since our initial neutralization tests with the truncated spikes showed no alteration to neutralization sensitivity, but much higher titers compared to full-length spike, we recommend using a truncated spike in future studies and will move forward with spike-$\triangle$21 in our future work.

Overall, we have described an easily accessible assay to study neutralizing antibody responses to SARS-CoV-2 in a biosafety-level-2 laboratory. This assay allows human sera or plasma samples to be screened in a convenient 96-well format, which will help facilitate the testing of large numbers of patient samples to better understand the development of immunity and to potentially screen donors for passive transfer of convalescent plasma [43, 12].

2.5 Materials and Methods

2.5.1 Plasmids

The sequences of all plasmids used in this study are available in Genbank format at `https://github.com/jbloomlab/SARS-CoV-2_lentiviral_pseudotype/tree/master/plasmid_maps`. The plasmids themselves are available in BEI Resources (`https://www.beiresources.org/`) with the following catalog numbers:

- pHAGE2-EF1aInt-ACE2-WT (BEI catalog number NR52512): Lentiviral backbone plasmid expressing the human ACE2 gene (GenBank ID for human ACE2 is NM_021804) under an EF1a promoter with an intron to increase expression.

- pHAGE2-EF1aInt-ACE2-WT (BEI catalog number NR52512): Lentiviral backbone plasmid expressing the human ACE2 gene (GenBank ID for human ACE2 is NM_021804) under an EF1a promoter with an intron to increase expression.

- HDM-IDTSpike-fixK-HA-tail (BEI catalog number NR52513): Plasmid expressing under a CMV promoter the Spike from SARS-CoV-2 strain Wuhan-Hu-1 (Genbank NC_045512) codon-optimized using IDT, with the Spike cytoplasmic tail replaced by that from the HA protein of A/WSN/1933 (H1N1) influenza, and the Kozak sequence in the plasmid fixed compared to an earlier version of this plasmid.

- HDM-IDTSpike-fixK (BEI catalog number NR-52514): Plasmid expressing under a CMV promoter the Spike from SARS-CoV-2 strain Wuhan-Hu-1 (Genbank NC_045512) codon-optimized using IDT and the Kozak sequence in the plasmid fixed compared to an earlier version of this plasmid.

- HDM-nCoV-Spike-IDTopt-ALAYT (BEI catalog number NR-52515): plasmid expressing under a CMV promoter the Spike from SARS-CoV-2 strain Wuhan-Hu-1 (Gen-

bank NC_045512) codon-optimized using IDT, with the Spike containing two mutations in the cytoplasmic tail such that the last five amino acids are ALAYT.

- pHAGE-CMV-Luc2-IRES-ZsGreen-W (BEI catalog number NR-52516): Lentiviral backbone plasmid that uses a CMV promoter to express luciferase followed by an IRES and ZsGreen.

- HDM-Hgpm2 (BEI catalog number NR-52517): lentiviral helper plasmid expressing HIV Gag-Pol under a CMV promoter.

- HDM-tat1b (NR-52518): Lentiviral helper plasmid expressing HIV Tat under a CMV promoter.

- pRC-CMV-Rev1b (NR-52519): Lentiviral helper plasmid expressing HIV Rev under a CMV promoter.

- pHAGE2-CMV-ZsGreen-W (NR-52520): Lentiviral backbone plasmid that uses a CMV promoter to express ZsGreen.

- HDM-IDTSpike-delta21 (BEI catalog number NR-53742): Plasmid expressing under a CMV promoter the Spike from SARS-CoV-2 strain Wuhan-Hu-1 (Genbank NC_045512) codon-optimized using IDT with the last 21 amino acids deleted. The spike is also cloned into a slightly differentt 5' cloning site than HDM-IDTSpike-fixK to shift the spike coding sequence out of frame of upstream ATG sequences in the plasmid backbone.

Note that all of these plasmids have ampicillin resistance. The two plasmids used in this study that are not in the BEI Resources catalog are the HDM-VSV G plasmid and the HDM-IDTSpike-delta18 plasmids. The HDM-VSV G plasmid expresses VSV G under a

CMV promoter, and was used to create the positive control lentivirus pseudotyped with VSV G. However, numerous VSV G expressing plasmids are available from AddGene and other repositories. The HDM-IDTSpike-delta18 plasmid was not deposited in BEI Resources since we did not move forward with using it for future work.

Following completion of this work, we also made a spike plasmid with the 21 amino acid c-terminal deletion and the D614G mutation. This plasmid is available in BEI Resources as NR-53765 and is what we now recommend for spike-pseudotyped lentiviral assays due to the dominance of the D614G mutation and the high titers we achieve with this plasmid.

2.5.2 Creation of 293T ACE2 Cells

VSV G-pseudotyped lentivirus packaging the human ACE2 was generated via co-transfecting 293T cells (ATCC, CRL-3216) with the pHAGE2-EF1aInt-ACE2-WT plasmid and lentiviral helper plasmids (HDM-VSVG, HDM-Hgpm2, HDM-tat1b, and pRC-CMV-Rev1b). The resulting lentivirus was used to infect more 293T cells in the presence of 5 μg/mL polybrene. The transduced cells were stained with anti-human ACE-2 polyclonal goat IgG (AF933, R&D Systems, Minneapolis, MN, USA) primary antibody at 1 μg/mL and donkey anti-goat IgG conjugated to Alexa Fluor 488 (ab150129, Abcam, Cambridge, UK) secondary antibody at a 1:2500 dilution and sorted based on antibody staining. Once single cell clones had grown sufficiently, they were screened for ACE2 expression via flow cytometry and a clone with high expression was expanded and named 293T-ACE2 (Figure 2.2A). For verifying expression via flow cytometry, cells were harvested with enzyme-free dissociation buffer (13151014, ThermoFisher, Waltham, MA, USA) and stained with the anti-human ACE-2 polyclonal goat IgG primary antibody at 2 μg/mL and donkey anti-goat IgG (Alexa Fluor 488) secondary antibody at a 1:1000 dilution. For each staining step, cells were incubated with antibody in the dark at 4 ℃ for 30 min. Cells were washed three times with

3% BSA in PBS following each stain.

The 293T-ACE2 cells can be grown in D10 growth media (DMEM with 10% heat-inactivated FBS, 2 mM l-glutamine, 100 U/mL penicillin, and 100 μg/mL streptomycin) at 37℃ and 5% carbon dioxide. Note that there was not a selectable marker for the ACE2 expression. We found that ACE2 expression remained stable overtime (Figure 2.2A), but if there is a concern about expression, ACE2 levels can be periodically re-confirmed via antibody staining and flow cytometry. The 293T-ACE2 cells are available from BEI Resources as catalog number NR-52511.

2.5.3 Detailed Protocol for Generation of Pseudotyped Lentiviral Particles

Pseudotyped lentiviruses can be generated by transfecting 293Ts as depicted in Figure 2.1A. We used the following protocol:

1. Seed 293T cells in D10 growth media (see Section 2.5.2 for media composition) so that they will be 50%–70% confluent the next day. For a six-well plate, this is 5 × 10^5 cells per well (2.5 × 10^5 cells per mL).

2. At 16-24 h after seeding, transfect the cells with the plasmids required for lentiviral production. We transfected using BioT (Bioland Scientific, Paramount, CA, USA) following the manufacturer's instructions and using the following plasmid mix per well of a six-well plate (plasmid amounts should be adjusted for larger plates):

    - 1 μg of lentiviral backbone–we used either the ZsGreen (NR-52520) or the Luciferase-IRES-ZsGreen (NR-52516) backbone
    - 0.22 μg each of plasmids HDM-Hgpm2 (NR-52517), pRC-CMV-Rev1b (NR-52519), and HDM-tat1b (NR-52518)

- 0.34 μg viral entry protein—either SARS-CoV-2 Spike (NR-52513, NR-52514, NR-52515, NR-53742, or NR-53765 (recommended)), VSV G (positive control), or transfection carrier DNA (E4881, Promega, Madison, WI, USA) as a negative control.

3. At 18 to 24 h post-transfection, change the media to fresh, pre-warmed D10.

4. At 60 h post transfection, collect virus by harvesting the supernatant from each well and filtering it through a 0.45 μm SFCA low protein-binding filter. Virus can be stored at 4℃ for immediate use or frozen at –80℃. The titers of Spike- and VSV G-pseudotyped lentiviruses were found to be unaffected by a single freeze-thaw cycle (data not shown). Nonetheless, we recommend freezing virus in small aliquots to avoid multiple freeze-thaw cycles. All titers presented here are from virus that was frozen at –80℃ prior to use and underwent a single freeze-thaw.

2.5.4 Detailed Protocol for Titering Pseudotyped Lentiviral Particles

To determine viral titers, we used either flow cytometry (for viruses packaging the ZsGreen backbone) or a luciferase assay (for viruses packaging the Luciferase-IRES-ZsGreen backbone). A detailed titering protocol is described below and differences between these two readouts are noted:

1. Coat a 96-well cell-culture plate with 25 μL poly-L-lysine per well (P4707, Millipore Sigma, Burlington, MA, USA) according to the manufacturer's protocol. Poly-L-lysine improves cell adherence and prevents cell disruption during infection. Pre-coated plates are also available (Greiner Bio-One 655930) and using a black-walled poly-L-lysine coated plate (Greiner Bio-One 655936) removes the need to transfer out of the tissue culture assay plate for the luciferase readout.

2. Seed a poly-l-lysine-coated 96-well plate with 1.25 × 10^4 293T-ACE2 cells per well in D10 media. Typically, we seed cells in a volume of 50 μL.

3. The next day (12–24 h post-seeding), if using a flow cytometry readout, count at least two wells of cells to determine the number of cells present at infection.

4. Prepare serial dilutions of the viruses to be titered in a final volume of 120 μL D10 growth media.

   (a) For ZsGreen virus, we started with a 1:5 dilution and made three 1:5 serial dilutions.

   (b) For Spike-pseudotyped Luciferase_IRES_ZsGreen virus, we started with undiluted virus and made three 1:3 dilutions. For VSV G-pseudotyped Luciferase_IRES_ZsGreen virus, we started with a 1:50 dilution.

5. Slowly add 100 μL of the virus dilutions to the pre-seeded cells (already in 50 μL of media) for a final infection volume of 150 μL.

6. Optional: Add polybrene (TR-1003-G, Sigma Aldrich, St. Louis, MO, USA) to a final concentration of 5 μg/mL. Polybrene is a polycation that helps facilitate lentiviral infection through minimizing charge-repulsion between the virus and cells [35]. However, we found this only minimally improved spike-pseudotyped lentiviral titers (data not shown) and now skip this step.

7. At 48–60 h post-infection, collect cells for analysis:

   (a) For flow cytometry:

      i. Look at the cells under a fluorescent microscope and select wells that appear $\approx$1%–10% positive. Harvest cells from these wells using trypsin and

transfer them to a V-bottom plate or microcentrifuge tubes. Pellet cells at 300×g for 4 min and wash twice with 3% BSA in PBS. After the final wash, resuspend in 1% BSA in PBS and analyze via flow cytometry. We used a Becton Dickinson Celesta cell analysis machine with a 530/30 filter to detect ZsGreen in the FITC channel. Resulting FCS files were analyzed using FlowJo (v10) (BD Life Sciences, Ashland, OR, USA).

ii. Calculate titers using the Poisson formula. If P is the percentage of cells that are ZsGreen positive, then the titer per ml is:

$$\frac{-ln(1 - P/100) \times (number\ of\ cells\ per\ well)}{volume\ of\ virus\ per\ well\ in\ mL}$$

Note that when the percentage of cells that are ZsGreen positive is low, this formula is approximately equal to:

$$\frac{(\%\ ZsGreen\ positive/100) \times (number\ of\ cells\ per\ well)}{volume\ of\ virus\ per\ well\ in\ mL}$$

Furthermore, the titers using even the Poisson equation will only be accurate if the percentage of cells that are ZsGreen positive is relatively low (ideally 1–10%).

(b) For luciferase:

i. Thaw luciferase reagent at room temperature. We used the Bright-Glo Luciferase Assay System (E2610, Promega, Madison, WI, USA).

ii. Prepare cells by removing 100 μL media from each well. Accounting for evaporation, this leaves $\approx$30 μL of media in each well.

iii. Add 30 μL of luciferase reagent and mix well, avoiding bubbles. If not using a black-walled plate, transfer all $\approx$60 μL to a black-bottom plate (Costar 96-well solid black, 07-200-590, Fisher Scientific, Waltham, MA, USA). If using a black-walled plate, either continue on to the next step or, to minimize

background, add a black back-sticker (Fisher Scientific, NC9425162) to the bottom of the plate.

iv. Incubate plate for 2 min at room temperature in the dark, then measure luminescence using a plate reader. We used a Tecan Infinite M1000 Pro plate reader with no attenuation and a luminescence integration time of 1 s.

v. Plot RLUs vs. volume of virus added. Select an amount of virus for further assays where there is sufficient ($>$1000-fold) signal above virus-only background and a linear relationship between virus added and RLU. Typically, we aim for $\approx$2 x 10^5 RLUs per well.

2.5.5 Detailed Protocol for Neutralization Assays

The following protocol was developed to streamline neutralization assays with spike-pseudotyped lentiviral particles. This protocol can be performed with either human sera or plasma, or monoclonal antibodies. Note that for safety, sera or plasma should be heat-inactivated in a biosafety cabinet prior to use as described in Section 2.5.6.

1. Seed a black-walled poly-L-lysine-coated 96-well plate with 1.25 × 10^4 293T-ACE2 cells (BEI NR-52511) per well in 50 μL D10 (2.5 × 10^5 cells per mL). Plan to infect this plate 8–24 h post-seeding.

2. About 1.5 h prior to infecting cells, begin preparing serum and/or ACE2 dilutions in D10:

   (a) In a separate 96-well "setup" plate, serially dilute serum samples, leaving 60 μL diluted serum in each well. Remember that these samples will be diluted an additional 2x by the addition of virus. For the data in Figure 2.5A,C, we

started at a serum dilution of 1:80 (1:40 in the ”setup” plate) and did serial 2.5-fold dilutions, meaning each replicate of the assay required 5 μL of sera. For the data in 2.4C, we started at a serum dilution of 1:20 (1:10 in the ”setup” plate) and did serial 3-fold dilutions. For ACE2 (Figure 2.5B), we started with a concentration of 200 μg/mL and did serial three-fold dilutions.

(b) Add 60 μL of D10 to wells corresponding to virus only and virus plus cells control wells. Add 120 μL of D10 to media only and cells only control wells. See Figure 2.6 for example plate layouts.

3. Dilute virus to $\approx$2–4 × 10^6 RLU per mL. Add 60 μL of diluted virus to all wells containing serum dilutions and the virus only and virus plus cells control wells.

4. Incubate virus and serum at 37 ℃ for 1 h.

5. Carefully add 100 μL from each well of the setup plate containing the sera and virus dilutions to the corresponding wells of the plate of 293T-ACE2 cells.

6. Incubate at 37 ℃ for 48–60 h before reading out luminescence or fluorescence as described in Section 2.5.4.

7. Plot the data. For our analysis, we first subtracted out the background signal (average of the “virus only” and “virus + 293Ts” wells) and then calculated the “maximum infectivity” for each plate as the average signal from the wells without serum (“virus + cells” wells). We then calculated the “fraction infectivity” for each well, as the luciferase reading from each well divided by the “maximum infectivity” for that plate. If using layouts similar to those in 2.6, we recommend calculating the ”maximum infectivity” as the average of the two ”virus + cells” wells in each row (for Figure 2.6A) or column (for Figure 2.6B) and calculating ”fraction infectivty” for each well based

on its row or column's "maximum infectivity." For the curves shown in Figure 2.5 and Figure 2.4C, we then fit and plotted the fraction infectivity data using the neutcurve Python package (`https://jbloomlab.github.io/neutcurve/`). This package fits a three-parameter Hill curve, with the top baseline being a free parameter (Figure 2.5) or fixed to 1 (Figure 2.4C) and bottom baseline fixed to zero.

2.5.6 Human Plasma Sample and Soluble ACE2

The human plasma sample used in Figure 2.5A was collected at 19 days post symptom onset from a patient with a confirmed SARS-CoV-2 infection. The human serum sample used in Figure 2.4C was was collected at 43 days post symptom onset from a patient with a confirmed SARS-CoV-2 infection. Prior to use, these samples were heat-inactivated in a biosafety cabinet at 56 ℃ for one hour. This duration of heat treatment has been shown to be sufficient to inactivate SARS-CoV-2 [3, 25], which has also not been reported to be present at high titers in the blood [162, 40]. The negative control serum pools came from Gemini Biosciences, West Sacramento, CA, USA (Cat:100-110). The naïve serum pool collected in 2017–2018 is lot H86W03J. The age-matched negative control serum comes from serum residuals collected by Bloodworks Northwest. It was collected on 12/19/1989, stored at –80℃, and heat inactivated at 56℃ prior to use.

Soluble human ACE2 protein fused to the Fc region of human IgG1 was produced as described by the authors of [157]. This ACE2-Fc fusion protein was used in Figure 2.5B. Following the original publication of this manuscript, an error in the production of this ACE2-Fc was identified and it was determined that the ACE2-Fc used in this study was the macaque ACE2, not the human ACE2 sequence. This potentially contributed to differences in ACE2-Fc IC50 between our work and previously published data [88], but does not affect the utility of this assay for measuring SARS-CoV-2 neutralization.

A

Virus Only	Virus Only	Virus Only	Virus Only	Virus Only	Virus Only	Virus Only	Virus Only	Virus + 293Ts	Virus + 293Ts	Virus + 293Ts	Virus + 293Ts
Cells Only	Virus+Cells	Serum 1 – A	Serum 1 – B	Serum 2 – A	Serum 2 – B	Serum 3 – A	Serum 3 – B	Serum 4 – A	Serum 4 – B	Virus+Cells	Cells Only
Cells Only											Cells Only
Cells Only											NoVEP (60 uL)
Cells Only											NoVEP (60 uL)
Cells Only											NoVEP (60 uL)
Cells Only											Cells Only
Cells Only											Cells Only

B

Virus Only	Virus Only	Virus Only	Virus Only	Virus Only	Virus Only	Virus Only	Virus Only	Virus Only	Virus Only	Virus Only	Virus Only
Virus+Cells											
Serum 2 – B											
Serum 2 – A											
Serum 1 – B											
Serum 1 – A											
Virus+Cells											
Cells Only	Cells Only	Cells Only	Cells Only	Cells Only	Cells Only	Cells Only	Cells Only	Cells Only	Cells Only	Cells Only	Cells Only

Figure 2.6: **Example plate layouts for neutralization assays**. It is possible to run full-dilution series of 2-4 sera or plasma samples in duplicate on each plate with the necessary controls. These controls include cells only and virus-only wells. Additional controls include four wells of virus-infecting 293T cells to confirm the lack of infection with Spike-pseudotyped lentivirus in the absence of ACE2 and/or several wells of ”bald” lentiviral particles without a viral entry protein (labelled as ’NoVEP’). The average signal from the “Virus Only” and “Virus + 293Ts” wells provides the background signal. The “Virus + Cells” wells represent maximum infection without any serum and provide a metric for 100% virus infectivity. Note that “cells” here refers to the 293T-ACE2 cells. The different colors simply denote different conditions, such as different serum samples or cells. These conditions are labeled in the top two rows **(A)** or left-most column **(B)** of the layout (or in each individual cell for the “Virus + 293Ts” condition).

2.6 Acknowledgements

We thank Caelan Radford, Andrew McGuire, and Abigail Powell for helpful suggestions and feedback on assay development. We also thank Dr. David Koelle and Dr. Anna Wald at the University of Washington for sharing the serum sample used in Figure 2.4C with us.

2.6.1 Funding

This research was supported by the following grants from the NIAID of the NIH: R01AI141707 (to J.D.B.), F30AI149928 (to K.H.D.C.) and HHSN272201700059C (to D.V.). This study was also supported by the National Institute of General Medical Sciences (R01GM120553, D.V.), a Pew Biomedical Scholars Award (D.V.), and Investigators in the Pathogenesis of Infectious Disease Awards from the Burroughs Wellcome Fund (J.D.B. and D.V.). A.B.B. is supported by the National Institutes for Drug Abuse (NIDA) Avenir New Innovator Award DP2DA040254. J.D.B. is an Investigator of the Howard Hughes Medical Institute.

2.6.2 Conflicts of Interest

H.Y.C. is a consultant for Merck and Glaxo Smith Kline and receives research funding from Sanofi Pasteur. The other authors declare no conflicts of interest.

2.7 Applications

2.7.1 ***Children infected with SARS-CoV-2 produce neutralizing antibodies***

In the spring of 2020, Adam Dingens—a staff scientist in the Bloom lab—collaborated with Dr. Janet Englund from Seattle Children's Hospital to screen pediatric serum samples for serological evidence of previous SARS-CoV-2 infection [38]. Adam screened samples from 1,076 children collected in March and April 2020 for IgG antibodies that could bind

to SARS-CoV-2 spike or RBD using a previously published ELISA protocol and confirmed positive samples using the Abbott Architect assay that measures anti-nucleoprotein IgG antibodies [3, 16]. Individuals needed to test positive in both ELISAs and the Abbott Architext assay to be considered seropositive. Of the 1,076 children in the study, 8 were determined to be seropositive for antibodies that could bind to SARS-CoV-2 [38].

To assess the neutralizing antibody response in children seropositive for SARS-CoV-2, I used the neutralization assay described in this chapter to measure neutralizing antibodies in all seropositive children as well as several positive control samples from children and adults with known SARS-CoV-2 infections and negative control serum samples collected prior to 2019 Figure 2.7. All pediatric serum samples that were seropositive by both the ELISA and Abbott assays mounted detectable neutralizing antibody titers (reciprocal IC50 $>$25). None of the seropositive children with no positive PCR test had COVID-19 symptoms, so it was encouraging to find that they still mounted a neutralizing antibody response within the range seen for symptomatic adults 3-8 weeks post symptom onset. One child with a known COVID-19 diagnosis ('child 4 wks') mounted one of the most potently neutralizing antibody responses we have ever measured with a reciprocal IC50 of $>$18,000. More recent studies, led by Lauren Gentles in the Bloom lab in collaboration with Dr. Janet Englund and her team at Seattle Children's Hospital, have begun to investigate potential differences in the neutralizing antibody response between children and adults.

Acknowledgements

We are grateful to all study participants for contributing samples. We also thank Abigail Powell, Peter Rupert, and Roland Strong for sharing antigens, Elizabeth Ahearn for laboratory management at Seattle Children's Hospital, and Mike Famulare and Alex Greninger for helpful comments on this paper. This work was supported by the NI-

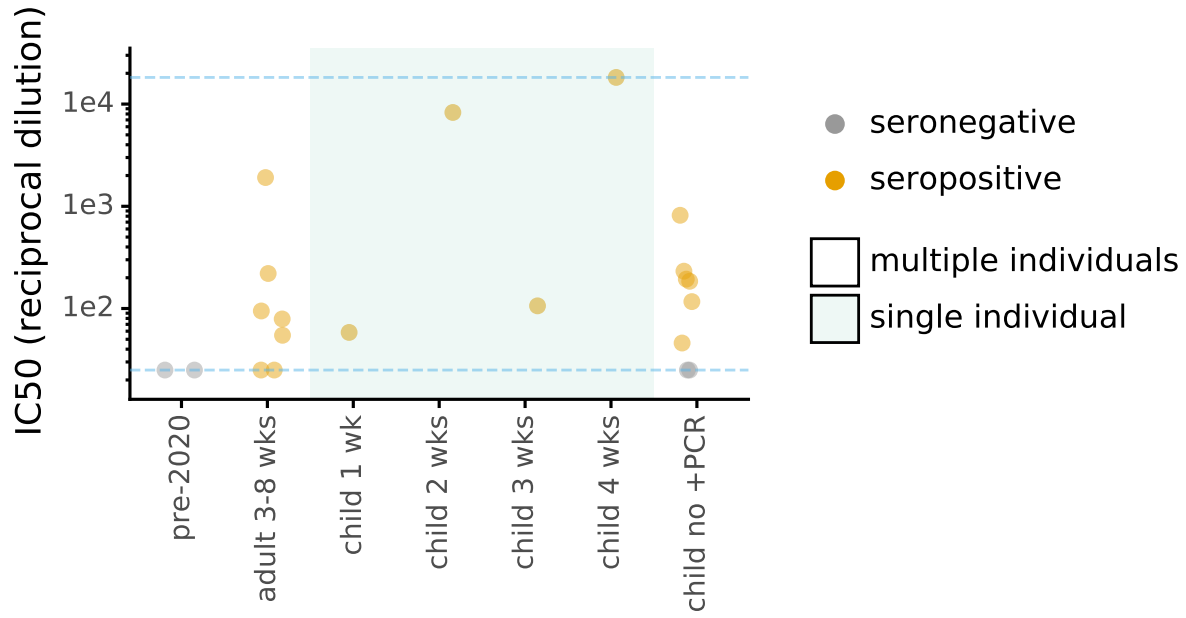

Figure 2.7: **Children seropositive for SARS-CoV-2 mount a neutralizing antibody response.** Serum samples from children with (shaded box) or without (far right) positive PCR tests for SARS-CoV-2 were measured alongside positive and negative control adult samples (left of shaded box) using the spike-pseudotyped lentivirus neutralization assay described above. The spike plasmid used in these assays encoded full-length spike without any cytoplasmic tail deletions or modifications. The duration of time between symptom onset and sample collection is indicated in the labels for individuals who tested positive for SARS-CoV-2 by PCR. The y-axis is the reciprocal dilution of serum that inhibits infection by 50% (IC50). The blue dashed lines indicate the limits of the dilution series with the lower bound being a dilution of 1:25 and the upper bound a dilution of 1:18,225. All seropositive children mounted a detectable neutralizing antibody response.

AID/NIH (R01AI141707 and R01AI140891 to J.D.B., HHSN272201700059C to D.V., and F30AI149928 to K.H.D.C.), the NIMGS/NIH (R01GM120553 to D.V.), the Bill & Melinda Gates Foundation (OPP1156262 to N.P.K.), a Pew Biomedical Scholars Award (to D.V.), and Burroughs Wellcome Investigators in the Pathogenesis of Infectious Diseases awards (to D.V. and J.D.B.). J.D.B. is an investigator of the Howard Hughes Medical Institute.

Work in the Krammer laboratory was partially supported by the NIAID Centers of Excellence for Influenza Research and Surveillance (CEIRS) contract HHSN272201400008C, Collaborative Influenza Vaccine Innovation Centers (CIVIC) contract 75N93019C00051, and philanthropic donations.

Competing Interests

H.Y.C. is a consultant for Merck and Glaxo Smith Kline and receives research funding from Sanofi Pasteur, outside of the submitted work. N.P.K. is a co-founder, shareholder, and chair of the scientific advisory board of Icosavax, Inc. Mount Sinai has licensed serological assays to commercial entities and has filed for patent protection for serological assays. J.A.E. is a consultant for Sanofi Pasteur and Meissa Vaccines. The remaining authors declare no competing interests.

2.7.2 ***Early evidence that SARS-CoV-2 neutralizing antibodies correlate with protection from infection***

Retrospective analyses of COVID-19 outbreaks can provide important insight into the spread of SARS-CoV-2. In early summer 2020, a fishing vessel that departed from Seattle, WA had an outbreak of SARS-CoV-2 with a high attack rate. Despite pre-departure screening, testing upon returning to shore found that 104 of the 122 individuals on board became infected with SARS-CoV-2 [1]. Pre-departure serological samples were available for 120 of the 122 people on the ship's manifest and these samples were further analyzed following identification of the outbreak. This analysis was originally done by Alex Greninger and his lab. Six individuals' pre-departure samples tested positive for IgG antibodies against SARS-CoV-2 nucleoprotein using the Abbott Architect assay. These samples were then shared with Adam Dingens and myself to run ELISAs and neutralization assays. Only three of the individuals with positive Abbott tests had measurable

neutralizing antibody titers at the time of their pre-departure screening Figure 2.8. Notably, the three individuals who did not have detectable neutralizing antibodies prior to departure also had markedly lower levels of anti-spike and anti-RBD binding antibodies by ELISA, perhaps indicating that these individuals had false positives in the initial serological screening [1].

Of the 120 individuals with pre-departure samples, 103 of them were infected in the subsequent outbreak on the fishing vessel—including the three individuals who had tested positive in the Abbott Architect assay, but did not have neutralizing antibodies Figure 2.8. None of the three individuals with detectable neutralizing antibody titers were infected with SARS-CoV-2 on the boat. The overall rate of infection was 0 out of 3 for individuals with neutralizing antibodies and 103 out of 117 for individuals without. These infection rates indicate a statistically significant (Fisher's exact test: $P = 0.002$) association between neutralizing antibodies and protection from infection with SARS-CoV-2.

Since the summer of 2020, data (especially from vaccine trials) have continued to indicate that neutralizing antibodies against SARS-CoV-2 correlate with protection from infection [8]. However, in the summer of 2020, the analysis of this shipping vessel outbreak was some of the earliest evidence that individuals with SARS-CoV-2-neutralizing antibodies were less likely to be infected with the virus. Although this correlation between neutralizing antibodies and protection from infection is expected, it nonetheless remains encouraging, especially as more individuals get vaccinated and begin mounting their own neutralizing antibody responses to SARS-CoV-2.

Acknowledgements

We thank Nicole Lieberman for helpful comments, Nathan Breit for data pulls, and Ann Jarris and Mark Wener for protocol development. We also thank Brooke Fiala, Samuel Wrenn, Deleah Pettie, and Neil P. King at the Institute for Protein Design for sharing

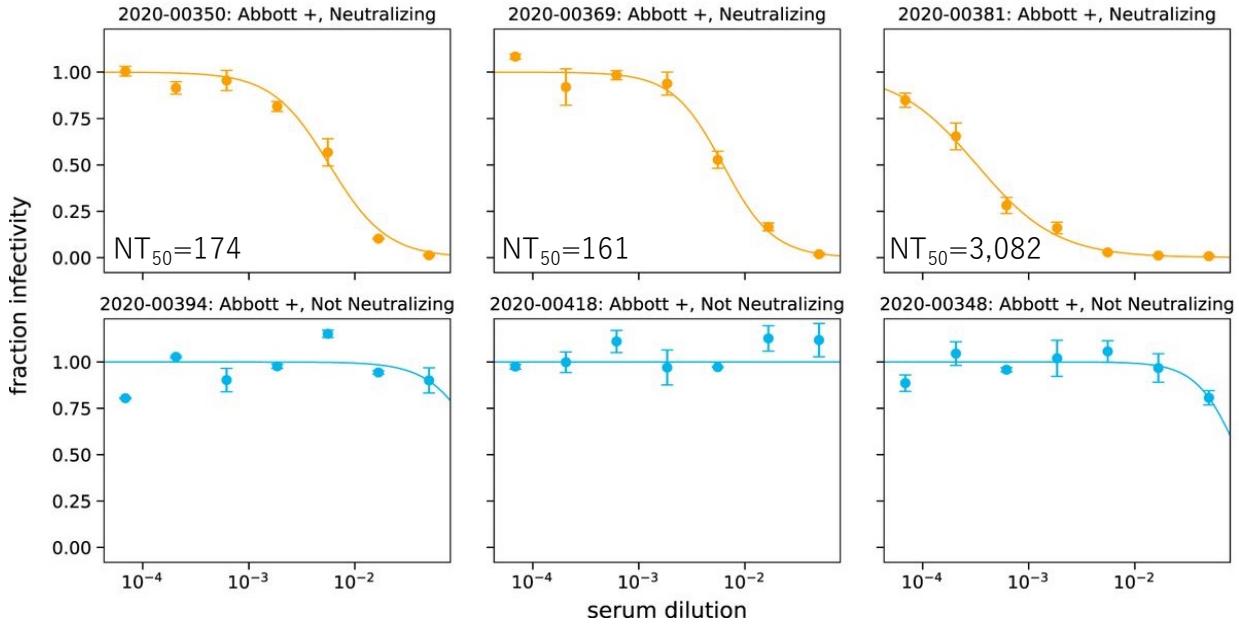

Figure 2.8: **SARS-CoV-2 neutralizing antibodies correlate with protection from infection** Pre-departure serum from all six individuals who tested positive for SARS-CoV-2 anti-nucleoprotein antibodies was tested for neutralizing antibodies using the SARS-CoV-2 spike-pseudotyped lentivirus neutralization assay described above (using full-length spike with no cytoplasmic tail modifications). None of the individuals with neutralizing antibodies (top row) were subsequently infected with SARS-CoV-2 during the outbreak on their fishing vessel. All three individuals without neutralizing antibodies (bottom row) were infected during the outbreak. The lower limit of the serum dilution series was a 1:20 dilution. For individuals with detectable neutralizing titers, the reciprocal of the serum dilution that neutralized infection by 50% (NT_{50}) is provided on the plot.

reagents for ELISA assays.

Work performed in the clinical laboratory was supported by the Department of Laboratory Medicine and Pathology. This research was supported by the following grants from the NIAID of the NIH: R01AI141707 (to J.D.B.) and F30AI149928 (to K.H.D.C.). J.D.B. is an Investigator of the Howard Hughes Medical Institute.

2.7.3 ***Assessing the impact of a circulating variant on SARS-CoV-2 spike-mediated entry***

During the summer of 2020, a SARS-CoV-2 variant rose in frequency in Europe and was identified by Emma Hodcroft and her collaborators [69]. This variant made up the 20E (EU1) cluster and included an A222V mutation in the N-terminal domain of spike, as well as the widely circulating D614G mutation. To test if the A222V mutation had an effect on spike-mediated viral entry, I pseudotyped lentiviral particles with spike with G at site 614 and either A or V at site 222. I then measured the ability of these viral particles to infect 293T-ACE2 cells [32]. I made two A222V D614G spike plasmids with different synonymous codons used to introduce the A222V mutation. I made all spike-pseudotyped viruses in at least biological triplicate and measured entry using two different lentiviral backbones and readouts (Figure 2.9. Titers of spike-pseudotyped lentiviral particles with both the A222V and D614G mutations were slightly ($\approx$1.3-fold) higher than titers with D614G alone, but the difference was not statistically significant 2.9.

A pseudotyped lentiviral system is not a perfect proxy for the effects of mutations to spike on infection in the human population, so it is possible that the A222V mutation may have a more notable effect on transmission in natural infections. However, in concordance with my pseudotyped lentiviral titer results, Emma and her team did not find any clear evidence that the A222V mutation was affecting viral transmission or infectivity. Instead, they found that most of the increased spread of the 20E (EU1) cluster could be explained by epidemiological factors, such as travel patterns between European countries in the summer of 2020.

Acknowledgements

We are grateful to researchers, clinicians, and public health authorities for making SARS-CoV-2 sequence data available in a timely manner. We also wish to thank the COVID-19

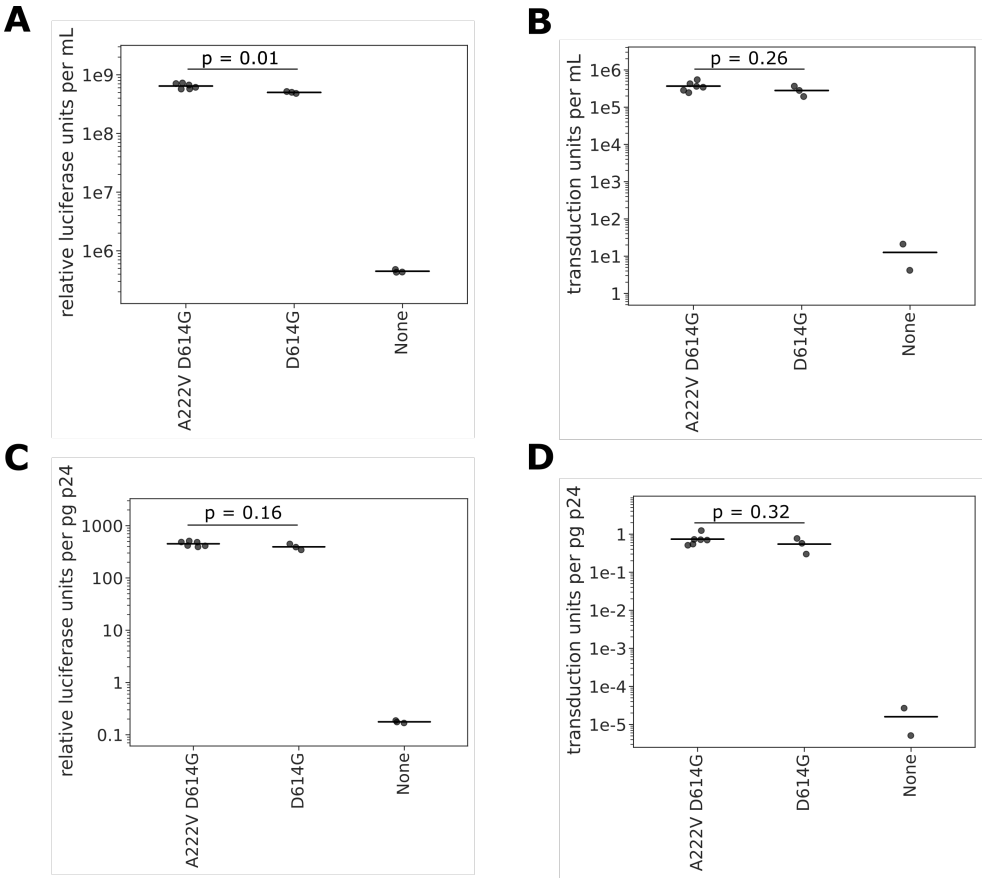

Figure 2.9: **Titers of lentiviral particles pseudotyped with spike with or without the A222V mutation.** The x-axis describes the viral entry protein used for pseudotyping. A222V and D614G describe mutations in spike and ”None” indicates negative control particles with no viral entry protein. The spike plasmid used to make the A222V D614G and D614G spike-pseudotyped particles also included the 21 amino acid cytoplasmic tail truncation (see Figure 2.4) A) Titers of lentiviral particles carrying luciferase in the viral genome. B) Titers of lentiviral particles carrying the fluorescent protein ZsGreen in the viral genome. In both cases, titers with the A222V mutation are on average higher by a factor of 1.3. C) Titers of lentiviral particles carrying luciferase in the viral genome normalized by the p24 concentration (pg/mL) of each viral supernatant. After p24 normalization, the titer difference shrinks from 1.28 to 1.14 fold, increasing the p-value to 0.16. D) Titers of lentiviral particles carrying ZsGreen in the viral genome normalized by the p24 concentration (pg/mL) of each viral supernatant. All horizontal lines indicate mean titers for the respective groups and p-values were calculated using a two-sided T-test.

Genomics UK consortium for their no-table sequencing efforts, which have provided more than half of the sequences currently publicly available. We would also like to thank the Swiss Federal Office of Public Health (FOPH) for providing access to their data. This work was supported by the Swiss National Science Foundation (SNSF) through grant numbers 31CA30 196046 (to RAN, EBH, CLA), 31CA30 196267 (to TS), European Union's Horizon 2020 research and innovation programme - project EpiPose (No 101003688) (MLR, CLA), core funding by the University of Basel and ETH Zürich, the National Institute of General Medical Sciences (R01GM120553 to DV), the National Institute of Allergy and Infectious Diseases (DP1AI158186 and HHSN272201700059C to DV), a Pew Biomedical Scholars Award (DV), an Investigators in the Pathogenesis of Infectious Disease Awards from the Burroughs Wellcome Fund (DV and JDB), a Fast Grants (DV), and NIAID grants R01AI141707 (JDB) and F30AI149928 (KHDC). SeqCOVID-SPAIN is funded by the Instituto de Salud Carlos III project COV20/00140, Spanish National Research Council and ERC StG 638553 to IC and BFU2017-89594R from MICIN to FGC. JDB is an Investigator of the Howard Hughes Medical Institute.

Competing Interests

DV is a consultant for Vir Biotechnology Inc. DC is an employee of Vir Biotechnology and may hold shares in Vir Biotechnology. The Veesler laboratory has received an unrelated sponsored research agreement from Vir Biotechnology Inc. AH is a co-founder of Kido Dynamics, DM is employed by Kido Dynamics. The other authors declare no competing interests.

2.7.4 ***Measuring the neutralizing antibody response to RBD nanoparticle vaccine candidates***

The SARS-CoV-2 pandemic has spurred the rapid development of several vaccines, but there remains a need for highly effective, thermostable vaccines that can be easily manufactured at scale. The King lab at the University of Washington's Institute for Protein Design has developed a self-assembling nanoparticle platform for protein subunit vaccines [98]. Their initial RBD nanoparticle vaccine candidate was highly immunogenic in pre-clinical studies, but there was room for improving the thermostability and ease of manufacturing [156]. Using deep mutational scanning data from yeast-displayed deep mutational scanning of RBD [143], Dan Ellis lead the efforts to develop RBD immunogens with stabilizing mutations that would facilitate their ease of use as vaccine candidates [46]. These mutations involved ”re-packing” the RBD to fill a hole in isolated RBD that is usually stabilized by binding linoleic acid in the context of full-length spike trimers. These ”re-packed” RBDs (Rpk4 and Rpk9) are more thermostable and are more resistant to aggregation than the wildtype RBD.

Dan and his team also wanted to confirm that these repacked RBDs maintained potent immunogenicity and immunized mice with their repacked RBD nanoparticle vaccine candidates as well as several controls, including spike trimers (”Hexapro-foldon”), wildtype RBD nanoparticles, and RBD trimers that cannot assemble into nanoparticles. Using the spike-pseudotyped lentivirus neutralization assay I developed, I measured the neutralizing antibody response in serum collected from these mice (Figure 2.10. Results of these neutralization assays showed that the nanoparticle vaccine candidates made with all three RBD sequences (wildtype, Rpk4, and Rpk9) induced potent neutralizing antibody responses, with no decrease in neutralizing antibody titers for the RBDs with ”re-packing” mutations (Figure 2.10. The increased ease of production and improved thermostability of these re-packed RBDs makes them promising vaccine candidates. These ”re-packed”

RBDs also highlight the promise of using data from the deep mutational scanning of viral entry proteins to inform and refine structure-based vaccine design.

Acknowledgements

We thank Ratika Krishnamurty for program management. This study was supported by the Bill & Melinda Gates Foundation (OPP1156262 to D.V. and N.P.K., and OPP1126258 to K.K.L.), a generous gift from the Audacious Project, a generous gift from Jodi Green and Mike Halperin, a generous gift from the Hanauer family, the Defense Threat Reduction Agency (HDTRA1-18-1-0001 to N.P.K.), grant R01 AI141707 from the NIAID/NIH, and grant F30 AI149928 from the NIAID/NIH to K.H.D.C. T.N.S. is an HHMI Fellow of the Damon Runyon Cancer Research Foundation. J.D.B. is an Investigator of the Howard Hughes Medical Institute.

Competing Interests

D.E., A.C.W, T.N.S., A.G., J.B., D.V., and N.P.K. are named as inventors on patent applications filed by the University of Washington based on the studies presented in this paper. N.P.K. is a co-founder, shareholder, paid consultant, and chair of the scientific advisory board of Icosavax, Inc. and has received an unrelated sponsored research agreement from Pfizer. D.V. is a consultant for and has received an unrelated sponsored research agreement from Vir Biotechnology Inc. J.D.B. consults for Moderna on viral evolution and epidemiology. J.D.B. and K.H.D.C. have the potential to receive a share of IP revenue as an inventor on a Fred Hutch optioned technology/patent (application WO2020006494) related to deep mutational scanning of viral proteins.

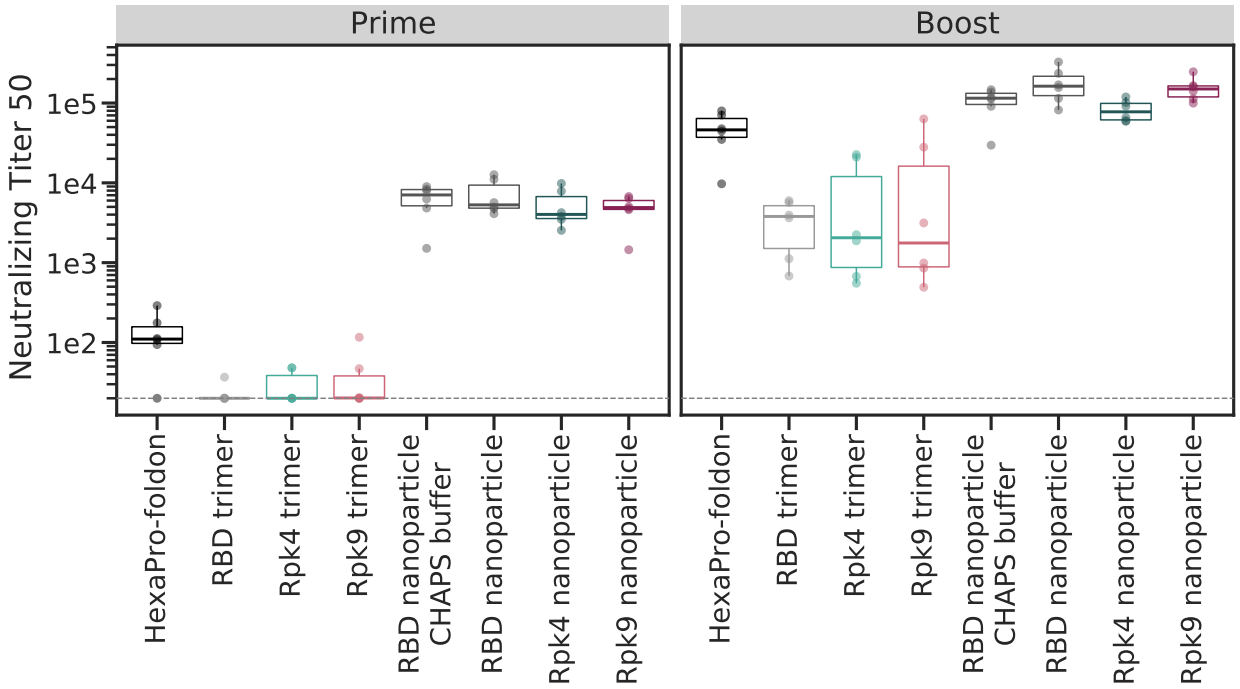

Figure 2.10: **Serum from mice vaccinated with RBD nanoparticle vaccine candidates potently neutralizes spike-pseudotyped lentiviral particles.** Serum was collected from mice immunized with trimerized spike ("Hexapro"), RBD trimers, or RBD nanoparticle vaccine candidates two weeks after each of two immunizations—an initial "prime" immunization was followed 3 weeks later by a "boost" with the same immunogen. The y-axis is the reciprocal of the serum dilution that neutralizes infection by 50%. The lower limit of detection (dashed grey line) was a neutralizing titer 50 of 20. Mice immunized with the RBD nanoparticle vaccine candidates mounted potent neutralizing responses. These neutralizing antibody responses remained high in mice immunized with RBD nanoparticles where the RBD had been engineered to be easier to manufacture ("Rpk4" and "Rpk9"). The spike-pseudotyped lentiviral particles used in these neutralization assays were pseudotyped with a spike with a 21 amino acid cytoplasmic tail truncation (see Figure 2.4) and the D614G mutation.

Chapter 3

DYNAMICS OF NEUTRALIZING ANTIBODY TITERS IN THE MONTHS AFTER SEVERE ACUTE RESPIRATORY SYNDROME CORONAVIRUS 2 INFECTION

A version of this chapter has been previously published as:

Crawford KHD, Dingens AS, Eguia R, Wolf CR, Wilcox N, et al. Dynamics of neutralizing antibody titers in the months after SARS-CoV-2 infection. J Infect Dis. 2020 Sep 30:jiaa618. doi: 10.1093/infdis/jiaa618.

3.1 Abstract

Most individuals infected with severe acute respiratory syndrome coronavirus 2 (SARS-CoV-2) develop neutralizing antibodies that target the viral spike protein. In this study, we quantified how levels of these antibodies change in the months after SARS-CoV-2 infection by examining longitudinal samples collected approximately 30–152 days after symptom onset from a prospective cohort of 32 recovered individuals with asymptomatic, mild, or moderate-severe disease. Neutralizing antibody titers declined an average of about 4-fold from 1 to 4 months after symptom onset. This decline in neutralizing antibody titers was accompanied by a decline in total antibodies capable of binding the viral spike protein or its receptor-binding domain. Importantly, our data are consistent with the expected early immune response to viral infection, where an initial peak in antibody levels is followed by a decline to a lower plateau. Additional studies of long-lived B cells and antibody titers over longer time frames are necessary to determine the durability of immunity

to SARS-CoV-2.

3.2 Introduction

Within a few weeks of being infected with severe acute respiratory syndrome coronavirus 2 (SARS-CoV-2), individuals develop antibodies that bind to viral proteins [163, 169, 89, 95, 137, 176, 174, 72]. A few weeks after symptom onset, serum from most infected individuals can bind to the viral spike protein and neutralize infection in vitro [137, 174, 146]. The reciprocal dilution of serum required to inhibit viral infection by 50% (neutralizing antibody titer at 50% inhibition [NT50]) is typically in the range of 100–200 at 3–4 weeks after symptom onset [126], although neutralizing titers range from undetectable to greater than 10,000 [169, 137, 146].

There are currently limited data on the dynamics of neutralizing antibodies in the months after recovery from SARS-CoV-2. For most acute viral infections, neutralizing antibodies rapidly rise after infection owing to a burst of short-lived antibody-secreting cells and then decline from this peak before reaching a stable plateau that can be maintained for years to decades by long-lived plasma and memory B cells [85, 4]. These dynamics have been observed for many viruses, including influenza [160], respiratory syncytial virus [60], Middle East respiratory syndrome coronavirus [26], SARS coronavirus 1 [148, 68], and the seasonal human coronavirus 229E [17].

Several recent studies have tracked antibody levels in individuals who have recovered from infection with SARS-CoV-2 for the first few months after symptom onset [137, 174, 72, 10, 96, 155, 171]. Most of these studies have reported that over the first 3 months, antibodies targeting the spike protein decline several-fold from a peak reached a few weeks after symptom onset [137, 174, 10], suggesting that the early dynamics of the antibody response to SARS-CoV-2 are similar to those for other acute viral infections.

Here we build on these studies by measuring both the neutralizing and binding anti-

body levels in serial plasma samples from 32 SARS-CoV-2–infected individuals across a range of disease severity with follow-up as long as 152 days after symptom onset. On average, neutralizing titers decreased about 4-fold from approximately 30 to $>$90 days after symptom onset. This decline in neutralizing titers was paralleled by a decrease in levels of antibodies that bind the spike protein and its receptor-binding domain (RBD). Nonetheless, most recovered individuals still had substantial neutralizing titers at 3–4 months after symptom onset.

3.3 Methods

3.3.1 Study Population

Plasma samples were collected as part of a prospective longitudinal cohort study of individuals with SARS-CoV-2 infection. Individuals aged $\geq$18 years with laboratory-confirmed SARS-CoV-2 infection were eligible for inclusion. Individuals who were human immunodeficiency virus positive were excluded from this study owing to concerns that antiretroviral treatment may affect our pseudotyped lentivirus neutralization assay. Individuals were recruited from 3 groups: inpatients, outpatients, and asymptomatic individuals. Inpatients were hospitalized at Harborview Medical Center, University of Washington Medical Center, or Northwest Hospital in Seattle, Washington, and were enrolled while hospitalized. Outpatients were identified through a laboratory alert system, email and flyer advertising, and through identification of positive coronavirus disease 2019 cases reported by the Seattle Flu Study [27]. Asymptomatic individuals in this study were recruited through outpatient testing and identified when they answered “None” on their symptom questionnaire. They were confirmed to be symptom free for the first 30 days after diagnosis.

We initially enrolled 34 individuals after reverse-transcription quantitative polymerase chain reaction (RT-qPCR) confirmation of SARS-CoV-2 infection. Two individuals (participant identifiers [PIDs] 19C and 196C) were seronegative at all time points in the neu-

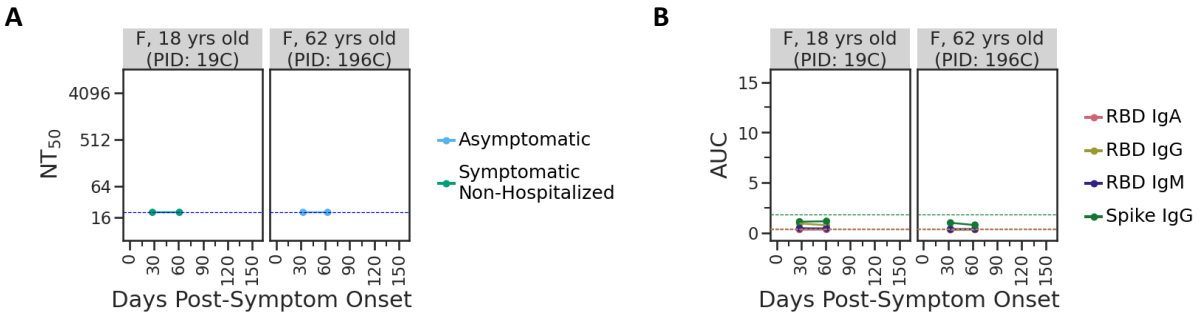

Figure 3.1: **Neutralizing and binding antibody levels are not above background for participants 19C and 196C. (A)** Neither PID 19C nor 196C had detectable neutralizing titers at any time point. The limit of detection for our neutralization assay (NT50 = 20) is shown with a dashed blue line. **(B)** Neither PID 19C nor 196C had detectable spike or RBD binding antibodies at any time point. The binding levels for the negative control sample (2017-2018 sera pool) are shown as dashed lines colored by assay.

tralization assay and all RBD and spike protein enzyme-linked immunosorbent assays (ELISAs) (Figure 3.1). We then tested these individuals using the Abbott Architect antinucleoprotein assay, with which they were also seronegative, with index values of 0.01 (for both samples from PID 196C) or 0.02 (for both samples from PID 19C), far below the threshold for seropositivity of 1.40 [16]. Because these individuals had only a single positive RT-qPCR result (and PID 196C tested negative in 6 subsequent RT-qPCR tests conducted within 15 days of the initial test) and because the Abbott Architect assay has been validated to have very high (95.1%–100%) sensitivity by day 17 after symptom onset [16], we assessed that these 2 individuals were likely not truly infected but rather false-positives in a single RT-qPCR viral test. Therefore, they were excluded from all further analyses, resulting in a final cohort of 32 individuals.

Participants or their legally authorized representatives completed electronic informed consent. Sociodemographic and clinical data were collected from electronic chart review and from participants via a data collection questionnaire (Project REDCap [62]) at the

time of enrollment. The questionnaire collected data on the nature and duration of symptoms, medical comorbid conditions, and care-seeking behavior (Table A.1). Based on these data, individuals were classified by disease severity as asymptomatic, symptomatic nonhospitalized, or symptomatic hospitalized.

Individuals who were recruited as inpatients were enrolled during their hospital admission and had samples collected during their hospitalization. After hospital discharge, these participants subsequently returned to an outpatient clinical research site approximately 30 days after symptom onset for follow-up. In-person follow-up occurred only if participants were asymptomatic, per Centers for Disease Control and Prevention guidelines. Outpatients and asymptomatic individuals completed their enrollment, data collection questionnaire, and first blood sample collection at an outpatient visit approximately 30 days after symptom onset (or positive test for asymptomatic individuals). All participants subsequently were asked to return on day 60 and then on day 90 or 120 for follow-up.

The majority of samples collected from participants were from outpatient visits after recovery. However, the first sample from PID 13, the first 3 from PID 23, and the first 6 from PID 25 were collected during their hospitalizations.

For some of the analyses shown in Figures 3.2 and 3.4, samples from individuals were divided into 3 time points: approximately 30 days after symptom onset (or after positive test for asymptomatic individuals; range, 22–48 days), approximately 60 days after symptom onset or positive test (range, 55–79 days), and $>$90 days after symptom onset or positive test (range, 94–152 days). Three individuals (PIDs 2C, 23, and 25) had multiple samples in the first time range. For aggregated analyses that required samples be divided into these 3 groups, we included only the sample closest to 30 days after symptom onset for those individuals. No individuals had multiple samples collected approximately 60 days after symptom onset. One individual (PID 12C) had 2 samples collected $>$90 days after symptom onset. For this individual, we included only the latest sample collected in

aggregated analyses that required classification into groups. The numbers of samples at each time point overall and for each disease severity classification are shown in Table 3.1. For analyses of fold change, we required individuals to have a sample collected at the 30-day time point. The numbers of individuals included in the fold-change analyses are also indicated in Table 3.1. This study was approved by the University of Washington Human Subjects Institutional Review Board.

3.3.2 Laboratory Methods

Whole-blood samples were collected in acid citrate dextrose tubes and then spun down, aliquoted, and frozen at –20℃ within 6 hours of collection. Before use in this study, plasma samples were heat inactivated at 56℃ for 60 minutes and stored at 4℃. Some samples from the early time points were stored at –80℃ after heat inactivation and underwent no more than 2 freeze-thaw cycles. Plasma samples were spun at 2000g for 15 minutes at 4℃ immediately before use to pellet platelets.

3.3.3 Protein Expression and Purification

SARS-CoV-2 RBD and spike (S-2P trimer [157]) proteins were produced in mammalian cells, as described elsewhere [157, 38, 156]. Proteins were purified from clarified supernatants as described elsewhere [156]. Sodium dodecyl sulfate–polyacrylamide gel electrophoresis was used to assess purity before flash freezing and storage at –80℃.

3.3.4 Abbott Architect

Testing of serum samples with the Abbott Architect SARS-CoV-2 immunoglobulin (Ig) G assay was performed according to the manufacturer's instructions for use and as described elsewhere [16]. Index values associated with the Abbott test are chemilumines-

Table 3.1: **Demographic characteristics of study participants by disease severity categories**

	Asymptomatic (N=6)	Symptomatic Non-hospitalized (N=21)	Symptomatic Hospitalized (N=5)	Overall (N=32)
Age Median [Min, Max]	64 [24, 79]	43 [22, 76]	54 [31, 64]	45.5 [22, 79]
Sex:				
Male	2 (33.3%)	9 (42.9%)	3 (60.0%)	14 (43.8%)
Female	4 (66.7%)	12 (57.1%)	2 (40.0%)	18 (56.3%)
Samples per Participant Median [Min, Max]	2 [2-3]	3 [2-3]	3 [2-8]	3 [2-8]
Samples at each time point {Included in fold-change analyses}:				
≈30 days	4 {4}	20 {20}	4 {4}	28 {28}
≈60 days	6 {4}	18 {17}	3 {2}	27 {23}
>90 days	3 {1}	15 {14}	4 {3}	22 {18}
Days of Follow Up[a] Median [Min, Max]	89 [60-131]	104 [58-152]	113 [76-121]	104 [58-152]

[a]Days between symptom onset date and collection date of last sample. For asymptomatic individuals, test date - calculated as Wednesday of the week of RT-qPCR test - was used in place of symptom onset date.

cent signal values relative to a calibrator control and are broadly similar to optical density values for an ELISA. An index value $\geq$1.40 is qualitatively reported as positive.

3.3.5 ELISAs

The IgG ELISAs for spike protein and RBD were conducted as described elsewhere [38], and were based on a published protocol that recently received emergency use authorization from New York State and the Food and Drug Administration (FDA) [3, 142]. Plasma samples were diluted with 5 serial 3-fold dilutions in phosphate-buffered saline with 0.1% Tween nonfat dry milk, starting at a 1:25 dilution. Each plate contained a negative control dilution series of pooled human serum samples collected in 2017–2018 (Gemini Biosciences; nos. 100–110, lot H86W03J; pooled from 75 donors) and a CR3022 monoclonal antibody positive control dilution series starting at 1 μg/mL.

IgA and IgM RBD ELISAs were performed as described elsewhere for IgG ELISAs [38], with the following changes. The IgA secondary antibody was Peroxidase AffiniPure Goat Anti-Human Serum IgA, α-chain specific (The Jackson Laboratory; no. 109-035-011), and the IgM secondary antibody was goat Anti-Human IgM (μ-chain specific)-Peroxidase antibody (Sigma Aldrich; A6907); both were diluted 1:3000 in phosphate-buffered saline–Tween containing 1% milk. For these ELISAs, plasma samples were analyzed at 6 serial 4-fold dilutions, starting at a 1:25 dilution, again with each plate containing a negative control dilution series (pooled human serum samples obtained in 2017–2018). The area under the curve (AUC) was calculated as the area under the titration curve after putting the serial dilutions on a log-scale.

3.3.6 Neutralization Assays

Neutralization assays were conducted using pseudotyped lentiviral particles, as described elsewhere [32], with a few modifications. First, we used a spike protein with a cytoplas-

mic tail truncation that removes the last 21 amino acids (spike $\triangle$21). The map for this plasmid, HDM-SARS2-Spike-delta21, is available at `https://github.com/jbloomlab/SARS-CoV-2_lentiviral_pseudotype/tree/master/plasmid_maps`, and the plasmid is available from Addgene (plasmid no. 155130) or BEI Resources (NR-35742). We used a spike protein with a C-terminal deletion because, since publication of our original protocol [32], other groups have reported that deleting the spike protein's cytoplasmic tail improves titers of spike-pseudotyped viruses [36, 20, 129, 113]. Indeed, we found that the C-terminal deletion increased the titers of our pseudotyped lentiviral particles without affecting neutralization sensitivity (Figure 2.4).

For our neutralization assays, we seeded black-walled, clear bottom, poly-L-lysine coated 96-well plates (Greiner; no. 655936) with 1.25×10^4 293T-ACE2 (NR-52511) cells per well in 50 μL of D10 medium (Dulbecco modified Eagle medium with 10% heat-inactivated fetal bovine serum, 2 mmol/L L-glutamine, 100 U/mL penicillin, and 100 μg/mL streptomycin) at 37ºC with 5% carbon dioxide. About 12 hours later, we diluted the plasma samples in D10, starting with a 1:20 dilution followed by 6 or 11 serial 3-fold dilutions (11 dilutions were used for samples from individuals in whom we had previously measured high neutralizing antibody responses; PIDs 13, 23, and 25). We then diluted the spike-$\triangle$21 pseudotyped lentiviral particles 1:6 (1 mL of virus plus 5 mL of D10 per plate) and added a volume of virus equal to the volume of plasma dilution to each well of the plasma dilution plates. We incubated the virus and plasma for 1 hour at 37ºC and then added 100 μL of the virus-plus-plasma dilutions to the cells.

At 50–52 hours after infection, luciferase activity was measured using the Bright-Glo Luciferase Assay System (Promega; E2610) as described elsewhere [32], except that luciferase activity was measured directly in the assay plates. Two "no-plasma" wells were included in each row of the neutralization plate, and the fraction infectivity was calculated by dividing the luciferase readings from the wells with plasma by the average of

the no-plasma wells in the same row. After calculating fraction infectivities, we used the neutcurve Python package (`https://jbloomlab.github.io/neutcurve/`) to calculate the plasma dilution that inhibited infection by 50% (IC50), fitting a Hill curve with the bottom fixed at 0 and the top at 1. The NT50 for each plasma sample was calculated as the reciprocal of the IC50. Individuals whose plasma was not sufficiently neutralizing to interpolate an IC50 using the Hill curve fit were assigned an NT50 of 20 (the limit of our dilution series) for plotting (Figures 3.2A, 3.2C, and 3.4B) and for fold-change analyses (Figure 3.2B). Neutralization curves for all samples are provided in Figure A.2 in Appendix A.

All samples were assayed at least in duplicate. We analyzed all samples from the same individual in the same batch of neutralization assays and on the same plate when possible. Each batch of samples included a negative control of pooled serum samples collected from 2017–2018 (Gemini Biosciences; nos. 100–110, lot H86W03J; pooled from 75 donors), and 1 plasma sample known to be neutralizing (from PID 4C at the 30-day time point). These samples were used to confirm consistency between batches.

Results from SARS-CoV-2 spike-pseudotyped lentivirus neutralization assays have been shown to correlate well with full virus SARS-CoV-2 neutralization assays [75, 147]. Nonetheless, in an effort to help standardize comparisons between neutralization assays, we also performed our assay with a standard serum sample from the National Institute for Biological Standards and Control (NIBSC) (Research Reagent for Anti-SARS-CoV-2 Ab; NIBSC code 20/130). This sample had an NT50 of approximately 3050 (Figure A.1).

3.3.7 Data Availability

Raw data for each sample, including IC50, NT50, AUC, and relevant demographic data (age, sex, disease severity, days after symptom onset) are available in Appendix A (Table A.2). Clinical data were analyzed using R software, version 3.6.0 (2019).

3.4 Results

3.4.1 Longitudinal Plasma Samples From a Cohort of SARS-CoV-2 Infected Individuals

We enrolled 32 individuals after RT-qPCR–confirmed SARS-CoV-2 infection, of whom 5 were symptomatic hospitalized, 21 were symptomatic nonhospitalized, and 6 were asymptomatic (Tables 3.1 and A.1). This cohort included slightly more female than male participants (56.3% female overall), with ages ranging from 22 to 79 years. The age and sex distributions, overall and based on disease severity, are provided in Table 3.1. Four individuals had comorbid conditions. Information on participant race or ethnicity, symptoms, comorbid conditions, and level of medical care required is provided in Table A.1.

At least 2 samples were collected from all individuals in this study (median, 3 samples) with the last sample collected 58–152 days after symptom onset (median, 104 days). The majority of individuals (22 of 32) had their last sample collected $>$90 days after symptom onset.

3.4.2 Dynamics of Neutralizing Antibody Titers Over Time

We used spike-pseudotyped lentiviral particles [32] to measure neutralizing antibody titers in the longitudinal plasma samples from all 32 infected individuals (Figure 3.2A). All individuals had detectable neutralizing antibody titers (NT50 $>$20) in their first convalescent plasma sample, which was generally collected roughly 1 month after symptom onset. These data are consistent with prior studies showing that most SARS-CoV-2–infected individuals develop neutralizing antibodies [137, 174, 146]. Qualitative inspection of Figure 3.2A shows that these titers modestly decreased for most individuals over the next few months, although the dynamics were highly heterogeneous across individuals.

To quantify the dynamics of neutralizing antibody titers over time, we calculated the fold change at approximately 60 and $>$90 days after symptom onset, relative to the ap-

Figure 3.2: **Change in neutralizing antibody titer over time**. **(A)** Neutralizing antibody titer at 50% inhibition (NT50) for each individual in the study, with facets colored according to disease severity (see key below plot). Facet titles indicate sex (F, female; M, male), age, and participant identifier (PID). Dashed blue line indicates the limit of detection for our assay (NT50=20). **(B)** Fold change in NT50 compared with 30-day time point, including only individuals with a neutralizing sample at day 30. P values were calculated using the Wilcoxon signed rank test. **(C)** Distribution of NT50 values at the 3 time points, with box plots colored by disease severity and the blue dashed line indicating the limit of detection as in panel A. P values are indicated when there is a significant difference ($P \leq 0.05$) between NT50 values for different disease severity categories at a time point and were calculated using the Wilcoxon rank sum test.

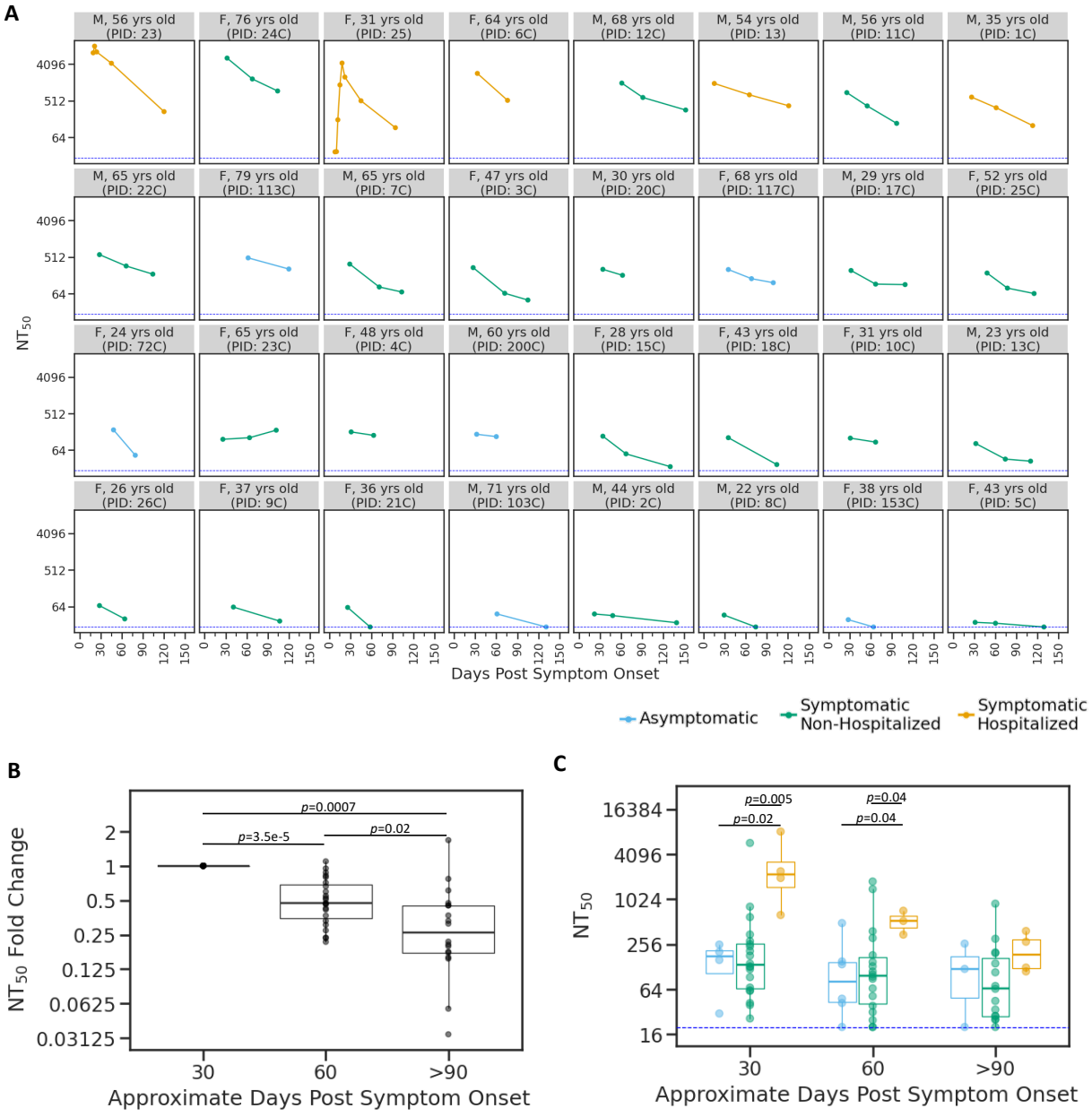
A
M, 56 yrs old (PID: 23)
F, 76 yrs old (PID: 24C)
F, 31 yrs old (PID: 25)
F, 64 yrs old (PID: 6C)
M, 68 yrs old (PID: 12C)
M, 54 yrs old (PID: 13)
M, 56 yrs old (PID: 11C)
M, 35 yrs old (PID: 1C)
M, 65 yrs old (PID: 22C)
F, 79 yrs old (PID: 113C)
M, 65 yrs old (PID: 7C)
F, 47 yrs old (PID: 3C)
M, 30 yrs old (PID: 20C)
F, 68 yrs old (PID: 117C)
M, 29 yrs old (PID: 17C)
F, 52 yrs old (PID: 25C)
F, 24 yrs old (PID: 72C)
F, 65 yrs old (PID: 23C)
F, 48 yrs old (PID: 4C)
M, 60 yrs old (PID: 200C)
F, 28 yrs old (PID: 15C)
F, 43 yrs old (PID: 18C)
F, 31 yrs old (PID: 10C)
M, 23 yrs old (PID: 13C)
F, 26 yrs old (PID: 26C)
F, 37 yrs old (PID: 9C)
F, 36 yrs old (PID: 21C)
M, 71 yrs old (PID: 103C)
M, 44 yrs old (PID: 2C)
M, 22 yrs old (PID: 8C)
F, 38 yrs old (PID: 153C)
F, 43 yrs old (PID: 5C)
NT50
4096
512
64
0
30
60
90
120
150
Days Post Symptom Onset
Asymptomatic
Symptomatic Non-Hospitalized
Symptomatic Hospitalized
B
NT50 Fold Change
2
1
0.5
0.25
0.125
0.0625
0.03125
p=0.0007
p=3.5e-5
p=0.02
30
60
>90
Approximate Days Post Symptom Onset
C
NT50
16384
4096
1024
256
64
16
p=0.005
p=0.02
p=0.04
p=0.04
30
60
>90
Approximate Days Post Symptom Onset

proximately 30-day time point, excluding any individuals who lacked a 30-day sample. Taken across all individuals, neutralizing titers significantly declined from 30 to 60 days, and again from 60 to 90 days (see legend to Figure 3.2B for details). At >90 days, the median neutralizing titer was reduced 3.8-fold relative to the 30-day value (Figure 3.2B). However, most individuals (27 of 32) still had detectable neutralizing titers at the last time point.

We compared the dynamics of neutralizing antibody titers between individuals with different disease severities (Figure 3.2C). Individuals with more severe disease tended to have higher neutralizing antibody titers during early convalescence, consistent with prior studies [137, 161, 133]. Specifically, at both approximately 30 and approximately 60 days after symptom onset, individuals who required hospitalization had significantly higher neutralizing antibody titers than those who did not (Figure 3.2C). From approximately 30 to >90 days after symptom onset, the NT50 for symptomatic hospitalized individuals decreased about 18-fold, significantly more than the approximately 3-fold decrease in the NT50 for nonhospitalized individuals (P=0.03; Wilcoxon rank sum test) (Figure 3.3). By >90 days after symptom onset, neutralization titers did not differ significantly between disease severity groups (Figure 3.2C). At all time points, asymptomatic individuals had neutralization titers similar to those of symptomatic nonhospitalized individuals.

3.4.3 Dynamics of Spike Protein-Binding and RBD-Binding Antibodies Over Time

For all plasma samples, we also used ELISAs to measure IgA, IgM, and IgG binding to the RBD of the spike protein, and IgG binding to the full spike protein ectodomain [3]. Figure 3.4A shows each individual's IgA, IgM, and IgG binding antibody titers as quantified by the AUC of the ELISA readings (see Methods for detailed description). Like neutralizing antibody titers, these antibody binding titers tended to decrease over time, although there was substantial variation among individuals. All of the ELISA-measured antibody-binding

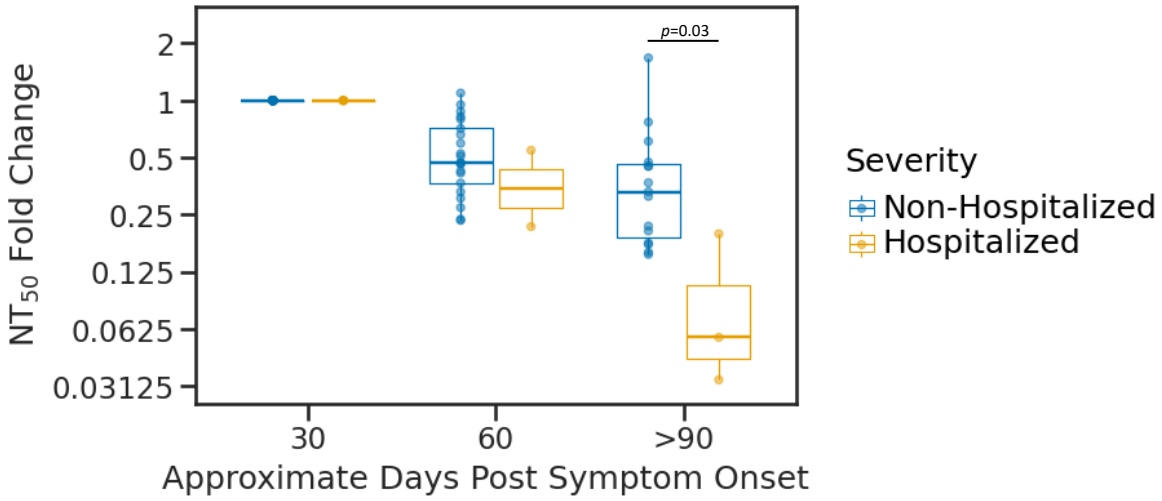

Figure 3.3: **Fold change in NT50 at each time point colored by disease severity.** There was only one asymptomatic individual with a 30-day time point and 90-day time point, so this individual was included in the Non-Hospitalized group. As in Figure 1B, only individuals with a sample at ∼30 days post-symptom onset are included. P value calculated using the Wilcoxon rank-sum test.

titers are clearly correlated with neutralizing antibody titers (Figure 3.4B).

Individuals with severe disease had higher antibody binding titers at early time points. Specifically, individuals who were hospitalized as part of their care had higher IgG, IgA, and IgM binding responses than asymptomatic or symptomatic nonhospitalized individuals at approximately 30 days after symptom onset (Figure 3.4C). By approximately 60 days after symptom onset, anti-RBD IgM levels were no longer significantly different between severity groups, and by $>$90 days after symptom onset, binding responses did not differ between severity groups for any antibody subtype. This trend is consistent with data in Figure 3.2C showing that neutralizing antibody responses were higher for individuals with more severe disease early during convalescence but reached similar levels across all disease severity groups by $>$90 days after symptom onset. Among all patients, regardless of disease severity, IgA and IgM levels decreased more than IgG levels from approximately 30 to $>$90 days after symptom onset, consistent with findings of other studies [174, 72, 10, 171].

3.5 Discussion

We have measured the dynamics of neutralizing antibody titers over the first 3–4 months after infection with SARS-CoV-2 in a well-characterized prospective longitudinal cohort of individuals across a range of disease severity. The titers of neutralizing antibodies declined modestly, with the titers at 3–4 months after symptom onset generally about 4-fold lower than those at 1 month. This decline in neutralizing antibodies was paralleled by a decline in antibodies binding to the viral spike protein and its RBD. This decline is generally similar in magnitude to that reported in several other recent studies of antibody dynamics in the months immediately after SARS-CoV-2 infection [137, 174, 10].

Individuals with more severe disease tended to have higher peak antibody responses at 1–2 months after symptom onset, consistent with many other studies reporting higher

Figure 3.4: **Immunoglobulin (Ig) A, IgM, and IgG antibody binding titers over time.** **(A)** Longitudinal binding antibody titers for each individual as quantified by area under the curve (AUC) of enzyme-linked immunosorbent assays (ELISAs). Facets are arranged by maximal neutralizing antibody titer at 50% inhibition (NT50) from top left to bottom right, as in Figure 3.2A. Dashed lines indicate the AUC value for the negative control sample (2017–2018 serum sample pool) for each assay, colored by assay. Abbreviations: F, female; M, male; PID, participant identifier; RBD, receptor-binding domain. **(B)** Correlation plots between AUC for each ELISA and neutralization titer (NT50) for all samples. Vertical dashed line indicates the limit of detection for the neutralization assay; horizontal dashed lines, the AUC values for the negative control sample (2017–2018 serum sample pool) for each assay, colored based on the assay as in A. **(C)** For each antibody type measured, individuals who were symptomatic and required hospitalization as part of their care had significantly higher antibody levels during the first 1–2 months after symptom onset. *$P \leq 0.05$; **$P \leq 0.01$. P values were calculated using the Wilcoxon rank sum test. As in A and B, the dashed line in each facet indicates the AUC value for the negative control sample for each assay, colored by assay.

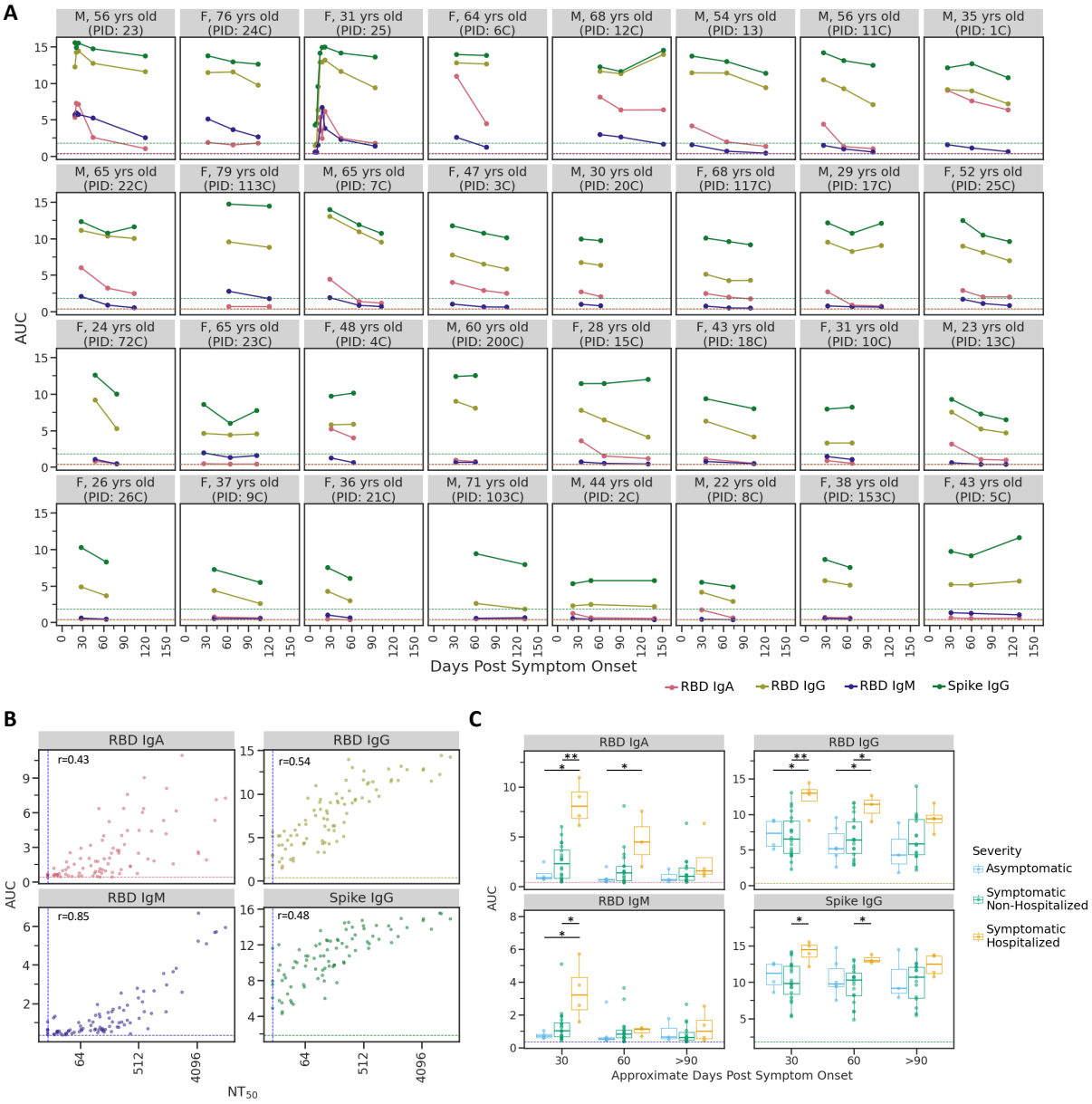
A
M, 56 yrs old (PID: 23)
F, 76 yrs old (PID: 24C)
F, 31 yrs old (PID: 25)
F, 64 yrs old (PID: 6C)
M, 68 yrs old (PID: 12C)
M, 54 yrs old (PID: 13)
M, 56 yrs old (PID: 11C)
M, 35 yrs old (PID: 1C)
M, 65 yrs old (PID: 22C)
F, 79 yrs old (PID: 113C)
M, 65 yrs old (PID: 7C)
F, 47 yrs old (PID: 3C)
M, 30 yrs old (PID: 20C)
F, 68 yrs old (PID: 117C)
M, 29 yrs old (PID: 17C)
F, 52 yrs old (PID: 25C)
F, 24 yrs old (PID: 72C)
F, 65 yrs old (PID: 23C)
F, 48 yrs old (PID: 4C)
M, 60 yrs old (PID: 200C)
F, 28 yrs old (PID: 15C)
F, 43 yrs old (PID: 18C)
F, 31 yrs old (PID: 10C)
M, 23 yrs old (PID: 13C)
F, 26 yrs old (PID: 26C)
F, 37 yrs old (PID: 9C)
F, 36 yrs old (PID: 21C)
M, 71 yrs old (PID: 103C)
M, 44 yrs old (PID: 2C)
M, 22 yrs old (PID: 8C)
F, 38 yrs old (PID: 153C)
F, 43 yrs old (PID: 5C)
AUC
Days Post Symptom Onset
RBD IgA
RBD IgG
RBD IgM
Spike IgG
B
RBD IgA
r=0.43
RBD IgG
r=0.54
RBD IgM
r=0.85
Spike IgG
r=0.48
AUC
NT50
C
RBD IgA
RBD IgG
RBD IgM
Spike IgG
AUC
Approximate Days Post Symptom Onset
Severity
Asymptomatic
Symptomatic Non-Hospitalized
Symptomatic Hospitalized

early titers in severely ill SARS-CoV-2–infected individuals [137, 176, 161, 133]. However, by 3–4 months after symptom onset, neutralizing antibody titers among individuals with severe disease were no longer significantly higher than those of individuals with mild symptoms or even asymptomatic infections. Therefore, it seems possible that the large peak in antibody production in severely ill individuals wanes more dramatically than in milder cases, consistent with severe disease often leading to an exaggerated burst of short-lived antibody-secreting cells [83, 144].

Importantly, most individuals in our study still had substantial neutralizing antibody titers at 3–4 months after symptom onset. While some recent studies have interpreted a modest drop in titers in the first few months after infection as alarming, it is entirely consistent with antibody responses to other respiratory viruses. Acute infection is always associated with an initial peak in antibody titers due to a burst of short-lived antibody-secreting cells [48]. For many other infections, titers decline from this initial peak but then reach a stable plateau that is maintained for years or even decades by long-lived plasma cells and memory B cells that can be recalled during subsequent infections [4, 160, 60, 26, 148, 17, 82, 6].

The modest declines in antibody titers that we observe over time do have implications for efforts to collect convalescent patient plasma for use in treatment of sick individuals [49]. FDA guidelines suggest minimum cutoffs for the antibody activity in such convalescent plasma (eg, NT50 $>$160; [133]). Our results suggest that plasma from convalescent donors collected in the first few months after symptom onset will be more likely to meet these cutoffs; others have made a similar observation [117]. In addition, our results indicate that if an individual is donating convalescent plasma over time, each plasma sample should be tested for antibody titers to ensure that they remain above the FDA cutoff.

The limitations of the current study include the small number of samples, particularly in the asymptomatic and symptomatic hospitalized groups, and recruitment of partici-

pants from a single study site, which potentially limits the generalizability of these results. Furthermore, since symptom-onset date relies on individual recollections, it is difficult to precisely match the timing of blood draws across all participants. In addition, we had follow-up only to about 4 months after symptom onset, and we only measured plasma antibody responses. Further studies over longer time frames and with direct interrogation of plasma and memory B cells will be necessary to determine longer term durability of immunity to SARS-CoV-2, as well as its relationship to protection against reinfection [1].

Despite these limitations, our study shows that titers of neutralizing and binding antibodies targeting SARS-CoV-2 spike protein remain detectable in most individuals up to $>$90 days after symptom onset. Although titers decline modestly from approximately 30 to $>$90 days after symptom onset, we found that the dynamics of the antibody response to SARS-CoV-2 in the first several months after infection are consistent with what would be expected from knowledge of other acute viral infections [160, 60, 26, 148, 68, 17].

3.6 Notes

3.6.1 Acknowledgments

We thank Marion Pepper, PhD for helpful input, David Koelle, MD and Anna Wald, MD for sharing reagents, Andrea Loes, PhD and Meei-Li Huang, PhD for experimental assistance, and Ariana Magedson, Dylan McDonald, and Nicholas Franko for assistance with enrollment. We also thank all research participants in the Hospitalized or Ambulatory Adults with Respiratory Viral Infections (HAARVI) study for their generosity in participation.

3.6.2 Financial support

This work was supported by the National Institute of Allergy and Infectious Diseases, National Institutes of Health (grants R01AI141707 to J. D. B. and F30AI149928 to K. H. D. C.), the Bill & Melinda Gates Foundation (H. Y. C.; grant OPP1156262 to N. P. K.), and the Burroughs Wellcome Fund (Investigators in the Pathogenesis of Infectious Disease award to J. D. B.) J.D.B. is an Investigator of the Howard Hughes Medical Institute.

3.6.3 Conflicts of Interest

N. P. K. is a cofounder, shareholder, and chair of the scientific advisory board of Icosavax, Inc. A. L. G. has consulted for Abbott Molecular, outside the submitted work. H. Y. C. is a consultant for Merck and Pfizer and receives research funds from Cepheid, Ellume, Genentech, and Sanofi-Pasteur. All other authors report no potential conflicts. All authors have submitted the ICMJE Form for Disclosure of Potential Conflicts of Interest. Conflicts that the editors consider relevant to the content of the manuscript have been disclosed.

Chapter 4

ALIGNPARSE: A PYTHON PACKAGE FOR PARSING COMPLEX FEATURES FROM HIGH-THROUGHPUT LONG-READ SEQUENCING

A version of this chapter has been previously published as:

Crawford KHD, Bloom JD. alignparse: A Python package for parsing complex features from high-throughput long-read sequencing. J Open Source Softw. 2019;4(44):1915. doi: 10.21105/joss.01915. Epub 2019 Dec 11.

4.1 Summary & Purpose

Advances in sequencing technology have made it possible to generate large numbers of long, high-accuracy sequencing reads. For instance, the new PacBio Sequel platform can generate hundreds of thousands of high-quality circular consensus sequences in a single run [125, 65]. Good programs exist for aligning these reads for genome assembly [21, 93]. However, these long reads can also be used for other purposes, such as sequencing PCR amplicons that contain various features of interest. For instance, PacBio circular consensus sequences have been used to identify the mutations in influenza viruses in single cells [130], or to link barcodes to gene mutants in deep mutational scanning [99]. For such applications, the alignment of the sequences to the targets may be fairly trivial, but it is not trivial to then parse specific features of interest (such as mutations, unique molecular identifiers, cell barcodes, and flanking sequences) from these alignments.

Here we describe alignparse, a Python package for parsing complex sets of features from long sequences that map to known targets. Specifically, it allows the user to provide

complex target sequences in Genbank Flat File format that contain an arbitrary number of user-defined sub-sequence features [134]. It then aligns the sequencing reads to these targets and filters alignments based on whether the user-specified features are present with the desired identities (which can be set to different thresholds for different features). Finally, it parses out the sequences, mutations, and/or accuracy (sequence quality) of these features as specified by the user. The flexibility of this package therefore fulfills the need for a tool to extract and analyze complex sets of features in large numbers of long sequencing reads.

4.2 Uses & Examples

Below are two example use cases of alignparse from our research. Code, data, and example output are included in the alignparse documentation.

4.2.1 Sequencing deep mutational scanning libraries

In deep mutational scanning experiments, researchers use mutant libraries to assay the effects of tens of thousands of individual mutations to a gene-of-interest in one experiment [51]. One way to make deep mutational scanning of long gene variants work efficiently with short-read Illumina sequencing is to link the mutations in each variant to a unique molecular barcode [67]. This barcode linking can be done by long-read PacBio sequencing of the variant library [99], but it is then necessary to parse the resulting long reads to associate the barcode with the mutations in the variant.

The alignparse package provides a standard tool for parsing barcodes and linked mutations from the long-read sequencing data. It also allows for the parsing of additional sequence features necessary for validating the quality of deep mutational scanning libraries, such as the presence of terminal sequences or other identifying tags. The RecA deep mutational scanning library example demonstrates this use.

4.2.2 Single-cell viral sequencing

Some viral genomes are sufficiently small to be sequenced in their entirety using long-read sequencing technology. Recent work has shown that such long-read sequencing of viral genes can be combined with standard single-cell transcriptomic technologies (such as 10x Chromium) to simultaneously sequence the infecting virus and characterize the transcriptome in single infected cells [130]. Such experiments require parsing the long-read viral sequences to identify viral mutations as well as cell barcodes, unique molecular identifiers, and other flanking sequences. The single-cell virus sequencing example shows how such parsing can readily be performed using alignparse.

4.3 How alignparse works

alignparse takes the following inputs:

1. One or more user-defined Genbank files containing the sequence of one or more alignment targets with an arbitrary number of user-defined features. These Genbank files can be readily generated using sequence editing programs, such as ApE or Benchling.

2. A YAML file containing parsing specifications for each feature. These specifications include filters indicating the maximal allowed mutations in each feature, as well as information on what output should be parsed for each feature (e.g., its sequence, its mutations, or simply if it is present).

3. A FASTQ file containing the long-read sequencing data. This file can be gzipped. There is no need to decompress gzipped FASTQ files first.

These inputs are used to define a Targets object. alignparse then uses this Targets

object to create sequence alignments and parse sequence features defined in the input Genbank and YAML files.

alignparse aligns sequencing reads to the targets using minimap2. The alignparse.minimap2 submodule provides alignment specifications optimized for the two example use cases described above. alignparse uses the cs tags generated by minimap2 to extract the relevant features from the alignments into intuitive data frames or CSV files.

We expect most users to align sequences and parse features in a single step using the alignparse.targets.Targets.align_and_parse function. However, these aligning and parsing steps can be carried out separately, as seen in the Lassa virus glycoprotein example. Indeed, the alignparse.targets.Targets.parse_alignment function should be able to parse features from any alignment file (in SAM format) as long as the alignments have cs tags and a corresponding Targets object has been defined that identifies the targets to which the query sequences were aligned and specifies the features to parse and filters to use.

Downstream analyses of parsed features are facilitated by the alignparse.consensus submodule. This submodule provides tools for grouping reads by shared barcodes, determining consensus sequences for barcoded reads, and further processing mutation information for downstream analyses. Since the main outputs from alignparse are in intuitive data frame formats, downstream analyses can be highly customized by the user. Thus, alignparse provides a flexible and useful tool for parsing complex sets of features from high-throughput long-read sequencing of pre-defined targets.

4.4 Code Availability

The alignparse source code is on GitHub at `https://github.com/jbloomlab/alignparse` and the documentation is at `https://jbloomlab.github.io/alignparse`.

4.5 Acknowledgements

We would like to thank members of the Bloom lab for helpful discussions and beta testing. This work was supported by the following grants from NIAID of the NIH: R01 AI141707 and R01 AI140891. JDB is an Investigator of the Howard Hughes Medical Institute.

Chapter 5
CONCLUSIONS

The emergence of SARS-CoV-2 in late 2019 challenged the scientific community to learn as much as possible, as quickly as possible about this novel coronavirus. An important aspect of addressing this challenge was the development of easy-to-use, scalable tools to study SARS-CoV-2 and, in particular, its viral entry protein, spike.

This research effort was a global undertaking of which the pseudotyped lentivirus-based system described in Chapter 2 was one small part. The reagents and protocol described in Chapter 2 were shared with scientists around the world within weeks of the protocol being developed. The wide-spread use of this and similar systems further highlights the important role pseudotyped viral particles play in advancing our understanding of emerging viruses.

The work described at the end of Chapter 2 and throughout Chapter 3 highlights several important uses of spike-pseudotyped lentiviral particles. The results of Chapter 3 contributed to our early understanding of how neutralizing antibody titers to SARS-CoV-2 change in the first several months post symptom onset. At the time of the study in July 2020, our cohort included samples from individuals with some of the longest follow-up published at the time. I remain grateful to the individuals who participated in the study for facilitating this early research into the neutralizing antibody response to SARS-CoV-2.

In the months since conducting the experiments described in Chapter 3, additional studies have confirmed the main findings. Levels of SARS-CoV-2 neutralizing antibodies do decline a few fold in the months following infection, but most individuals continue to have detectable neutralizing antibody titers several months post infection, with recent

studies showing a sustained antibody response at least 6 months post infection [53, 171]. Our finding that individuals with more severe disease have higher initial antibody titers against SARS-CoV-2 spike has also continued to be seen by many groups [152, 161]. However, whether individuals with severe disease maintain higher titers than individuals with mild, moderate, or asymptomatic disease overtime remains a little less certain. We found that although individuals with severe disease had significantly higher neutralizing antibody titers at early time points, by $>$90 days post symptom onset this trend was no longer significant. Other groups have found that IgG antibodies that bind to spike or RBD remain elevated in individuals with more severe disease, even at $>$4 months post symptom onset [53, 116]. However, as we found, this trend is not always statistically significant for measurements of neutralizing antibodies at later time points [116]. Nonetheless, disease severity does seem to correlate with anti-spike antibody levels and, regardless of disease severity, most individuals will maintain detectable neutralizing antibody titers for many months following infection with SARS-CoV-2.

More than one year after the beginning of the COVID-19 pandemic, it feels like we can now take for granted the fact that the neutralizing antibody response to SARS-CoV-2 generally resembles that of other respiratory viruses, but going into the summer of 2020, that was uncertain. We should continue to monitor the neutralizing antibody response to SARS-CoV-2 as individuals get further out from infection and/or vaccination. Almost one year after my initial study, it remains encouraging, but not surprising, that scientists continue to detect SARS-CoV-2 neutralizing antibodies in most individuals many months after infection [53].

Now, in the summer of 2021, research into SARS-CoV-2 neutralizing antibodies is focused on whether mutations to spike can evade a previously infected individual's neutralizing antibody response. With several SARS-CoV-2 variants increasing in frequency [86], the main question is not *if* an individual will have neutralizing antibodies several

months after infection with SARS-CoV-2, but whether those antibodies can still neutralize circulating viruses that have mutations in spike [121]. Recent studies indicate that neutralizing antibodies from individuals previously infected with SARS-CoV-2 are somewhat less effective at neutralizing some of the currently circulating variants, such as B.1.351, but serum from most individuals still has detectable neutralizing antibodies against tested variants six months post infection [11].

Spike-pseudotyped lentiviral particles can easily be produced with different spike sequences. Research into the effects of mutations to spike on neutralizing antibodies has taken advantage of this to measure the neutralizing antibody response not only to currently circulating variants, but also to other combinations of spike mutations [55, 84]. These studies are important for the continued assessment of an individual's vaccine- or infection-elicited neutralizing antibody response, especially as the virus continues to change.

Below I discuss current progress and future directions using the flexibility of a pseudotyped lentiviral system can be used to profile mutations to viral entry proteins from emerging viruses—such as SARS-CoV2 spike or Lassa virus glycoprotein (LASV GP)—at high-throughput using deep mutational scanning.

5.1 Viral entry protein deep mutational scanning moving forward

A generalizable and high-throughput platform for assessing the effects of mutations to viral entry proteins from emerging viruses is necessary to fully understand the functional and antigenic effects of mutations to these important proteins, which include SARS-CoV-2 spike or LASV GP. Based in part on the pseudotyped lentivirus work discussed in the preceding chapters, I have helped develop a platform to conduct deep mutational scanning experiments on viral entry proteins using pseudotyped lentiviral particles. Establishing this system required optimizing several molecular engineering steps, which I will not dis-

cuss in detail, but which are shown in Figure 5.1. Importantly, this lentiviral vector system removes the need to optimize a separate reverse genetics system for every viral entry protein we wish to study. Furthermore, since pseudotyped lentiviruses can be safely grown under biosafety level 2 conditions [2], these experiments enable the study of viral entry proteins from emerging viruses that usually require high biosafety level containment.

This platform makes it possible to prospectively characterize the effects of mutations to viral entry proteins from numerous emerging viruses. This information will both increase our scientific understanding of these viruses and improve the speed with which we can identify mutants that mediate escape from potential therapeutics. This has proven exceedingly useful for the current SARS-CoV-2 pandemic [143, 57, 55, 56], and will certainly prove only more useful in a system that can measure the effects of mutations on viral entry protein function, not just binding.

Other members of the Bloom lab have now taken the lead in applying this pseudotyped lentivirus deep mutational scanning system to SARS-CoV-2 spike. I have instead focused on applying this system to the deep mutational scanning of LASV GP. This work is ongoing and I will briefly introduce my current progress and next steps below.

5.1.1 Lassa virus glycoprotein deep mutational scanning

Lassa virus is an Old World arenavirus that is endemic in West Africa and causes Lassa fever—a viral hemorrhagic fever that causes several hundred thousand cases and thousands of deaths annually [131]. Most human infections with Lassa virus are the result of zoonotic spillover from a rodent reservoir [107]. Lassa virus is considered a priority pathogen by the WHO and Center for Epidemic Preparedness Innovations [15, 112]. There are currently no approved targeted treatments, but antibody therapeutics are being developed [104]. LASV GP deep mutational scanning will help improve our understanding of how mutations to LASV GP affect entry into human cells and allow us to readily identify

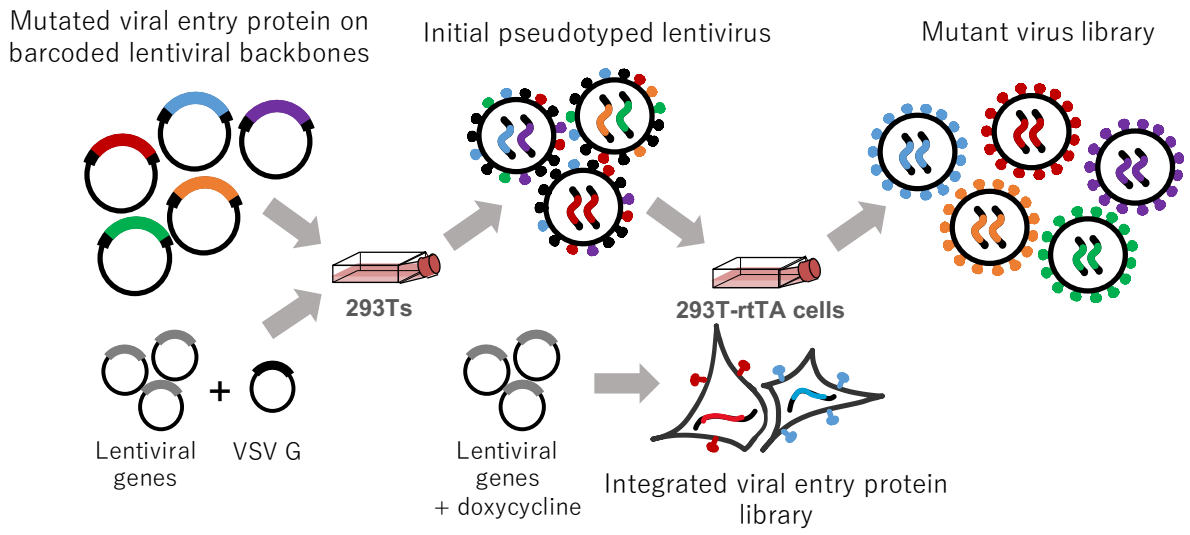

Figure 5.1: **Generation of viral entry protein deep mutational scanning libraries using pseudotyped lentiviral particles.** The generation of pseudotyped lentivirus deep mutational scanning libraries starts with generating mutant viral entry protein plasmid libraries using a PCR mutagenesis technique commonly used in the Bloom lab [41, 61]. Importantly, these viral entry protein mutants are cloned into plasmids (i.e. "lentiviral backbones") such that they can be packaged into lentiviral particles. These plasmids have been further engineered to include barcodes, include full-length 5' and 3' lentiviral long terminal repeats (necessary to recover virus from transduced cells), express the viral entry protein from a doxycycline-inducible promoter, and constitutively express a green fluorescent protein (ZsGreen). Transfecting HEK-293Ts (293Ts) with the mutant viral entry protein plasmids, lentiviral helper plasmids (encoding Gag/Pol, Tat, and Rev), and a plasmid expressing VSV G produces pseudotyped lentiviral particles that can infect target cells without relying on the viral entry protein of interest. These lentiviral particles can then be used to infect 293T-rtTA cells—293Ts that express a reverse tetracycline transactivator (rtTA)—at a low MOI ($<$0.02). Infected cells should largely be infected by a single virion and contain one genome-integrated viral entry protein sequence. These cells can then be sorted based on the expression of ZsGreen. Sorted cells should each encode a different viral entry protein variant that can be expressed by the addition of doxycycline thanks to the rtTA protein in the transduced cells. These cells can then be expanded and transfected with the required lentiviral helper plasmids to produce pseudotyped lentivirus viral libraries with a genotype-phenotype link. Once mutant virus libraries are generated, they can be used in typical deep mutational scanning selection experiment workflows, such as those previously used for influenza HA or HIV Env [41, 42, 87, 61, 39, 37].

mutations that could affect neutralization by the therapeutic antibodies being developed.

Currently, I am in the process of finishing selection experiments with initial LASV GP-pseudotyped lentivirus deep mutational scanning libraries using the GP sequence from the prototypical Lassa virus strain, Josiah. I have finished growing the LASV GP-pseudotyped mutant viruses libraries, have completed PacBio long-read sequencing of all variants in the library, and have linked barcodes with their associated mutations using the alignparse package described in Chapter 4. I have biological replicate libraries, one with $\approx$40,000 LASV GP variants and the other with $\approx$50,000 variants. In total, these libraries include $>$99% of all possible single amino acid mutations to LASV GP, with $>$80% of those mutations present at least once as the only mutation in the gene. While further optimizations to library production—such as sorting more cells with integrated viral entry protein variants—could improve library diversity, these libraries are sufficient for initial functional and antibody escape selections. I am currently conducting these selection experiments by infecting 293Ts with these LASV GP-pseudotyped lentivirus libraries both with and without neutralizing antibodies. I am conducting initial antibody selections with 8.9F, an antibody that potently neutralizes LASV in non-human primate and cell culture models [104]. A LASV GP mutation (Y150D) has also already been identified as escaping neutralization by 8.9F [104]. This will provide a good starting point for validating my results.

I look forward to completing functional and antigenic selections with my LASV GP deep mutational scanning libraries as a proof-of-principle for the use of pseudotyped lentiviral particles for viral entry protein deep mutational scanning. I think the full potential of viral entry protein deep mutational scanning is only beginning to be realized. A pseudotyped lentivirus-based viral entry protein deep mutational scanning platform, such as the one I have contributed to throughout my PhD, will greatly facilitate the application of deep mutational scanning to viral entry proteins from difficult-to-work-with—or even currently

unknown—viruses that could lead to future pandemics. The information gained from such experiments will facilitate our understanding of these important viruses, aid in developing effective viral therapeutics or vaccines, and help us respond rapidly to future viral threats.

BIBLIOGRAPHY

[1] Amin Addetia, Katharine HD Crawford, Adam Dingens, Haiying Zhu, Pavitra Roychoudhury, Meei-Li Huang, Keith R Jerome, Jesse D Bloom, and Alexander L Greninger. Neutralizing antibodies correlate with protection from sars-cov-2 in humans during a fishery vessel outbreak with a high attack rate. *Journal of clinical microbiology*, 58(11), 2020.

[2] American Biological Safety Association Alliance. Lentivirus vector fact sheet. `https://absa.org/wp-content/uploads/2018/05/LentivirusVectorFactSheet.pdf`, 2018. Accessed: 2021-05-10.

[3] Fatima Amanat, Daniel Stadlbauer, Shirin Strohmeier, Thi HO Nguyen, Veronika Chromikova, Meagan McMahon, Kaijun Jiang, Guha Asthagiri Arunkumar, Denise Jurczyszak, Jose Polanco, et al. A serological assay to detect sars-cov-2 seroconversion in humans. *Nature medicine*, 26(7):1033–1036, 2020.

[4] Ian J Amanna, Nichole E Carlson, and Mark K Slifka. Duration of humoral immunity to common viral and vaccine antigens. *New England Journal of Medicine*, 357(19):1903–1915, 2007.

[5] Kristian G Andersen, B Jesse Shapiro, Christian B Matranga, Rachel Sealfon, Aaron E Lin, Lina M Moses, Onikepe A Folarin, Augustine Goba, Ikponmwonsa Odia, Philomena E Ehiane, et al. Clinical sequencing uncovers origins and evolution of lassa virus. *Cell*, 162(4):738–750, 2015.

[6] Claudia P Arevalo, Valerie Le Sage, Marcus J Bolton, Theresa Eilola, Jennifer E Jones, Karen A Kormuth, Eric Nturibi, Angel Balmaseda, Aubree Gordon, Seema S Lakdawala, et al. Original antigenic sin priming of influenza virus hemagglutinin stalk antibodies. *Proceedings of the National Academy of Sciences*, 117(29):17221–17227, 2020.

[7] I Made Artika and Chairin Nisa Ma'roef. Laboratory biosafety for handling emerging viruses. *Asian Pacific journal of tropical biomedicine*, 7(5):483–491, 2017.

[8] Lindsey R Baden, Hana M El Sahly, Brandon Essink, Karen Kotloff, Sharon Frey, Rick Novak, David Diemert, Stephen A Spector, Nadine Rouphael, C Buddy Creech, et al. Efficacy and safety of the mrna-1273 sars-cov-2 vaccine. *New England Journal of Medicine*, 384(5):403–416, 2021.

[9] Christopher O Barnes, Anthony P West Jr, Kathryn E Huey-Tubman, Magnus AG Hoffmann, Naima G Sharaf, Pauline R Hoffman, Nicholas Koranda, Harry B Gristick, Christian Gaebler, Frauke Muecksch, et al. Structures of human antibodies bound to sars-cov-2 spike reveal common epitopes and recurrent features of antibodies. *Cell*, 182(4):828–842, 2020.

[10] Guillaume Beaudoin-Bussières, Annemarie Laumaea, Sai Priya Anand, Jérémie Prévost, Romain Gasser, Guillaume Goyette, Halima Medjahed, Josée Perreault, Tony Tremblay, Antoine Lewin, et al. Decline of humoral responses against sars-cov-2 spike in convalescent individuals. *MBio*, 11(5), 2020.

[11] Maureen Betton, Marine Livrozet, Delphine Planas, Antoine Fayol, Blandine Monel, Benoit Védie, Timothée Bruel, Eric Tartour, Nicolas Robillard, Jean-Claude Manuguerra, et al. Sera neutralizing activities against sars-cov-2 and multiple variants six month after hospitalization for covid-19. *Clinical Infectious Diseases*, 2021.

[12] Evan M Bloch, Shmuel Shoham, Arturo Casadevall, Bruce S Sachais, Beth Shaz, Jeffrey L Winters, Camille Van Buskirk, Brenda J Grossman, Michael Joyner, Jeffrey P Henderson, et al. Deployment of convalescent plasma for the prevention and treatment of covid-19. *The Journal of clinical investigation*, 130(6):2757–2765, 2020.

[13] Anna Bootz, Astrid Karbach, Johannes Spindler, Barbara Kropff, Nina Reuter, Heinrich Sticht, Thomas H Winkler, William J Britt, and Michael Mach. Protective capacity of neutralizing and non-neutralizing antibodies against glycoprotein b of cytomegalovirus. *PLoS pathogens*, 13(8):e1006601, 2017.

[14] Berend Jan Bosch, Ruurd Van der Zee, Cornelis AM De Haan, and Peter JM Rottier. The coronavirus spike protein is a class i virus fusion protein: structural and functional characterization of the fusion core complex. *Journal of virology*, 77(16):8801–8811, 2003.

[15] Børge Brende, Jeremy Farrar, Diane Gashumba, Carlos Moedas, Trevor Mundel, Yasuhisa Shiozaki, Harsh Vardhan, Johanna Wanka, and John-Arne Røttingen.

Cepi—a new global r&d organisation for epidemic preparedness and response. *The Lancet*, 389(10066):233–235, 2017.

[16] Andrew Bryan, Gregory Pepper, Mark H Wener, Susan L Fink, Chihiro Morishima, Anu Chaudhary, Keith R Jerome, Patrick C Mathias, and Alexander L Greninger. Performance characteristics of the abbott architect sars-cov-2 igg assay and seroprevalence in boise, idaho. *Journal of clinical microbiology*, 58(8), 2020.

[17] KA Callow, HF Parry, M Sergeant, and DAJ Tyrrell. The time course of the immune response to experimental coronavirus infection of man. *Epidemiology & Infection*, 105(2):435–446, 1990.

[18] Kathleen A Callow. Effect of specific humoral immunity and some non-specific factors on resistance of volunteers to respiratory coronavirus infection. *Epidemiology & Infection*, 95(1):173–189, 1985.

[19] George Carnell, Keith Grehan, Francesca Ferrara, Eleonora Molesti, and Nigel J Temperton. An optimised method for the production using pei, titration and neutralization of sars-cov spike luciferase pseudotypes. *Bio-protocol*, 7(16), 2017.

[20] James Brett Case, Paul W Rothlauf, Rita E Chen, Zhuoming Liu, Haiyan Zhao, Arthur S Kim, Louis-Marie Bloyet, Qiru Zeng, Stephen Tahan, Lindsay Droit, et al. Neutralizing antibody and soluble ace2 inhibition of a replication-competent vsv-sars-cov-2 and a clinical isolate of sars-cov-2. *Cell host & microbe*, 28(3):475–485, 2020.

[21] M.J. Chaisson and G. Tesler. Mapping single molecule sequencing reads using basic local alignment with successive refinement (blasr): application and thory. *BMC Bioinformatics*, 13, 2012.

[22] Xiangyu Chen, Ren Li, Zhiwei Pan, Chunfang Qian, Yang Yang, Renrong You, Jing Zhao, Pinghuang Liu, Leiqiong Gao, Zhirong Li, et al. Human monoclonal antibodies block the binding of sars-cov-2 spike protein to angiotensin converting enzyme 2 receptor. *Cellular & molecular immunology*, 17(6):647–649, 2020.

[23] Y Cheng, R Wong, YOY Soo, WS Wong, CK Lee, MHL Ng, P Chan, KC Wong, CB Leung, and G Cheng. Use of convalescent plasma therapy in sars patients in hong kong. *European Journal of Clinical Microbiology and Infectious Diseases*, 24(1):44–46, 2005.

[24] Xiaojing Chi, Xiuying Liu, Conghui Wang, Xinhui Zhang, Xiang Li, Jianhua Hou, Lili Ren, Qi Jin, Jianwei Wang, and Wei Yang. Humanized single domain antibodies neutralize sars-cov-2 by targeting the spike receptor binding domain. *Nature communications*, 11(1):1–7, 2020.

[25] Alex W H Chin, Julie T S Chu, Mahen R A Perera, Kenrie P Y Hui, Hui-Ling Yen, Michael C W Chan, Malik Peiris, and Leo L M Poon. Stability of sars-cov-2 in different environmental conditions. *The Lancet Microbe*, 1(1):e10, 2020.

[26] Pyoeng Gyun Choe, RAPM Perera, Wan Beom Park, Kyoung-Ho Song, Ji Hwan Bang, Eu Suk Kim, Hong Bin Kim, Long Wei Ronald Ko, Sang Won Park, Nam-Joong Kim, et al. Mers-cov antibody responses 1 year after symptom onset, south korea, 2015. *Emerging infectious diseases*, 23(7):1079, 2017.

[27] Helen Y Chu, Janet A Englund, Lea M Starita, Michael Famulare, Elisabeth Brandstetter, Deborah A Nickerson, Mark J Rieder, Amanda Adler, Kirsten Lacombe, Ashley E Kim, et al. Early detection of covid-19 through a citywide pandemic surveillance platform. *New England Journal of Medicine*, 383(2):185–187, 2020.

[28] Mary Dawn T Co, Masanori Terajima, Stephen J Thomas, Richard G Jarman, Kamonthip Rungrojcharoenkit, Stefan Fernandez, In-Kyu Yoon, Darunee Buddhari, John Cruz, and Francis A Ennis. Relationship of preexisting influenza hemagglutination inhibition, complement-dependent lytic, and antibody-dependent cellular cytotoxicity antibodies to the development of clinical illness in a prospective study of a (h1n1) pdm09 influenza in children. *Viral immunology*, 27(8):375–382, 2014.

[29] Davide Corti, Jincun Zhao, Mattia Pedotti, Luca Simonelli, Sudhakar Agnihothram, Craig Fett, Blanca Fernandez-Rodriguez, Mathilde Foglierini, Gloria Agatic, Fabrizia Vanzetta, et al. Prophylactic and postexposure efficacy of a potent human monoclonal antibody against mers coronavirus. *Proceedings of the National Academy of Sciences*, 112(33):10473–10478, 2015.

[30] François-Loic Cosset, Philippe Marianneau, Geraldine Verney, Fabrice Gallais, Noel Tordo, Eve-Isabelle Pécheur, Jan ter Meulen, Vincent Deubel, and Birke Bartosch. Characterization of lassa virus cell entry and neutralization with lassa virus pseudoparticles. *Journal of virology*, 83(7):3228–3237, 2009.

[31] Katharine HD Crawford, Adam S Dingens, Rachel Eguia, Caitlin R Wolf, Naomi Wilcox, Jennifer K Logue, Kiel Shuey, Amanda M Casto, Brooke Fiala, Samuel Wrenn, et al. Dynamics of neutralizing antibody titers in the months after severe

acute respiratory syndrome coronavirus 2 infection. *The Journal of infectious diseases*, 223(2):197–205, 2021.

[32] Katharine HD Crawford, Rachel Eguia, Adam S Dingens, Andrea N Loes, Keara D Malone, Caitlin R Wolf, Helen Y Chu, M Alejandra Tortorici, David Veesler, Michael Murphy, et al. Protocol and reagents for pseudotyping lentiviral particles with sars-cov-2 spike protein for neutralization assays. *Viruses*, 12(5):513, 2020.

[33] Adam P Cribbs, Alan Kennedy, Bernard Gregory, and Fionula M Brennan. Simplified production and concentration of lentiviral vectors to achieve high transduction in primary human t cells. *BMC biotechnology*, 13(1):1–8, 2013.

[34] James Cronin, Xian-Yang Zhang, and Jakob Reiser. Altering the tropism of lentiviral vectors through pseudotyping. *Current gene therapy*, 5(4):387–398, 2005.

[35] Warren Denning, Suvendu Das, Siqi Guo, Jun Xu, John C Kappes, and Zdenek Hel. Optimization of the transductional efficiency of lentiviral vectors: effect of sera and polycations. *Molecular biotechnology*, 53(3):308–314, 2013.

[36] M Eugenia Dieterle, Denise Haslwanter, Robert H Bortz III, Ariel S Wirchnianski, Gorka Lasso, Olivia Vergnolle, Shawn A Abbasi, J Maximilian Fels, Ethan Laudermilch, Catalina Florez, et al. A replication-competent vesicular stomatitis virus for studies of sars-cov-2 spike-mediated cell entry and its inhibition. *Cell host & microbe*, 28(3):486–496, 2020.

[37] Adam S Dingens, Dana Arenz, Haidyn Weight, Julie Overbaugh, and Jesse D Bloom. An antigenic atlas of hiv-1 escape from broadly neutralizing antibodies distinguishes functional and structural epitopes. *Immunity*, 50(2):520–532, 2019.

[38] Adam S Dingens, Katharine HD Crawford, Amanda Adler, Sarah L Steele, Kirsten Lacombe, Rachel Eguia, Fatima Amanat, Alexandra C Walls, Caitlin R Wolf, Michael Murphy, et al. Serological identification of sars-cov-2 infections among children visiting a hospital during the initial seattle outbreak. *Nature communications*, 11(1):1–6, 2020.

[39] Adam S Dingens, Hugh K Haddox, Julie Overbaugh, and Jesse D Bloom. Comprehensive mapping of hiv-1 escape from a broadly neutralizing antibody. *Cell host & microbe*, 21(6):777–787, 2017.

[40] Roger Y Dodd and Susan L Stramer. Covid-19 and blood safety: help with a dilemma. *Transfusion medicine reviews*, 2020.

[41] Michael B Doud and Jesse D Bloom. Accurate measurement of the effects of all amino-acid mutations on influenza hemagglutinin. *Viruses*, 8(6):155, 2016.

[42] Michael B Doud, Scott E Hensley, and Jesse D Bloom. Complete mapping of viral escape from neutralizing antibodies. *PLoS pathogens*, 13(3):e1006271, 2017.

[43] Kai Duan, Bende Liu, Cesheng Li, Huajun Zhang, Ting Yu, Jieming Qu, Min Zhou, Li Chen, Shengli Meng, Yong Hu, et al. Effectiveness of convalescent plasma therapy in severe covid-19 patients. *Proceedings of the National Academy of Sciences*, 117(17):9490–9496, 2020.

[44] Tom Dull, Romain Zufferey, Michael Kelly, RJ Mandel, Minh Nguyen, Didier Trono, and Luigi Naldini. A third-generation lentivirus vector with a conditional packaging system. *Journal of virology*, 72(11):8463–8471, 1998.

[45] Debra M Eckert and Peter S Kim. Mechanisms of viral membrane fusion and its inhibition. *Annual review of biochemistry*, 70(1):777–810, 2001.

[46] Daniel Ellis, Natalie Brunette, Katharine HD Crawford, Alexandra C Walls, Minh N Pham, Chengbo Chen, Karla-Luise Herpoldt, Brooke Fiala, Michael Murphy, Deleah Pettie, et al. Stabilization of the sars-cov-2 spike receptor-binding domain using deep mutational scanning and structure-based design. *bioRxiv*, 2021.

[47] Christine M Fennessey, Mykola Pinkevych, Taina T Immonen, Arnold Reynaldi, Vanessa Venturi, Priyanka Nadella, Carolyn Reid, Laura Newman, Leslie Lipkey, Kelli Oswald, et al. Genetically-barcoded siv facilitates enumeration of rebound variants and estimation of reactivation rates in nonhuman primates following interruption of suppressive antiretroviral therapy. *PLoS pathogens*, 13(5):e1006359, 2017.

[48] Katja Fink. Origin and function of circulating plasmablasts during acute viral infections. *Frontiers in immunology*, 3:78, 2012.

[49] US Food and Drug Administration. Recommendations for investigational covid-19 convalescent plasma. `https://www.fda.gov/vaccines-blood-biologics/investigational-new-drug-ind-or-device-exemption-ide-process-cber/recommendations-investigational-covid-19-convalescent-plasma`, 2020. Accessed: 2020-07-20.

[50] Center for Systems Science and Engineering (CSSE). Covid-19 dashboard. `https://coronavirus.jhu.edu/map.html`, 2021. Accessed: 2021-05-11.

[51] D.M. Fowler and S. Fields. Deep mutational scanning: a new style ofo protein science. *Nature Methods*, 11, 2014.

[52] Shuetsu Fukushi, Tetsuya Mizutani, Masayuki Saijo, Shutoku Matsuyama, Naoko Miyajima, Fumihiro Taguchi, Shigeyuki Itamura, Ichiro Kurane, and Shigeru Morikawa. Vesicular stomatitis virus pseudotyped with severe acute respiratory syndrome coronavirus spike protein. *Journal of General Virology*, 86(8):2269–2274, 2005.

[53] Christian Gaebler, Zijun Wang, Julio CC Lorenzi, Frauke Muecksch, Shlomo Finkin, Minami Tokuyama, Alice Cho, Mila Jankovic, Dennis Schaefer-Babajew, Thiago Y Oliveira, et al. Evolution of antibody immunity to sars-cov-2. *Nature*, 591(7851):639–644, 2021.

[54] Tsanan Giroglou, Jindrich Cinatl, Holger Rabenau, Christian Drosten, Harald Schwalbe, Hans Wilhelm Doerr, and Dorothee Von Laer. Retroviral vectors pseudotyped with severe acute respiratory syndrome coronavirus s protein. *Journal of virology*, 78(17):9007–9015, 2004.

[55] Allison J Greaney, Andrea N Loes, Katharine HD Crawford, Tyler N Starr, Keara D Malone, Helen Y Chu, and Jesse D Bloom. Comprehensive mapping of mutations to the sars-cov-2 receptor-binding domain that affect recognition by polyclonal human plasma antibodies. *Cell host & microbe*, 29(3):463–476, 2021.

[56] Allison J Greaney, Andrea N Loes, Lauren E Gentles, Katharine HD Crawford, Tyler N Starr, Keara D Malone, Helen Y Chu, and Jesse D Bloom. The sars-cov-2 mrna-1273 vaccine elicits more rbd-focused neutralization, but with broader antibody binding within the rbd. *bioRxiv*, 2021.

[57] Allison J Greaney, Tyler N Starr, Pavlo Gilchuk, Seth J Zost, Elad Binshtein, Andrea N Loes, Sarah K Hilton, John Huddleston, Rachel Eguia, Katharine HD Crawford, et al. Complete mapping of mutations to the sars-cov-2 spike receptor-binding domain that escape antibody recognition. *Cell host & microbe*, 29(1):44–57, 2021.

[58] Keith Grehan, Francesca Ferrara, and N Temperton. An optimised method for the production of mers-cov spike expressing viral pseudotypes. *MethodsX*, 2:379–384, 2015.

[59] Bronwyn M Gunn, Wen-Han Yu, Marcus M Karim, Jennifer M Brannan, Andrew S Herbert, Anna Z Wec, Peter J Halfmann, Marnie L Fusco, Sharon L Schendel, Karthik Gangavarapu, et al. A role for fc function in therapeutic monoclonal antibody-mediated protection against ebola virus. *Cell host & microbe*, 24(2):221–233, 2018.

[60] Maximillian S Habibi, Agnieszka Jozwik, Spyridon Makris, Jake Dunning, Allan Paras, John P DeVincenzo, Cornelis AM de Haan, Jens Wrammert, Peter JM Openshaw, and Christopher Chiu. Impaired antibody-mediated protection and defective iga b-cell memory in experimental infection of adults with respiratory syncytial virus. *American journal of respiratory and critical care medicine*, 191(9):1040–1049, 2015.

[61] Hugh K Haddox, Adam S Dingens, and Jesse D Bloom. Experimental estimation of the effects of all amino-acid mutations to hiv's envelope protein on viral replication in cell culture. *PLoS pathogens*, 12(12):e1006114, 2016.

[62] Paul A Harris, Robert Taylor, Robert Thielke, Jonathon Payne, Nathaniel Gonzalez, and Jose G Conde. Research electronic data capture (redcap)—a metadata-driven methodology and workflow process for providing translational research informatics support. *Journal of biomedical informatics*, 42(2):377–381, 2009.

[63] Stephen C Harrison. Viral membrane fusion. *Virology*, 479:498–507, 2015.

[64] Kathryn M Hastie, Michelle A Zandonatti, Lara M Kleinfelter, Megan L Heinrich, Megan M Rowland, Kartik Chandran, Luis M Branco, James E Robinson, Robert F Garry, and Erica Ollmann Saphire. Structural basis for antibody-mediated neutralization of lassa virus. *Science*, 356(6341):923–928, 2017.

[65] P.D.N. Hebert, T.W.A. Braukmann, S.W.J. Prosser, S. Ratnasingham, J.R. deWaard, N.V. Ivanova, D.H. Janzen, W. Hallwachs, S. Naik, J.E. Sones, and E.V. Zakharov. A sequel to sanger: amplicon sequencing that scales. *BMC Genomics*, 19, 2018.

[66] Gunilla B Karlsson Hedestam, Ron AM Fouchier, Sanjay Phogat, Dennis R Burton, Joseph Sodroski, and Richard T Wyatt. The challenges of eliciting neutralizing antibodies to hiv-1 and to influenza virus. *Nature Reviews Microbiology*, 6(2):143–155, 2008.

[67] J.B. Hiatt, R.P. Patwardhan, E.H. Turner, C. Lee, and J. Shendure. Parallel, tag-directed assembly of locally derived short sequence reads. *Nature Methods*, 7, 2010.

[68] Mei-Shang Ho, Wei-Ju Chen, Hour-Young Chen, Szu-Fong Lin, Min-Chin Wang, Jiali Di, Yen-Ta Lu, Ching-Lung Liu, Shan-Chwen Chang, Chung-Liang Chao, et al. Neutralizing antibody response and sars severity. *Emerging infectious diseases*, 11(11):1730, 2005.

[69] Emma B Hodcroft, Moira Zuber, Sarah Nadeau, Timothy G Vaughan, Katharine HD Crawford, Christian L Althaus, Martina L Reichmuth, John E Bowen, Alexandra C Walls, Davide Corti, et al. Spread of a sars-cov-2 variant through europe in the summer of 2020. *Nature*, pages 1–9, 2021.

[70] Markus Hoffmann, Hannah Kleine-Weber, Simon Schroeder, Nadine Krüger, Tanja Herrler, Sandra Erichsen, Tobias S Schiergens, Georg Herrler, Nai-Huei Wu, Andreas Nitsche, et al. Sars-cov-2 cell entry depends on ace2 and tmprss2 and is blocked by a clinically proven protease inhibitor. *cell*, 181(2):271–280, 2020.

[71] Yuan Huang, Chan Yang, Xin-feng Xu, Wei Xu, and Shu-wen Liu. Structural and functional properties of sars-cov-2 spike protein: potential antivirus drug development for covid-19. *Acta Pharmacologica Sinica*, 41(9):1141–1149, 2020.

[72] Baweleta Isho, Kento T Abe, Michelle Zuo, Alainna J Jamal, Bhavisha Rathod, Jenny H Wang, Zhijie Li, Gary Chao, Olga L Rojas, Yeo Myong Bang, et al. Persistence of serum and saliva antibody responses to sars-cov-2 spike antigens in covid-19 patients. *Science immunology*, 5(52), 2020.

[73] Wei Jiang, Rui Hua, Mengping Wei, Chenhong Li, Zilong Qiu, Xiaofei Yang, and Chen Zhang. An optimized method for high-titer lentivirus preparations without ultracentrifugation. *Scientific reports*, 5(1):1–9, 2015.

[74] M Gordon Joyce, Rajeshwer S Sankhala, Wei-Hung Chen, Misook Choe, Hongjun Bai, Agnes Hajduczki, Lianying Yan, Spencer L Sterling, Caroline E Peterson, Ethan C Green, et al. A cryptic site of vulnerability on the receptor binding domain of the sars-cov-2 spike glycoprotein. *bioRxiv*, 2020.

[75] Bin Ju, Qi Zhang, Jiwan Ge, Ruoke Wang, Jing Sun, Xiangyang Ge, Jiazhen Yu, Sisi Shan, Bing Zhou, Shuo Song, et al. Human neutralizing antibodies elicited by sars-cov-2 infection. *Nature*, 584(7819):115–119, 2020.

[76] Sagar U Kapadia, John K Rose, Elaine Lamirande, Leatrice Vogel, Kanta Subbarao, and Anjeanette Roberts. Long-term protection from sars coronavirus infection conferred by a single immunization with an attenuated vsv-based vaccine. *Virology*, 340(2):174–182, 2005.

[77] Saahir Khan, Rie Nakajima, Aarti Jain, Rafael Ramiro De Assis, Al Jasinskas, Joshua M Obiero, Oluwasanmi Adenaiye, Sheldon Tai, Filbert Hong, Donald K Milton, et al. Analysis of serologic cross-reactivity between common human coronaviruses and sars-cov-2 using coronavirus antigen microarray. *bioRxiv*, 2020.

[78] Robert N Kirchdoerfer, Christopher A Cottrell, Nianshuang Wang, Jesper Pallesen, Hadi M Yassine, Hannah L Turner, Kizzmekia S Corbett, Barney S Graham, Jason S McLellan, and Andrew B Ward. Pre-fusion structure of a human coronavirus spike protein. *Nature*, 531(7592):118–121, 2016.

[79] Natsuko Kishishita, Naokazu Takeda, Atchareeya Anuegoonpipat, and Surapee Anantapreecha. Development of a pseudotyped-lentiviral-vector-based neutralization assay for chikungunya virus infection. *Journal of clinical microbiology*, 51(5):1389–1395, 2013.

[80] Gary P Kobinger, Daniel J Weiner, Qian-Chun Yu, and James M Wilson. Filovirus-pseudotyped lentiviral vector can efficiently and stably transduce airway epithelia in vivo. *Nature biotechnology*, 19(3):225–230, 2001.

[81] Bette Korber, Will M Fischer, Sandrasegaram Gnanakaran, Hyejin Yoon, James Theiler, Werner Abfalterer, Nick Hengartner, Elena E Giorgi, Tanmoy Bhattacharya, Brian Foley, et al. Tracking changes in sars-cov-2 spike: evidence that d614g increases infectivity of the covid-19 virus. *Cell*, 182(4):812–827, 2020.

[82] Akshay T Krishnamurty, Christopher D Thouvenel, Silvia Portugal, Gladys J Keitany, Karen S Kim, Anthony Holder, Peter D Crompton, David J Rawlings, and Marion Pepper. Somatically hypermutated plasmodium-specific igm+ memory b cells are rapid, plastic, early responders upon malaria rechallenge. *Immunity*, 45(2):402–414, 2016.

[83] Leticia Kuri-Cervantes, M Betina Pampena, Wenzhao Meng, Aaron M Rosenfeld, Caroline AG Ittner, Ariel R Weisman, Roseline S Agyekum, Divij Mathew, Amy E Baxter, Laura A Vella, et al. Comprehensive mapping of immune perturbations associated with severe covid-19. *Science immunology*, 5(49), 2020.

[84] Alona Kuzmina, Yara Khalaila, Olga Voloshin, Ayelet Keren-Naus, Liora Boehm-Cohen, Yael Raviv, Yonat Shemer-Avni, Elli Rosenberg, and Ran Taube. Sars-cov-2 spike variants exhibit differential infectivity and neutralization resistance to convalescent or post-vaccination sera. *Cell host & microbe*, 29(4):522–528, 2021.

[85] Jonathan H Lam and Nicole Baumgarth. The multifaceted b cell response to influenza virus. *The Journal of Immunology*, 202(2):351–359, 2019.

[86] Adam S Lauring and Emma B Hodcroft. Genetic variants of sars-cov-2—what do they mean? *JAMA*, 2021.

[87] Juhye M Lee, John Huddleston, Michael B Doud, Kathryn A Hooper, Nicholas C Wu, Trevor Bedford, and Jesse D Bloom. Deep mutational scanning of hemagglutinin helps predict evolutionary fates of human h3n2 influenza variants. *Proceedings of the National Academy of Sciences*, 115(35):E8276–E8285, 2018.

[88] Changhai Lei, Kewen Qian, Tian Li, Sheng Zhang, Wenyan Fu, Min Ding, and Shi Hu. Neutralization of sars-cov-2 spike pseudotyped virus by recombinant ace2-ig. *Nature communications*, 11(1):1–5, 2020.

[89] Qing Lei, Yang Li, Hong-yan Hou, Feng Wang, Zhu-qing Ouyang, Yandi Zhang, Dan-yun Lai, Jo-Lewis Banga Ndzouboukou, Zhao-wei Xu, Bo Zhang, et al. Antibody dynamics to sars-cov-2 in asymptomatic covid-19 infections. *Allergy*, 76(2):551–561, 2021.

[90] Sandra Lester, Jennifer Harcourt, Michael Whitt, Hail M Al-Abdely, Claire M Midgley, Abdulrahim M Alkhamis, Hani A Aziz Jokhdar, Abdullah M Assiri, Azaibi Tamin, and Natalie Thornburg. Middle east respiratory coronavirus (mers-cov) spike (s) protein vesicular stomatitis virus pseudoparticle neutralization assays offer a reliable alternative to the conventional neutralization assay in human seroepidemiological studies. *Access microbiology*, 1(9), 2019.

[91] Michael Letko, Andrea Marzi, and Vincent Munster. Functional assessment of cell entry and receptor usage for sars-cov-2 and other lineage b betacoronaviruses. *Nature microbiology*, 5(4):562–569, 2020.

[92] Fang Li. Structure, function, and evolution of coronavirus spike proteins. *Annual review of virology*, 3:237–261, 2016.

[93] H. Li. Minimap2: pairwise alignment for nucleotide sequences. *Bioinformatics*, 34:3094–3100, 2018.

[94] Zhuoming Liu, Laura A VanBlargan, Louis-Marie Bloyet, Paul W Rothlauf, Rita E Chen, Spencer Stumpf, Haiyan Zhao, John M Errico, Elitza S Theel, Mariel J Liebeskind, et al. Identification of sars-cov-2 spike mutations that attenuate monoclonal and serum antibody neutralization. *Cell host & microbe*, 29(3):477–488, 2021.

[95] Quan-Xin Long, Bai-Zhong Liu, Hai-Jun Deng, Gui-Cheng Wu, Kun Deng, Yao-Kai Chen, Pu Liao, Jing-Fu Qiu, Yong Lin, Xue-Fei Cai, et al. Antibody responses to sars-cov-2 in patients with covid-19. *Nature medicine*, 26(6):845–848, 2020.

[96] Quan-Xin Long, Xiao-Jun Tang, Qiu-Lin Shi, Qin Li, Hai-Jun Deng, Jun Yuan, Jie-Li Hu, Wei Xu, Yong Zhang, Fa-Jin Lv, et al. Clinical and immunological assessment of asymptomatic sars-cov-2 infections. *Nature medicine*, 26(8):1200–1204, 2020.

[97] Huibin Lv, Nicholas C Wu, Owen Tak-Yin Tsang, Meng Yuan, Ranawaka APM Perera, Wai Shing Leung, Ray TY So, Jacky Man Chun Chan, Garrick K Yip, Thomas Shiu Hong Chik, et al. Cross-reactive antibody response between sars-cov-2 and sars-cov infections. *Cell reports*, 31(9):107725, 2020.

[98] Jessica Marcandalli, Brooke Fiala, Sebastian Ols, Michela Perotti, Willem de van der Schueren, Joost Snijder, Edgar Hodge, Mark Benhaim, Rashmi Ravichandran, Lauren Carter, et al. Induction of potent neutralizing antibody responses by a designed protein nanoparticle vaccine for respiratory syncytial virus. *Cell*, 176(6):1420–1431, 2019.

[99] K.A. Matreyek, L.M. Starita, J.J. Stephany, B. Martin, M.A. Chiasson, V.E. Gray, M. Kircher, A. Khechaduri, J.N. Dines, R.J. Hause, S Bhatia, W.E. Evans, M.V. Relling, W. Yang, J. Shendure, and D.M. Fowler. Multiplex assessment of protein variant abundance by massively parallel sequencing. *Nature Genetics*, 50:874–882, 2018.

[100] Mikhail Matrosovich, Alexander Tuzikov, Nikolai Bovin, Alexandra Gambaryan, Alexander Klimov, Maria R Castrucci, Isabella Donatelli, and Yoshihiro Kawaoka. Early alterations of the receptor-binding properties of h1, h2, and h3 avian influenza virus hemagglutinins after their introduction into mammals. *Journal of virology*, 74(18):8502–8512, 2000.

[101] Corrin E McBride, Jie Li, and Carolyn E Machamer. The cytoplasmic tail of the severe acute respiratory syndrome coronavirus spike protein contains a novel endoplasmic reticulum retrieval signal that binds copi and promotes interaction with membrane protein. *Journal of virology*, 81(5):2418–2428, 2007.

[102] Vineet D Menachery, Boyd L Yount, Amy C Sims, Kari Debbink, Sudhakar S Agnihothram, Lisa E Gralinski, Rachel L Graham, Trevor Scobey, Jessica A Plante, Scott R Royal, et al. Sars-like wiv1-cov poised for human emergence. *Proceedings of the National Academy of Sciences*, 113(11):3048–3053, 2016.

[103] Jean Kaoru Millet and Gary R Whittaker. Murine leukemia virus (mlv)-based coronavirus spike-pseudotyped particle production and infection. *Bio-protocol*, 6(23), 2016.

[104] Chad E Mire, Robert W Cross, Joan B Geisbert, Viktoriya Borisevich, Krystle N Agans, Daniel J Deer, Megan L Heinrich, Megan M Rowland, Augustine Goba, Mambu Momoh, et al. Human-monoclonal-antibody therapy protects nonhuman primates against advanced lassa fever. *Nature medicine*, 23(10):1146, 2017.

[105] Michael J Moore, Tatyana Dorfman, Wenhui Li, Swee Kee Wong, Yanhan Li, Jens H Kuhn, James Coderre, Natalya Vasilieva, Zhongchao Han, Thomas C Greenough, et al. Retroviruses pseudotyped with the severe acute respiratory syndrome coronavirus spike protein efficiently infect cells expressing angiotensin-converting enzyme 2. *Journal of virology*, 78(19):10628–10635, 2004.

[106] Kouki Morizono and Irvin SY Chen. Receptors and tropisms of envelope viruses. *Current opinion in virology*, 1(1):13–18, 2011.

[107] Adrian QN Mylne, David M Pigott, Joshua Longbottom, Freya Shearer, Kirsten A Duda, Jane P Messina, Daniel J Weiss, Catherine L Moyes, Nick Golding, and Simon I Hay. Mapping the zoonotic niche of lassa fever in africa. *Transactions of the Royal Society of Tropical Medicine and Hygiene*, 109(8):483–492, 2015.

[108] Luigi Naldini, Ulrike Blömer, Philippe Gallay, Daniel Ory, Richard Mulligan, Fred H Gage, Inder M Verma, and Didier Trono. In vivo gene delivery and stable transduction of nondividing cells by a lentiviral vector. *Science*, 272(5259):263–267, 1996.

[109] Jianhui Nie, Qianqian Li, Jiajing Wu, Chenyan Zhao, Huan Hao, Huan Liu, Li Zhang, Lingling Nie, Haiyang Qin, Meng Wang, et al. Establishment and validation of a pseudovirus neutralization assay for sars-cov-2. *Emerging microbes & infections*, 9(1):680–686, 2020.

[110] Jianhui Nie, Xiaohong Wu, Jian Ma, Shouchun Cao, Weijin Huang, Qiang Liu, Xuguang Li, Yuhua Li, and Youchun Wang. Development of in vitro and in vivo rabies virus neutralization assays based on a high-titer pseudovirus system. *Scientific reports*, 7(1):1–12, 2017.

[111] Nisreen MA Okba, Marcel A Müller, Wentao Li, Chunyan Wang, Corine H GeurtsvanKessel, Victor M Corman, Mart M Lamers, Reina S Sikkema, Erwin de Bruin, Felicity D Chandler, et al. Severe acute respiratory syndrome coronavirus

2- specific antibody responses in coronavirus disease patients. *Emerging infectious diseases*, 26(7):1478–1488, 2020.

[112] World Health Organization et al. Annual review of diseases prioritized under the research and development blueprint. In *Workshop on Prioritization of Pathogens*, 2018.

[113] Xiuyuan Ou, Yan Liu, Xiaobo Lei, Pei Li, Dan Mi, Lili Ren, Li Guo, Ruixuan Guo, Ting Chen, Jiaxin Hu, et al. Characterization of spike glycoprotein of sars-cov-2 on virus entry and its immune cross-reactivity with sars-cov. *Nature communications*, 11(1):1–12, 2020.

[114] Kathleen A Page, NATHANIEL R Landau, and DR Littman. Construction and use of a human immunodeficiency virus vector for analysis of virus infectivity. *Journal of virology*, 64(11):5270–5276, 1990.

[115] Jesper Pallesen, Nianshuang Wang, Kizzmekia S Corbett, Daniel Wrapp, Robert N Kirchdoerfer, Hannah L Turner, Christopher A Cottrell, Michelle M Becker, Lingshu Wang, Wei Shi, et al. Immunogenicity and structures of a rationally designed prefusion mers-cov spike antigen. *Proceedings of the National Academy of Sciences*, 114(35):E7348–E7357, 2017.

[116] Michael J Peluso, Saki Takahashi, Jill Hakim, J Daniel Kelly, Leonel Torres, Nikita S Iyer, Keirstinne Turcios, Owen Janson, Sadie E Munter, Cassandra Thanh, et al. Sars-cov-2 antibody magnitude and detectability are driven by disease severity, timing, and assay. *medRxiv*, 2021.

[117] Josée Perreault, Tony Tremblay, Marie-Josée Fournier, Mathieu Drouin, Guillaume Beaudoin-Bussières, Jérémie Prévost, Antoine Lewin, Philippe Bégin, Andrés Finzi, and Renée Bazin. Waning of sars-cov-2 rbd antibodies in longitudinal convalescent plasma samples within 4 months after symptom onset. *Blood, The Journal of the American Society of Hematology*, 136(22):2588–2591, 2020.

[118] Luca Piccoli, Young-Jun Park, M Alejandra Tortorici, Nadine Czudnochowski, Alexandra C Walls, Martina Beltramello, Chiara Silacci-Fregni, Dora Pinto, Laura E Rosen, John E Bowen, et al. Mapping neutralizing and immunodominant sites on the sars-cov-2 spike receptor-binding domain by structure-guided high-resolution serology. *Cell*, 183(4):1024–1042, 2020.

[119] Pedro A Piedra, Alan M Jewell, Stanley G Cron, Robert L Atmar, and W Paul Glezen. Correlates of immunity to respiratory syncytial virus (rsv) associated-hospitalization: establishment of minimum protective threshold levels of serum neutralizing antibodies. *Vaccine*, 21(24):3479–3482, 2003.

[120] Dora Pinto, Young-Jun Park, Martina Beltramello, Alexandra C Walls, M Alejandra Tortorici, Siro Bianchi, Stefano Jaconi, Katja Culap, Fabrizia Zatta, Anna De Marco, et al. Cross-neutralization of sars-cov-2 by a human monoclonal sars-cov antibody. *Nature*, 583(7815):290–295, 2020.

[121] Delphine Planas, Timothée Bruel, Ludivine Grzelak, Florence Guivel-Benhassine, Isabelle Staropoli, Françoise Porrot, Cyril Planchais, Julian Buchrieser, Maaran Michael Rajah, Elodie Bishop, et al. Sensitivity of infectious sars-cov-2 b. 1.1. 7 and b. 1.351 variants to neutralizing antibodies. *Nature medicine*, pages 1–8, 2021.

[122] Brian D Quinlan, Huihui Mou, Lizhou Zhang, Yan Guo, Wenhui He, Amrita Ojha, Mark S Parcells, Guangxiang Luo, Wenhui Li, Guocai Zhong, et al. The sars-cov-2 receptor-binding domain elicits a potent neutralizing response without antibody-dependent enhancement. *IMMUNITY-D-20-00389*, 2020.

[123] Sylvia E Reed. The behaviour of recent isolates of human respiratory coronavirus in vitro and in volunteers: evidence of heterogeneity among 229e-related strains. *Journal of medical virology*, 13(2):179–192, 1984.

[124] Felix A Rey and Shee-Mei Lok. Common features of enveloped viruses and implications for immunogen design for next-generation vaccines. *Cell*, 172(6):1319–1334, 2018.

[125] A. Rhoads and K.F. Au. Pacbio sequencing and its applications. *Genomics, Proteomics & Bioinformatics*, 13:278–279, October 2015.

[126] Davide F Robbiani, Christian Gaebler, Frauke Muecksch, Julio CC Lorenzi, Zijun Wang, Alice Cho, Marianna Agudelo, Christopher O Barnes, Anna Gazumyan, Shlomo Finkin, et al. Convergent antibody responses to sars-cov-2 in convalescent individuals. *Nature*, 584(7821):437–442, 2020.

[127] James E Robinson, Kathryn M Hastie, Robert W Cross, Rachael E Yenni, Deborah H Elliott, Julie A Rouelle, Chandrika B Kannadka, Ashley A Smira, Courtney E

Garry, Benjamin T Bradley, et al. Most neutralizing human monoclonal antibodies target novel epitopes requiring both lassa virus glycoprotein subunits. *Nature communications*, 7(1):1–14, 2016.

[128] Barry Rockx, Davide Corti, Eric Donaldson, Timothy Sheahan, Konrad Stadler, Antonio Lanzavecchia, and Ralph Baric. Structural basis for potent cross-neutralizing human monoclonal antibody protection against lethal human and zoonotic severe acute respiratory syndrome coronavirus challenge. *Journal of virology*, 82(7):3220–3235, 2008.

[129] Thomas F Rogers, Fangzhu Zhao, Deli Huang, Nathan Beutler, Alison Burns, Wanting He, Oliver Limbo, Chloe Smith, Ge Song, Jordan Woehl, et al. Isolation of potent sars-cov-2 neutralizing antibodies and protection from disease in a small animal model. *Science*, 369(6506):956–963, 2020.

[130] A.B. Russell, E. Elshina, J.R. Kowalsky, A.J.W. te Velthuis, and J.D. Bloom. Single-cell virus sequencing of influenza infections that trigger innate immunity. *Journal of Virology*, 93:e00500–19, 2019.

[131] Marion Russier, Delphine Pannetier, and Sylvain Baize. Immune responses and lassa virus infection. *Viruses*, 4(11):2766–2785, 2012.

[132] Jibin Sadasivan, Manmeet Singh, and Jayasri Das Sarma. Cytoplasmic tail of coronavirus spike protein has intracellular targeting signals. *Journal of biosciences*, 42(2):231–244, 2017.

[133] Eric Salazar, Suresh V Kuchipudi, Paul A Christensen, Todd Eagar, Xin Yi, Picheng Zhao, Zhicheng Jin, S Wesley Long, Randall J Olsen, Jian Chen, et al. Convalescent plasma anti–sars-cov-2 spike protein ectodomain and receptor-binding domain igg correlate with virus neutralization. *The Journal of clinical investigation*, 130(12):6728–6738, 2020.

[134] E.W. Sayers, M. Cavanaugh, K. Clark, J. Ostell, K.D. Pruitt, and I. Karsch-Mizrachi. Genbank. *Nucleic Acids Research*, October 2019. gkz956.

[135] Fabian Schmidt, Yiska Weisblum, Frauke Muecksch, Hans-Heinrich Hoffmann, Eleftherios Michailidis, Julio CC Lorenzi, Pilar Mendoza, Magdalena Rutkowska, Eva Bednarski, Christian Gaebler, et al. Measuring sars-cov-2 neutralizing antibody activity using pseudotyped and chimeric viruses. *Journal of Experimental Medicine*, 217(11), 2020.

[136] Christel Schwegmann-Weßels, Jörg Glende, Xiaofeng Ren, Xiuxia Qu, Hongkui Deng, Luis Enjuanes, and Georg Herrler. Comparison of vesicular stomatitis virus pseudotyped with the s proteins from a porcine and a human coronavirus. *Journal of general virology*, 90(7):1724–1729, 2009.

[137] Jeffrey Seow, Carl Graham, Blair Merrick, Sam Acors, Suzanne Pickering, Kathryn JA Steel, Oliver Hemmings, Aoife O'Byrne, Neophytos Kouphou, Rui Pedro Galao, et al. Longitudinal observation and decline of neutralizing antibody responses in the three months following sars-cov-2 infection in humans. *Nature Microbiology*, 5(12):1598–1607, 2020.

[138] Priyanka Shah, Gabriela A Canziani, Erik P Carter, and Irwin Chaiken. The case for s2: The potential benefits of the s2 subunit of the sars-cov-2 spike protein as an immunogen in fighting the covid-19 pandemic. *Frontiers in Immunology*, 12:508, 2021.

[139] Patrick L Sinn, Jeremy E Coffin, Natarajan Ayithan, Kathleen H Holt, and Wendy Maury. Lentiviral vectors pseudotyped with filoviral glycoproteins. In *Ebolaviruses*, pages 65–78. Springer, 2017.

[140] Rami Sommerstein, Lukas Flatz, Melissa M Remy, Pauline Malinge, Giovanni Magistrelli, Nicolas Fischer, Mehmet Sahin, Andreas Bergthaler, Sebastien Igonet, Jan Ter Meulen, et al. Arenavirus glycan shield promotes neutralizing antibody evasion and protracted infection. *PLoS pathogens*, 11(11):e1005276, 2015.

[141] YOY Soo, Y Cheng, R Wong, DS Hui, CK Lee, KKS Tsang, MHL Ng, P Chan, G Cheng, and JJY Sung. Retrospective comparison of convalescent plasma with continuing high-dose methylprednisolone treatment in sars patients. *Clinical microbiology and infection*, 10(7):676–678, 2004.

[142] Daniel Stadlbauer, Fatima Amanat, Veronika Chromikova, Kaijun Jiang, Shirin Strohmeier, Guha Asthagiri Arunkumar, Jessica Tan, Disha Bhavsar, Christina Capuano, Ericka Kirkpatrick, et al. Sars-cov-2 seroconversion in humans: a detailed protocol for a serological assay, antigen production, and test setup. *Current protocols in microbiology*, 57(1):e100, 2020.

[143] Tyler N Starr, Allison J Greaney, Sarah K Hilton, Daniel Ellis, Katharine HD Crawford, Adam S Dingens, Mary Jane Navarro, John E Bowen, M Alejandra Tortorici, Alexandra C Walls, et al. Deep mutational scanning of sars-cov-2 receptor binding

domain reveals constraints on folding and ace2 binding. *Cell*, 182(5):1295–1310, 2020.

[144] Delphine Sterlin, Alexis Mathian, Makoto Miyara, Audrey Mohr, François Anna, Laetitia Claër, Paul Quentric, Jehane Fadlallah, Hervé Devilliers, Pascale Ghillani, et al. Iga dominates the early neutralizing antibody response to sars-cov-2. *Science translational medicine*, 13(577), 2021.

[145] Kanta Subbarao, Josephine McAuliffe, Leatrice Vogel, Gary Fahle, Steven Fischer, Kathleen Tatti, Michelle Packard, Wun-Ju Shieh, Sherif Zaki, and Brian Murphy. Prior infection and passive transfer of neutralizing antibody prevent replication of severe acute respiratory syndrome coronavirus in the respiratory tract of mice. *Journal of virology*, 78(7):3572–3577, 2004.

[146] Mehul S Suthar, Matthew G Zimmerman, Robert C Kauffman, Grace Mantus, Susanne L Linderman, William H Hudson, Abigail Vanderheiden, Lindsay Nyhoff, Carl W Davis, Oluwaseyi Adekunle, et al. Rapid generation of neutralizing antibody responses in covid-19 patients. *Cell Reports Medicine*, 1(3):100040, 2020.

[147] Wanbo Tai, Xiujuan Zhang, Aleksandra Drelich, Juan Shi, Jason C Hsu, Larry Luchsinger, Christopher D Hillyer, Chien-Te K Tseng, Shibo Jiang, and Lanying Du. A novel receptor-binding domain (rbd)-based mrna vaccine against sars-cov-2. *Cell research*, 30(10):932–935, 2020.

[148] Nigel J Temperton, Paul K Chan, Graham Simmons, Maria C Zambon, Richard S Tedder, Yasuhiro Takeuchi, and Robin A Weiss. Longitudinally profiling neutralizing antibody response to sars coronavirus with pseudotypes. *Emerging infectious diseases*, 11(3):411, 2005.

[149] Xiaolong Tian, Cheng Li, Ailing Huang, Shuai Xia, Sicong Lu, Zhengli Shi, Lu Lu, Shibo Jiang, Zhenlin Yang, Yanling Wu, et al. Potent binding of 2019 novel coronavirus spike protein by a sars coronavirus-specific human monoclonal antibody. *Emerging microbes & infections*, 9(1):382–385, 2020.

[150] Kelvin KW To, Anna JX Zhang, Ivan FN Hung, Ting Xu, Whitney CT Ip, Rebecca TY Wong, Joseph CK Ng, Jasper FW Chan, Kwok-Hung Chan, and Kwok-Yung Yuen. High titer and avidity of nonneutralizing antibodies against influenza vaccine antigen are associated with severe influenza. *Clinical and Vaccine Immunology*, 19(7):1012–1018, 2012.

[151] Kamilla Toon, Emma M Bentley, and Giada Mattiuzzo. More than just gene therapy vectors: Lentiviral vector pseudotypes for serological investigation. *Viruses*, 13(2):217, 2021.

[152] Benjamin Trinité, Ferran Tarrés-Freixas, Jordi Rodon, Edwards Pradenas, Víctor Urrea, Silvia Marfil, María Luisa Rodríguez de la Concepción, Carlos Ávila-Nieto, Carmen Aguilar-Gurrieri, Ana Barajas, et al. Sars-cov-2 infection elicits a rapid neutralizing antibody response that correlates with disease severity. *Scientific reports*, 11(1):1–10, 2021.

[153] Konstantin A Tsetsarkin, Dana L Vanlandingham, Charles E McGee, and Stephen Higgs. A single mutation in chikungunya virus affects vector specificity and epidemic potential. *PLOS pathog*, 3(12):e201, 2007.

[154] Philip V'kovski, Annika Kratzel, Silvio Steiner, Hanspeter Stalder, and Volker Thiel. Coronavirus biology and replication: implications for sars-cov-2. *Nature Reviews Microbiology*, 19(3):155–170, 2021.

[155] Ania Wajnberg, Fatima Amanat, Adolfo Firpo, Deena R Altman, Mark J Bailey, Mayce Mansour, Meagan McMahon, Philip Meade, Damodara Rao Mendu, Kimberly Muellers, et al. Robust neutralizing antibodies to sars-cov-2 infection persist for months. *Science*, 370(6521):1227–1230, 2020.

[156] Alexandra C Walls, Brooke Fiala, Alexandra Schäfer, Samuel Wrenn, Minh N Pham, Michael Murphy, V Tse Longping, Laila Shehata, Megan A O'Connor, Chengbo Chen, et al. Elicitation of potent neutralizing antibody responses by designed protein nanoparticle vaccines for sars-cov-2. *Cell*, 183(5):1367–1382, 2020.

[157] Alexandra C Walls, Young-Jun Park, M Alejandra Tortorici, Abigail Wall, Andrew T McGuire, and David Veesler. Structure, function, and antigenicity of the sars-cov-2 spike glycoprotein. *Cell*, 181(2):281–292, 2020.

[158] Alexandra C Walls, M Alejandra Tortorici, Berend-Jan Bosch, Brandon Frenz, Peter JM Rottier, Frank DiMaio, Félix A Rey, and David Veesler. Cryo-electron microscopy structure of a coronavirus spike glycoprotein trimer. *Nature*, 531(7592):114–117, 2016.

[159] Chunyan Wang, Wentao Li, Dubravka Drabek, Nisreen MA Okba, Rien van Haperen, Albert DME Osterhaus, Frank JM van Kuppeveld, Bart L Haagmans,

Frank Grosveld, and Berend-Jan Bosch. A human monoclonal antibody blocking sars-cov-2 infection. *Nature communications*, 11(1):1–6, 2020.

[160] Ming Wang, Jun Yuan, Tiegang Li, Yang Liu, Jibin Wu, Biao Di, Xi Chen, Xinhong Xu, Enjie Lu, Kuibiao Li, et al. Antibody dynamics of 2009 influenza a (h1n1) virus in infected patients and vaccinated people in china. *PloS one*, 6(2):e16809, 2011.

[161] Pengfei Wang, Lihong Liu, Manoj S Nair, Michael T Yin, Yang Luo, Qian Wang, Ting Yuan, Kanako Mori, Axel Guzman Solis, Masahiro Yamashita, et al. Sars-cov-2 neutralizing antibody responses are more robust in patients with severe disease. *Emerging microbes & infections*, 9(1):2091–2093, 2020.

[162] Wenling Wang, Yanli Xu, Ruqin Gao, Roujian Lu, Kai Han, Guizhen Wu, and Wenjie Tan. Detection of sars-cov-2 in different types of clinical specimens. *Jama*, 323(18):1843–1844, 2020.

[163] Xiaoli Wang, Xianghua Guo, Qianqian Xin, Yang Pan, Yaling Hu, Jing Li, Yanhui Chu, Yingmei Feng, and Quanyi Wang. Neutralizing antibodies responses to sars-cov-2 in covid-19 inpatients and convalescent patients. *Clinical Infectious Diseases*, 2020.

[164] Judith M White, Sue E Delos, Matthew Brecher, and Kathryn Schornberg. Structures and mechanisms of viral membrane fusion proteins: multiple variations on a common theme. *Critical reviews in biochemistry and molecular biology*, 43(3):189–219, 2008.

[165] Ian A Wilson, John J Skehel, and DC Wiley. Structure of the haemagglutinin membrane glycoprotein of influenza virus at 3 å resolution. *Nature*, 289(5796):366–373, 1981.

[166] Daniel Wrapp, Nianshuang Wang, Kizzmekia S Corbett, Jory A Goldsmith, Ching-Lin Hsieh, Olubukola Abiona, Barney S Graham, and Jason S McLellan. Cryo-em structure of the 2019-ncov spike in the prefusion conformation. *Science*, 367(6483):1260–1263, 2020.

[167] Edward Wright, Suzanne McNabb, Trudy Goddard, Daniel L Horton, Tiziana Lembo, Louis H Nel, Robin A Weiss, Sarah Cleaveland, and Anthony R Fooks. A robust lentiviral pseudotype neutralisation assay for in-field serosurveillance of rabies and lyssaviruses in africa. *Vaccine*, 27(51):7178–7186, 2009.

[168] Edward Wright, Nigel J Temperton, Denise A Marston, Lorraine M McElhinney, Anthony R Fooks, and Robin A Weiss. Investigating antibody neutralization of lyssaviruses using lentiviral pseudotypes: a cross-species comparison. *The Journal of general virology*, 89(Pt 9):2204, 2008.

[169] Fan Wu, Aojie Wang, Mei Liu, Qimin Wang, Jun Chen, Shuai Xia, Yun Ling, Yuling Zhang, Jingna Xun, Lu Lu, Shibo Jiang, Hongzhou Lu, Yumei Wen, and Jinghe Huang. Neutralizing antibody responses to sars-cov-2 in a covid-19 recovered patient cohort and their implications. *medRxiv*, 2020.

[170] Fan Wu, Su Zhao, Bin Yu, Yan-Mei Chen, Wen Wang, Zhi-Gang Song, Yi Hu, Zhao-Wu Tao, Jun-Hua Tian, Yuan-Yuan Pei, et al. A new coronavirus associated with human respiratory disease in china. *Nature*, 579(7798):265–269, 2020.

[171] Jun Wu, Boyun Liang, Cunrong Chen, Hua Wang, Yaohui Fang, Shu Shen, Xiaoli Yang, Baoju Wang, Liangkai Chen, Qi Chen, et al. Sars-cov-2 infection induces sustained humoral immune responses in convalescent patients following symptomatic covid-19. *Nature Communications*, 12(1):1–9, 2021.

[172] Hua-Long Xiong, Yang-Tao Wu, Jia-Li Cao, Ren Yang, Ying-Xia Liu, Jian Ma, Xiao-Yang Qiao, Xiang-Yang Yao, Bao-Hui Zhang, Ya-Li Zhang, et al. Robust neutralization assay based on sars-cov-2 s-protein-bearing vesicular stomatitis virus (vsv) pseudovirus and ace2-overexpressing bhk21 cells. *Emerging microbes & infections*, 9(1):2105–2113, 2020.

[173] Ke Xia Yan, Wen Jie Tan, Xiang Min Zhang, Hui Juan Wang, Yan Li, and Li Ruan. Development and application of a safe sars-cov neutralization assay based on lentiviral vectors pseudotyped with sars-cov spike protein. *Bing du xue bao= Chinese Journal of Virology*, 23(6):440–446, 2007.

[174] Xiang-Yang Yao, Wei Liu, Zhi-Yong Li, Hua-Long Xiong, Ying-Ying Su, Tingdong Li, Shi-Yin Zhang, Xue-Jie Zhang, Zhao-Feng Bi, Chen-Xi Deng, et al. Neutralizing and binding antibody kinetics of covid-19 patients during hospital and convalescent phases. *medRxiv*, 2020.

[175] Meng Yuan, Nicholas C Wu, Xueyong Zhu, Chang-Chun D Lee, Ray TY So, Huibin Lv, Chris KP Mok, and Ian A Wilson. A highly conserved cryptic epitope in the receptor binding domains of sars-cov-2 and sars-cov. *Science*, 368(6491):630–633, 2020.

[176] Juanjuan Zhao, Quan Yuan, Haiyan Wang, Wei Liu, Xuejiao Liao, Yingying Su, Xin Wang, Jing Yuan, Tingdong Li, Jinxiu Li, et al. Antibody responses to sars-cov-2 in patients with novel coronavirus disease 2019. *Clinical infectious diseases*, 71(16):2027–2034, 2020.

[177] Peng Zhou, Xing-Lou Yang, Xian-Guang Wang, Ben Hu, Lei Zhang, et al. A pneumonia outbreak associated with a new coronavirus of probable bat origin. *Nature*, 579(7798):270–273, 2020.

[178] Na Zhu, Dingyu Zhang, Wenling Wang, Xingwang Li, Bo Yang, Jingdong Song, Xiang Zhao, Baoying Huang, Weifeng Shi, Roujian Lu, et al. A novel coronavirus from patients with pneumonia in china, 2019. *New England journal of medicine*, 2020.

[179] ZH Zhu, SS Chen, and Alice S Huang. Phenotypic mixing between human immunodeficiency virus and vesicular stomatitis virus or herpes simplex virus. *Journal of acquired immune deficiency syndromes*, 3(3):215–219, 1990.

[180] Seth J Zost, Nicholas C Wu, Scott E Hensley, and Ian A Wilson. Immunodominance and antigenic variation of influenza virus hemagglutinin: implications for design of universal vaccine immunogens. *The Journal of infectious diseases*, 219(Supplement_1):S38–S45, 2019.

[181] Romain Zufferey, Thomas Dull, Ronald J Mandel, Anatoly Bukovsky, Dulce Quiroz, Luigi Naldini, and Didier Trono. Self-inactivating lentivirus vector for safe and efficient in vivo gene delivery. *Journal of virology*, 72(12):9873–9880, 1998.

[182] Romain Zufferey, Dea Nagy, Ron J Mandel, Luigi Naldini, and Didier Trono. Multiply attenuated lentiviral vector achieves efficient gene delivery in vivo. *Nature biotechnology*, 15(9):871–875, 1997.

Appendix A

SUPPLEMENTARY FILES FOR CHAPTER 3

This appendix contains the supplementary data for Chapter 3.

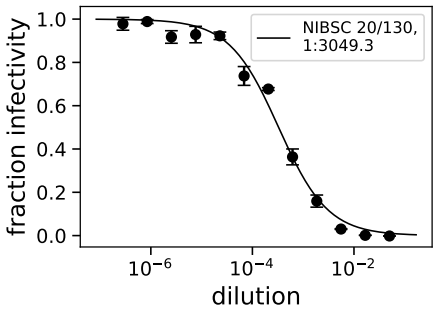

Figure A.1: **Neutralization curve for NIBSC standard reference serum** (product number 20/130). The NT50 for this sample was calculated to be ≈3050.

Figure A.2: **Neutralization curves for each participant.** For each participant, each sample is a different color with the legend specifying how many days post symptom onset each sample was collected.

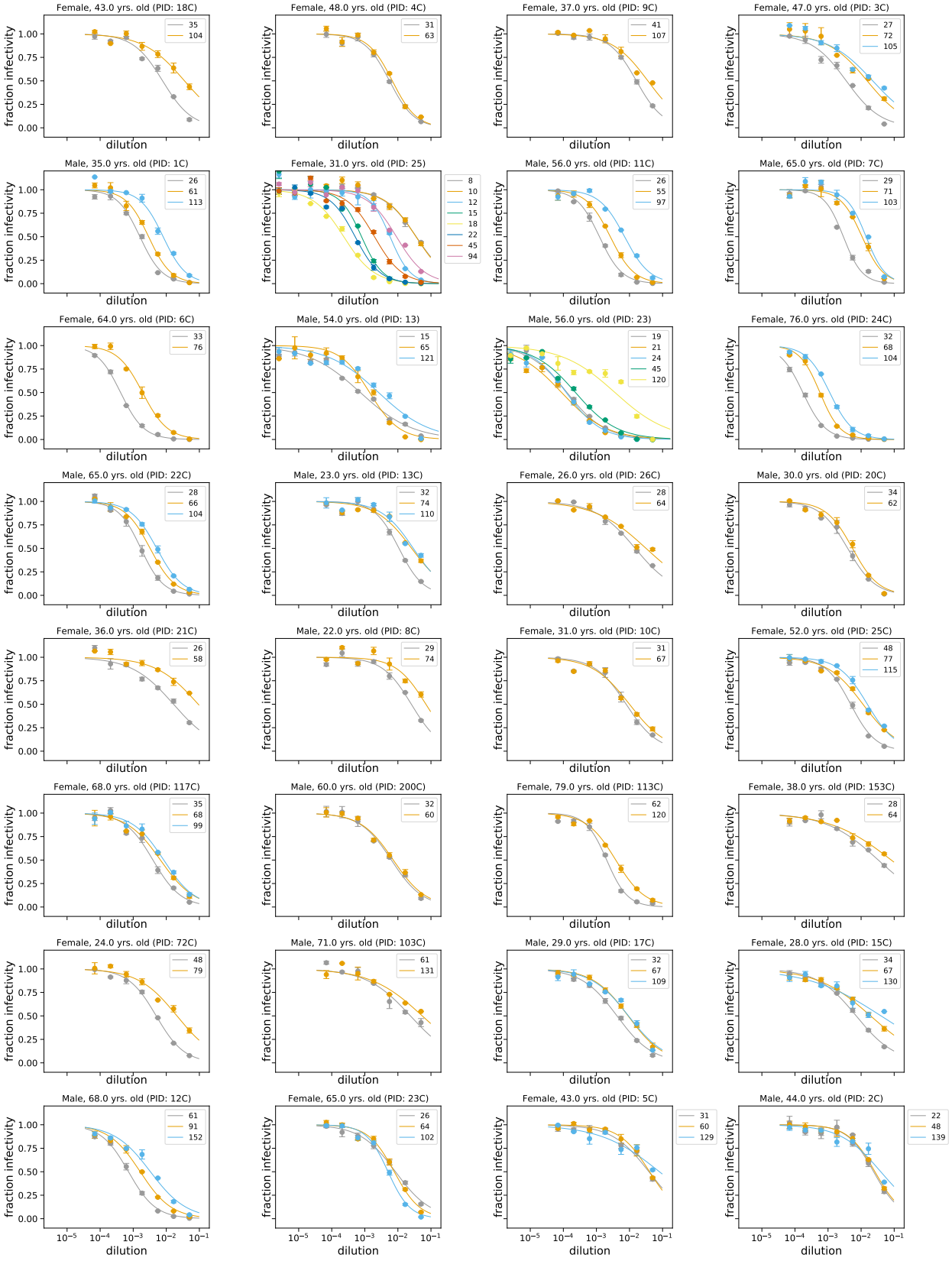
Female, 43.0 yrs. old (PID: 18C)
35
104
Female, 48.0 yrs. old (PID: 4C)
31
63
Female, 37.0 yrs. old (PID: 9C)
41
107
Female, 47.0 yrs. old (PID: 3C)
27
72
105
Male, 35.0 yrs. old (PID: 1C)
26
61
113
Female, 31.0 yrs. old (PID: 25)
8
10
12
15
18
22
45
94
Male, 56.0 yrs. old (PID: 11C)
26
55
97
Male, 65.0 yrs. old (PID: 7C)
29
71
103
Female, 64.0 yrs. old (PID: 6C)
33
76
Male, 54.0 yrs. old (PID: 13)
15
65
121
Male, 56.0 yrs. old (PID: 23)
19
21
24
45
120
Female, 76.0 yrs. old (PID: 24C)
32
68
104
Male, 65.0 yrs. old (PID: 22C)
28
66
104
Male, 23.0 yrs. old (PID: 13C)
32
74
110
Female, 26.0 yrs. old (PID: 26C)
28
64
Male, 30.0 yrs. old (PID: 20C)
34
62
Female, 36.0 yrs. old (PID: 21C)
26
58
Male, 22.0 yrs. old (PID: 8C)
29
74
Female, 31.0 yrs. old (PID: 10C)
31
67
Female, 52.0 yrs. old (PID: 25C)
48
77
115
Female, 68.0 yrs. old (PID: 117C)
35
68
99
Male, 60.0 yrs. old (PID: 200C)
32
60
Female, 79.0 yrs. old (PID: 113C)
62
120
Female, 38.0 yrs. old (PID: 153C)
28
64
Female, 24.0 yrs. old (PID: 72C)
48
79
Male, 71.0 yrs. old (PID: 103C)
61
131
Male, 29.0 yrs. old (PID: 17C)
32
67
109
Female, 28.0 yrs. old (PID: 15C)
34
67
130
Male, 68.0 yrs. old (PID: 12C)
61
91
152
Female, 65.0 yrs. old (PID: 23C)
26
64
102
Female, 43.0 yrs. old (PID: 5C)
31
60
129
Male, 44.0 yrs. old (PID: 2C)
22
48
139
fraction infectivity
dilution
0.00
0.25
0.50
0.75
1.00
10^{-5}
10^{-4}
10^{-3}
10^{-2}
10^{-1}

Table A.1: **Additional demographic and medical data**

	Asymptomatic (N=6)	Symptomatic Non-hospitalized (N=21)	Symptomatic Hospitalized (N=5)	Overall (N=32)
Race				
AIAN	1 (16.7%)	0 (0%)	0 (0%)	1 (3.1%)
White	5 (83.3%)	20 (95.2%)	1 (20.0%)	26 (81.2%)
Asian	0 (0%)	1 (4.8%)	3 (60.0%)	4 (12.5%)
Black	0 (0%)	0 (0%)	0 (0%)	0 (0%)
Multiple Races	0 (0%)	0 (0%)	1 (20.0%)	1 (3.1%)
Hispanic	0 (0%)	1 (4.8%)	0 (0%)	1 (3.1%)
Smoking				
Nonsmoker	5 (83.3%)	19 (90.5%)	5 (100%)	29 (90.6%)
Tobacco use	1 (16.7%)	2 (9.5%)	0 (0%)	3 (9.4%)
Electronic cigarettes/vapor pen use	0 (0%)	1 (4.8%)	0 (0%)	1 (3.1%)
Comorbidities[a]				
No comorbidities	6 (100%)	19 (90.5%)	3 (60.0%)	28 (87.5%)
Asthma	0 (0%)	0 (0%)	1 (20.0%)	1 (2.9%)
Hypertension	0 (0%)	2 (9.5%)	1 (20.0%)	3 (9.4%)

Diabetes	0 (0%)	0 (0%)	1 (20.0%)	1 (3.1%)
COPD/emphysema	0 (0%)	0 (0%)	1 (20.0%)	1 (3.1%)
Cancer	0 (0%)	0 (0%)	1 (20.0%)	1 (3.1%)
Obstructive Sleep Apnoea	0 (0%)	0 (0%)	1 (20.0%)	1 (3.1%)
Common Symptoms[a]				
Chills or shivering	0 (0%)	13 (61.9%)	5 (100%)	18 (56.2%)
Cough	0 (0%)	15 (71.4%)	5 (100%)	20 (62.5%)
Diarrhea	0 (0%)	6 (28.6%)	1 (20.0%)	7 (21.9%)
Ear pain or ear discharge	0 (0%)	0 (0%)	0 (0%)	0 (0%)
Fatigue	0 (0%)	16 (76.2%)	1 (20.0%)	17 (53.1%)
Feeling feverish	0 (0%)	13 (61.9%)	5 (100%)	18 (56.2%)
Increased trouble breathing	0 (0%)	4 (19.0%)	5 (100%)	9 (28.1%)
Loss of sense of taste or smell	0 (0%)	7 (33.3%)	0 (0%)	7 (21.9%)
Muscle or body aches	0 (0%)	13 (61.9%)	2 (40.0%)	15 (46.9%)
Nausea or vomiting	0 (0%)	3 (14.3%)	2 (40.0%)	5 (15.6%)
Rash	0 (0%)	1 (4.8%)	0 (0%)	1 (3.1%)

Runny or stuffy nose	0 (0%)	12 (57.1%)	1 (20.0%)	13 (40.6%)
Sore throat or itchy/scratchy throat	0 (0%)	9 (42.9%)	0 (0%)	9 (28.1%)
Sweats	0 (0%)	13 (61.9%)	4 (80.0%)	17 (53.1%)
Highest Level of Medical Treatment Received				
Outpatient - Testing Only	5 (83.3%)	13 (61.9%)	0 (0%)	18 (56.2%)
Outpatient - Saw Provider[b]	1 (16.7%)	8 (38.1%)	0 (0%)	9 (28.1%)
Inpatient (General Floor)	0 (0%)	0 (0%)	2 (40.0%)	2 (6.2%)
Inpatient (ICU)	0 (0%)	0 (0%)	3 (60.0%)	3 (9.4%)
Highest Level of Respiratory Support				
None	6 (100%)	21 (100%)	0 (0%)	29 (85.3%)
Nasal cannula	0 (0%)	0 (0%)	1 (20.0%)	1 (2.9%)
High-flow O2 or non-rebreather	0 (0%)	0 (0%)	1 (20.0%)	1 (2.9%)
Non-invasive ventilation (BiPAP)	0 (0%)	0 (0%)	1 (20.0%)	1 (2.9%)
Mechanical ventilation	0 (0%)	0 (0%)	2 (40.0%)	2 (5.9%)

Duration of mechanical ventilation (days) (N=2)				
Median [Min, Max]	NA [NA, NA]	NA [NA, NA]	11.5 [6.00, 17.0]	11.5 [6.00, 17.0]

[a]Categories not mutually exclusive

[b]Includes Primary care physician, Urgent care, Emergency Department

Table A.2: **Raw neutralization assay and ELISA data for analyses in Chapter 3**. [a]PID = Participant ID. [b]SH = Symptomatic Hospitalized, SNH = Symptomatic Non-Hospitalized, A = Asymptomatic. [c]PSO = Post Symptom Onset.

sample	PID[a]	Sex	Age	Severity[b]	Days PSO[c]	IC50	NT50	RBD IgA	RBD IgG	RBD IgM	Spike IgG
EBAD84C3	1C	M	35	SH	26	0.0016	627.43	9.02	9.12	1.57	12.11
3A8087A5	1C	M	35	SH	61	0.0029	342.97	7.56	8.94	1.12	12.66
948FA9B9	1C	M	35	SH	113	0.0080	124.46	6.34	7.17	0.62	10.74
16AFBA79	2C	M	44	SNH	22	0.0239	41.81	1.24	2.28	0.56	5.30
EEAEFD9B	2C	M	44	SNH	48	0.0262	38.15	0.64	2.46	0.44	5.72
6BE52F87	2C	M	44	SNH	139	0.0392	25.48	0.55	2.18	0.37	5.72
803BE443	3C	F	47	SNH	27	0.0036	281.26	4.00	7.75	1.03	11.75
597BF57E	3C	F	47	SNH	72	0.0152	65.62	2.89	6.50	0.65	10.73
C82692BD	3C	F	47	SNH	105	0.0224	44.62	2.50	5.83	0.62	10.11
A0D66F9E	4C	F	48	SNH	31	0.0056	179.62	5.20	5.78	1.23	9.69
48BAE426	4C	F	48	SNH	63	0.0068	147.62	3.98	5.86	0.60	10.12
1729101A	5C	F	43	SNH	31	0.0385	26.00	0.64	5.18	1.33	9.72
4D634A06	5C	F	43	SNH	60	0.0405	24.70	0.55	5.14	1.25	9.12
AA918415	5C	F	43	SNH	129	0.0500	20.00	0.59	5.65	1.05	11.60
65C28B8D	6C	F	64	SH	33	0.0004	2412.45	10.94	12.78	2.58	13.92
B82F21E3	6C	F	64	SH	76	0.0019	521.94	4.44	12.62	1.22	13.79

B0CB441F	7C	M	65	SNH	29	0.0029	344.15	4.43	13.02	1.90	13.96
B60A1A68	7C	M	65	SNH	71	0.0107	93.78	1.38	10.93	0.86	11.89
0401D9B0	7C	M	65	SNH	103	0.0142	70.67	1.16	9.50	0.70	10.71
0678DAA4	8C	M	22	SNH	29	0.0255	39.28	1.71	4.14	0.44	5.50
167A52E5	8C	M	22	SNH	74	0.0500	20.00	0.63	2.88	0.37	4.87
9FDB1F72	9C	F	37	SNH	41	0.0162	61.92	0.74	4.37	0.52	7.25
2C1A6676	9C	F	37	SNH	107	0.0358	27.92	0.61	2.58	0.51	5.47
1D1D9677	10C	F	31	SNH	31	0.0079	126.35	0.88	3.28	1.44	7.93
25A7121E	10C	F	31	SNH	67	0.0099	100.64	0.50	3.29	1.03	8.19
C3D4FC41	11C	M	56	SNH	26	0.0012	810.90	4.38	10.46	1.48	14.16
C3F06001	11C	M	56	SNH	55	0.0026	380.71	1.32	9.24	0.99	13.09
E3361F88	11C	M	56	SNH	97	0.0071	141.36	1.03	7.05	0.58	12.44
9EC82418	12C	M	68	SNH	61	0.0007	1392.22	8.09	11.62	2.96	12.23
EE87A018	12C	M	68	SNH	91	0.0016	614.60	6.33	11.29	2.62	11.59
79BD0F7A	12C	M	68	SNH	152	0.0033	301.78	6.35	13.93	1.64	14.50
191A5833	13	M	54	SH	15	0.0007	1364.86	4.14	11.42	1.56	13.71
C19DB21A	13	M	54	SH	65	0.0014	715.17	1.97	11.39	0.68	12.96
B5EBCB0D	13	M	54	SH	121	0.0026	383.58	1.34	9.38	0.43	11.35
611F3917	13C	M	23	SNH	32	0.0108	92.66	3.15	7.51	0.59	9.26
C98C6378	13C	M	23	SNH	74	0.0260	38.40	1.04	5.21	0.37	7.27

50BDD720	13C	M	23	SNH	110	0.0293	34.15	0.95	4.67	0.36	6.47
45099D7F	15C	F	28	SNH	34	0.0071	140.85	3.58	7.76	0.69	11.42
31FA5C80	15C	F	28	SNH	67	0.0193	51.69	1.51	6.44	0.50	11.43
C5E5DEE0	15C	F	28	SNH	130	0.0400	25.00	1.16	4.09	0.42	12.00
45DC80EB	17C	M	29	SNH	32	0.0042	239.10	2.71	9.50	0.78	12.15
E9ECA8DE	17C	M	29	SNH	67	0.0091	110.27	0.88	8.23	0.67	10.72
49CC2287	17C	M	29	SNH	109	0.0093	107.50	0.74	9.04	0.63	12.09
B7B37750	18C	F	43	SNH	35	0.0077	129.34	1.12	6.28	0.76	9.35
23517415	18C	F	43	SNH	104	0.0355	28.15	0.50	4.12	0.46	7.98
12DB8682	20C	M	30	SNH	34	0.0039	255.55	2.70	6.71	1.00	9.93
EAA0308A	20C	M	30	SNH	62	0.0055	182.06	2.05	6.34	0.80	9.72
21902307	21C	F	36	SNH	26	0.0165	60.59	0.46	4.25	1.01	7.50
B3505752	21C	F	36	SNH	58	0.0500	20.00	0.36	2.97	0.63	6.02
281BD693	22C	M	65	SNH	28	0.0017	588.50	6.00	11.12	2.08	12.32
6153F272	22C	M	65	SNH	66	0.0032	308.86	3.22	10.34	0.89	10.75
9E669CC3	22C	M	65	SNH	104	0.0051	194.42	2.47	10.01	0.53	11.60
EE14F19A	23	M	56	SH	19	0.0001	7768.01	5.31	12.22	5.68	15.54
EDD7CFC8	23	M	56	SH	21	0.0001	11346.78	7.24	14.22	5.93	14.89
5555A8C1	23	M	56	SH	24	0.0001	8183.31	7.11	14.41	5.71	15.48
331416C9	23	M	56	SH	45	0.0002	4292.30	2.57	12.72	5.22	14.70

96D33AAD	23	M	56	SH	120	0.0036	275.59	1.04	11.57	2.53	13.72
BDB764DB	23C	F	65	SNH	26	0.0085	118.26	0.45	4.60	1.94	8.57
F741505D	23C	F	65	SNH	64	0.0077	129.40	0.40	4.39	1.30	5.96
D715920D	23C	F	65	SNH	102	0.0050	198.32	0.40	4.53	1.57	7.73
2AD43D3B	24C	F	76	SNH	32	0.0002	5761.32	1.88	11.45	5.09	13.74
7B8AFF92	24C	F	76	SNH	68	0.0006	1758.67	1.54	11.53	3.64	12.91
1823354D	24C	F	76	SNH	104	0.0011	889.28	1.79	9.72	2.65	12.60
429A1FE7	25	F	31	SH	8	0.0357	28.01	0.60	1.45	0.54	4.27
90401AE1	25	F	31	SH	10	0.0352	28.38	0.57	1.69	0.56	4.47
462D516A	25	F	31	SH	12	0.0058	172.89	1.54	6.31	1.53	9.53
62FA7D27	25	F	31	SH	15	0.0008	1253.52	5.30	12.86	3.55	14.11
4B0E5065	25	F	31	SH	18	0.0002	4342.52	2.43	12.88	6.68	14.90
B571AC46	25	F	31	SH	22	0.0005	1960.56	6.14	13.16	3.81	14.94
775EA81A	25	F	31	SH	45	0.0020	509.96	2.46	11.60	2.28	14.12
D1337074	25	F	31	SH	94	0.0090	110.60	1.76	9.36	1.38	13.58
F89B0140	25C	F	52	SNH	48	0.0048	207.08	2.90	8.96	1.69	12.46
2DFDE3C7	25C	F	52	SNH	77	0.0114	87.98	2.01	8.11	1.11	10.47
C53B17AF	25C	F	52	SNH	115	0.0155	64.67	2.02	6.97	0.82	9.60
1996B4D1	26C	F	26	SNH	28	0.0148	67.37	0.50	4.87	0.60	10.26
E267499B	26C	F	26	SNH	64	0.0316	31.62	0.43	3.65	0.45	8.27

B7BA6AC9	72C	F	24	A	48	0.0050	201.75	0.80	9.17	1.04	12.58
C53AEB74	72C	F	24	A	79	0.0209	47.74	0.46	5.26	0.44	9.98
0CA2D4CB	103C	M	71	A	61	0.0239	41.86	0.50	2.60	0.57	9.41
D75ACCF6	103C	M	71	A	131	0.0500	20.00	0.47	1.82	0.65	7.92
CCBD6EF7	113C	F	79	A	62	0.0020	489.35	0.70	9.54	2.78	14.72
86BB2780	113C	F	79	A	120	0.0038	259.98	0.69	8.80	1.77	14.44
D5263562	117C	F	68	A	35	0.0040	252.70	2.48	5.11	0.76	10.06
F8138035	117C	F	68	A	68	0.0067	150.25	1.98	4.25	0.50	9.59
EEFFDE8A	117C	F	68	A	99	0.0084	119.43	1.75	4.28	0.48	9.15
7959DE8D	153C	F	38	A	28	0.0330	30.26	0.69	5.71	0.56	8.62
9730A048	153C	F	38	A	64	0.0500	20.00	0.62	5.11	0.49	7.52
37BB996C	200C	M	60	A	32	0.0064	157.26	0.93	9.00	0.64	12.40
482A935E	200C	M	60	A	60	0.0073	137.62	0.73	8.05	0.65	12.52